
Electronic Thesis and Dissertation Repository

8-24-2020 10:30 AM

Stable carbon and oxygen isotope investigation of Pleistocene growing-season paleoclimate using tree-ring cellulose from the Missinaibi Formation, Adam Creek, James Bay Lowland, Canada

Jumin Lee, *The University of Western Ontario*

Supervisor: Longstaffe, Fred J., *The University of Western Ontario*

Co-Supervisor: Webb, Elizabeth, *The University of Western Ontario*

A thesis submitted in partial fulfillment of the requirements for the Master of Science degree in Geology

© Jumin Lee 2020

Follow this and additional works at: <https://ir.lib.uwo.ca/etd>



Part of the [Geology Commons](#)

Recommended Citation

Lee, Jumin, "Stable carbon and oxygen isotope investigation of Pleistocene growing-season paleoclimate using tree-ring cellulose from the Missinaibi Formation, Adam Creek, James Bay Lowland, Canada" (2020). *Electronic Thesis and Dissertation Repository*. 7191.
<https://ir.lib.uwo.ca/etd/7191>

This Dissertation/Thesis is brought to you for free and open access by Scholarship@Western. It has been accepted for inclusion in Electronic Thesis and Dissertation Repository by an authorized administrator of Scholarship@Western. For more information, please contact wlsadmin@uwo.ca.

Abstract

The isotopic compositions of cellulose in tree rings provide a record of seasonal and annual climatic conditions such as precipitation and temperature. We analyzed stable isotopes of carbon ($\delta^{13}\text{C}_{\text{cellulose}}$) and oxygen ($\delta^{18}\text{O}_{\text{cellulose}}$) in early-wood and late-wood of five conifer sub-fossil wood samples from the Missinaibi Formation, which likely grew during the peak of Marine Isotope Substage (MIS) 5a (~82 kya) at Adam Creek, Ontario. There was no systematic difference between early-wood and late-wood for either $\delta^{13}\text{C}_{\text{cellulose}}$ or $\delta^{18}\text{O}_{\text{cellulose}}$, suggesting similar climatic conditions throughout the growing season. A shift to lower $\delta^{13}\text{C}_{\text{cellulose}}$ with growth age in most samples indicated rising water availability. The estimated value of $\delta^{18}\text{O}_{\text{precipitation}}$ was similar or slightly higher than modern $\delta^{18}\text{O}_{\text{precipitation}}$. Hence, the area may have experienced similar to slightly warmer and/or less humid conditions than today, which is in agreement with the few other studies of MIS 5a climate in this region.

Keywords

Stable carbon isotopes, Stable oxygen isotopes, Tree rings, Cellulose, Early-wood, Late-wood, Seasonality, James Bay Lowland, Paleoclimate, MIS 5, Missinaibi Formation

Summary for Lay Audience

Records of past interglacial (warm) and glacial (cold) stages during the last ice age are rare. Samples comprising these records are also commonly difficult to date. This study improves our knowledge of Ice Age climatic conditions in northern Canada through analysis of sub-fossil wood from the Quaternary Missinaibi Formation sediments of the James Bay Lowland, Canada. All samples were too old ($> 50,000$ kya) to date using radiocarbon methods. Nonetheless, most other data suggest that these trees grew between the retreat and advancement of the Laurentide Ice Sheet during a warm interval (interglacial) that peaked at ~ 82 kya, although some consider them to have been younger (71-57 kya). Tree rings are sensitive bioindicators of local environmental change and hence ideal for reconstructing past growing-season climate. Every year, trees form early-wood in the spring to early summer and late-wood from mid-summer to autumn. The cellulose in this wood systematically records growing-season carbon and oxygen-isotope compositions, which respond to changes in temperature and water availability. At the specific site studied here (Adam Creek, Ontario), these data suggest that growing-season conditions during the MIS 5a interglacial were similar to slightly warmer and/or less humid conditions than is the case today. However, the trees from Adam Creek at MIS 5a were still growing within the range of favourable conditions with temperature and water availability.

Acknowledgments

I consider myself fortunate to have two amazing supervisors, Dr. Elizabeth Webb and Dr. Fred. J. Longstaffe who showed continual support and patience throughout my studies. Dr. Elizabeth Webb, thank you for always encouraging me not to give up and helping me whenever I hit a roadblock in my research. Your positivity always helped me whenever I felt stressed and anxious. To Dr. Fred. J. Longstaffe, thank you for supporting and challenging me to grow in my critical thinking and my knowledge as a scientist. I would also like to thank Kim Law and Li Huang for their advice and assistance in the lab.

Thank you to Professor Paul Karrow for the provision of sub-fossil wood samples for this study.

This research was funded by the Natural Sciences and Engineering Research Council Discovery Grant and Canada Research Chairs Program to Dr. Fred. J. Longstaffe as well as the Canada Foundation for Innovation Infrastructure Grants and Ontario Research Fund Infrastructure Grants to Dr. Fred. J. Longstaffe and Dr. Elizabeth Webb.

I would like to thank my family, friends and colleagues for their support and encouragement throughout my studies. In particular, to my husband, Peter, thank you for always reminding me that I can accomplish my goals and for always being there for me during my stressful and tearful days. To my tiny human, Elizabeth Jihye, thank you for staying healthy in mommy's tummy and sleeping so well in daddy's arms during the final stretches on my studies. Mommy and daddy are so happy that you are in our lives. To my parents and sisters, Julia and Jennifer, thank you for showing your love in my life and for your patience and support throughout my long academic years.

Finally, I would like to thank God for His unconditional love and I acknowledge Him for creating everything in this world. My hope is in Him.

Table of Contents

Abstract.....	ii
Acknowledgments.....	iv
Table of Contents.....	v
List of Tables.....	viii
List of Figures.....	ix
List of Appendices.....	ii
Chapter 1.....	3
1 Introduction.....	3
1.1 Background.....	5
1.2 Sample Location.....	6
1.2.1 Site information.....	6
1.2.2 Stratigraphy of Missinaibi Formation.....	7
1.3 Isotope Dendrochronology.....	9
1.3.1 Wood growth.....	11
1.3.2 Stable carbon- and oxygen-isotope compositions of cellulose.....	11
1.3.3 Examples of tree ring isotope studies of fossil wood in Ontario.....	15
1.4 Objectives.....	16
Chapter 2.....	17
2 Methods.....	17
2.1 Sample Location and Samples.....	17
2.2 Cellulose Extraction.....	21
2.3 Isotopic Analyses of Cellulose.....	21
2.3.1 Oxygen isotopes.....	21
2.3.2 Stable carbon isotopes.....	22

2.4 Radiocarbon Dating	23
2.5 Statistical Methods.....	23
Chapter 3.....	24
3 Results	24
3.1 Physical Properties of Samples.....	24
3.2 Tree-ring Widths, Stable Isotope and Radiocarbon Results	28
3.2.1 Sample AC-77-A2	28
3.2.2 Sample AC-77-C3.....	35
3.2.3 Sample AC-77-D1	40
3.2.4 Sample AC-77-E3.....	45
3.2.5 Sample AC-77-F1	49
Chapter 4.....	54
4 Discussion	54
4.1 Juvenile Effect	55
4.2 Climate.....	58
4.2.1 $\delta^{13}\text{C}_{\text{cellulose}}$ and isotope dendrochronology	59
4.2.2 $\delta^{18}\text{O}_{\text{cellulose}}$, source water and temperature	65
4.2.3 Covariation between $\delta^{18}\text{O}_{\text{cellulose}}$ and $\delta^{13}\text{C}_{\text{cellulose}}$	72
4.3 Early-wood versus Late-Wood Cellulose Isotope Composition and Seasonality	74
4.4 Tree-ring Width and Seasonality	80
4.5 Climatic and Environment Conditions at Adam Creek during MIS 5a	84
Chapter 5.....	85
5 Conclusions	85
5.1 Future Work	86
References.....	87
Appendix.....	101

Curriculum Vitae 112

List of Tables

Table 1.1 Marine Isotope Stages (Lisiecki and Raymo 2005).....	4
Table 1.2 Stratigraphy of Adam Creek, James Bay Lowland, Ontario (Modified from Skinner (1973) and Nguyen and Hicock (2014).	8
Table 3.1 Physical properties of samples.....	24
Table 3.2 Radiocarbon dates for wood samples ¹	28
Table 3.3 Minimum, maximum and mean values of subfossil wood stable carbon- and oxygen-isotope compositions.....	30
Table 3.4 Summary of p-values (t-test) for tree-ring cellulose stable carbon- and oxygen-isotope compositions. Values of $p \leq 0.05$ are shown in bold font.....	31
Table 4.1 Calculated carbon-isotope composition and tree-ring # for whole tree-ring cellulose.	57
Table 4.2 Carbon-isotope composition and tree-ring # of late-wood cellulose.....	57
Table 4.3 Oxygen-isotope composition and tree ring # of early-wood cellulose.	67
Table 4.4 Oxygen-isotope composition and tree-ring # of late-wood cellulose.	67
Table 4.5 Correlation between late-wood $\delta^{18}\text{O}_{\text{cellulose}}$ and $\delta^{13}\text{C}_{\text{cellulose}}$	72
Table 4.6 Pearson correlation (r) between EW (early-wood) and the previous year's LW (late-wood), and between EW and LW of same year for $\delta^{13}\text{C}_{\text{cellulose}}$ or $\delta^{18}\text{O}_{\text{cellulose}}$	76
Table 4.7 p-values for two-tailed t-test for $\delta^{13}\text{C}_{\text{cellulose}}$ or $\delta^{18}\text{O}_{\text{cellulose}}$ between early- and late-wood within each tree-ring for all samples.....	76
Table 4.8 Average tree-ring widths (TRW) for isotopically analyzed sub-samples.....	80
Table 4.9 Pearson correlation between TRW and $\delta^{13}\text{C}_{\text{cellulose}}$ or $\delta^{18}\text{O}_{\text{cellulose}}$	82

List of Figures

Figure 1.1 Adam Creek Site Map (North America), which is located in the James Bay Lowland, Ontario (Modified from Ministry of Natural Resource, 2020)..... 7

Figure 1.2 Cross-sectioned tree rings of early-wood (light bands) and late-wood (dark bands) of Sample C (AC-77-C3) from Adam Creek, Ontario, Canada..... 10

Figure 2.1 Wood sample A (AC-77-A2). Tree-rings are symmetrical. (A) Bird’s-eye view of the wood; (B) Cross-section of the tree rings; (C) and (D) Photomicrographs of the tree rings. 18

Figure 2.2 Wood sample C (AC-77-C3). Tree-rings are radially asymmetric. (A) Bird’s-eye view of the wood; (B) Cross-section of the tree rings; (C) and (D) Photomicrographs of the tree rings..... 18

Figure 2.3 Wood sample D (AC-77-D1). Tree-rings are symmetrical. (Z) Bird’x-eye view of the wood; (B) Cross-section of the tree rings; (C) and (D) Photomicrographs of the tree rings. 19

Figure 2.4 Wood sample E (AC-77-E3). Tree-rings are radially asymmetric. (A) Bird’s-eye view of the wood; (b) Cross-section of the tree rings; (C) and (D) Photomicrographs of the tree rings..... 19

Figure 2.5 Wood sample F (AC-77-F1). Tree-rings are radial asymmetric. (A) Bird’s-eye view of the wood; (B) Cross-section of the tree rings; (C) and (D) Photomicrographs of the tree rings..... 20

Figure 3.1 Wood sample A (AC-77-A2). Wood not compressed. (A) Transverse thin-section of tree rings, showing prominent growth rings with a sharp transition from large early-wood cells to late-wood cells; and (B) Radial thin-section of tree rings. EW = early-wood; LW= late-wood; RD = resin duct; RT = ray tracheid. 25

Figure 3.2 Wood sample C (AC-77-C3). Wood compressed. (A) Transverse thin-section of tree-rings, showing prominent growth rings with a sharp transition from large earlywood

cells to latewood cells; and (B) Tangential thin-section of tree-rings. EW = early-wood; LW = late-wood; RB = ring boundary; RD = resin duct; RT = ray tracheid. 26

Figure 3.3 Wood sample D (AC-77-D1). Wood not compressed. (A) Transverse thin-section of tree-rings, showing prominent growth rings with a sharp transition from large early-wood cells to late-wood cells; and (B) Tangential thin-section of tree rings. EW = early-wood; LW = latewood; RB = ring boundary; RD = resin duct. 26

Figure 3.4 Wood sample E (AC-77-E3). Wood compressed. (A) Transverse thin-section tree-rings, not showing prominent growth rings with no sharp transition from large early-wood cells to late-wood cells; and (B) Tangential thin-section of tree-rings. RT = ray tracheid; RD = resin ducts. 27

Figure 3.5 Wood sample F (AC-77-F1). Wood compressed. (A) Transverse thin-section tree-rings, inadequate to show prominent growth rings with no sharp transition from large early-wood cells to late-wood cells; and (B) Radial thin-section of tree-rings. RD = resin duct; RT = ray tracheid. 27

Figure 3.6 $\delta^{18}\text{O}$ versus tree-ring number for sample AC-77-A2 for early-, late-, and whole-ring cellulose, as calculated annually, and for 3-year and 5-year running averages. 32

Figure 3.7 $\delta^{13}\text{C}$ versus tree-ring number for sample AC-77-A2 for early-, late-, and whole-ring cellulose, as calculated annually, and for 3-year and 5-year running averages. 33

Figure 3.8 Correlation between $\delta^{18}\text{O}$ (‰) (VSMOW) and $\delta^{13}\text{C}$ (‰) (VPDB) for: (A) early-wood cellulose, (B) late-wood cellulose, and (C) calculated whole-wood cellulose for sample AC-77-A2. 34

Figure 3.9 $\delta^{18}\text{O}$ versus tree-ring number for sample AC-77-C3 for early-, late-, and whole-ring cellulose, as calculated annually, and for 3-year and 5-year running averages. 37

Figure 3.10 $\delta^{13}\text{C}$ versus tree ring-number for sample AC-77-C3 for early-, late-, and whole-ring cellulose, as calculated annually, and for 3-year and 5-year running averages. 38

Figure 3.11 Correlation between $\delta^{18}\text{O}$ (‰) (VSMOW) and $\delta^{13}\text{C}$ (‰) (VPDB) for: (A) early-wood cellulose, (B) late-wood cellulose, and (C) calculated whole-wood cellulose for sample AC-77-C3..... 39

Figure 3.12 $\delta^{18}\text{O}$ versus tree-ring number for sample AC-77-D1 for early-, late-, and whole-ring cellulose, as calculated annually, and for 3-year and 5-year running averages. 42

Figure 3.13 $\delta^{13}\text{C}$ versus tree-ring number for sample AC-77-D1 for early-, late-, and whole-ring cellulose, as calculated annually, and for 3-year and 5-year running averages. 43

Figure 3.14 Correlation between $\delta^{18}\text{O}$ (‰) (VSMOW) and $\delta^{13}\text{C}$ (‰) (VPDB) for: (A) early-wood cellulose, (B) late-wood cellulose, and (C) calculated whole-wood cellulose for sample AC-77-D1. 44

Figure 3.15 $\delta^{18}\text{O}$ versus tree-ring number for sample AC-77-E3 for early-, late-, and whole-ring cellulose, as calculated annually, and for 3-year and 5-year running averages. 46

Figure 3.16 $\delta^{13}\text{C}$ versus tree-ring number for sample AC-77-E3 for early-, late-, and whole-ring cellulose, as calculated annually, and for 3-year and 5-year running averages. 47

Figure 3.17 Correlation between $\delta^{18}\text{O}$ (‰) (VSMOW) and $\delta^{13}\text{C}$ (‰) (VPDB) for: (A) early-wood cellulose, (B) late-wood cellulose, and (C) calculated whole-wood cellulose for sample AC-77-E3..... 48

Figure 3.18 $\delta^{18}\text{O}$ versus tree-ring number for sample AC-77-F1 for early-, late-, and whole-ring cellulose, as calculated annually, and for 3-year and 5-year running averages. 51

Figure 3.19 $\delta^{13}\text{C}$ versus tree-ring number for sample AC-77-F1 for early-, late-, and whole-ring cellulose, as calculated annually, and for 3-year and 5-year running averages. 52

Figure 3.20 Correlation between $\delta^{18}\text{O}$ (‰) (VSMOW) and $\delta^{13}\text{C}$ (‰) (VPDB) for: (A) early-wood cellulose, (B) late-wood cellulose, and (C) calculated whole-wood cellulose for sample AC-77-F1. 53

Figure 4.1 Calculated $\delta^{13}\text{C}_{\text{cellulose}}$ of whole tree-rings on an annual basis. 56

Figure 4.2 Frequency of $\delta^{13}\text{C}_{\text{cellulose}}$ obtained for late-wood..... 60

Figure 4.3 Tree-ring $\delta^{13}\text{C}_{\text{cellulose}}$ for boreal conifers from various locations. The red line indicates the average whole tree-ring and late-wood $\delta^{13}\text{C}_{\text{cellulose}}$ of Adam Creek samples AC-77-A2, -C3, -D1 and -E3. M = modern (¹McCarroll and Pawellek 2001, ²Tardif et al. 2008, ³Bégin et al. 2015, ⁴Edwards et al. 2008, ⁵Guerrieri et al. 2017, ⁶this thesis, ⁷Hunter et al. 2006, ⁸Leavitt and Kalin 1992). Late-wood cellulose: references 1 and 6; whole-ring cellulose: references 2-5 and 7-8. 63

Figure 4.4 The $\delta^{13}\text{C}_{\text{cellulose}}$ of early-wood (blue) and late-wood (orange) for AC-77-A2, AC-77-C3, AC-77-D1 and AC-77-E3. 64

Figure 4.5 The $\delta^{18}\text{O}_{\text{cellulose}}$ of early-wood (blue) and late-wood (orange) for AC-77-A2, AC-77-C3, AC-77-D1, AC-77-E3 and AC-77-F1..... 66

Figure 4.6 Frequency of $\delta^{18}\text{O}_{\text{cellulose}}$ obtained for late-wood for samples AC-77-A2, AC-77-C3, AC-77-D1, AC-77-E3 and AC-77-F1..... 68

Figure 4.7 $\delta^{18}\text{O}_{\text{cellulose}}$ from different locations. Red line displays Adam Creek oxygen-isotope compositions. M = modern. ¹Edwards and Fritz 1986, ²Edwards et al. 2008, ³Bégin et al. 2015, ⁴Guerrieri et al. 2017, ⁵thesis, ⁶Hunter et al. 2006, ⁷Kerr-Lawson et al. 1992. All data are for whole-wood except 6 (late-wood). 70

Figure 4.8 $\delta^{18}\text{O}_{\text{precipitation}}$ versus $\delta^{18}\text{O}_{\text{cellulose}}$ for localities shown in Figure 4.7..... 71

Figure 4.9 Correlations between late-wood $\delta^{18}\text{O}_{\text{cellulose}}$ and $\delta^{13}\text{C}_{\text{cellulose}}$ for samples AC-77-A2, AC-77-C3, AC-77-D1, AC-77-E3 and AC-77-F1. Data and trend-line shown in orange for AC-77-E3 represent the first four tree-ring sub-samples analyzed. 73

Figure 4.10 Comparison of same year, early-wood and late-wood $\delta^{13}\text{C}_{\text{cellulose}}$ for AC-77-A2, AC-77-C3, AC-77-D1, AC-77-E3 and AC-77-F1..... 77

Figure 4.11 Comparison of same year, early-wood and late-wood $\delta^{18}\text{O}_{\text{cellulose}}$ for AC-77-A2, AC-77-C3, AC-77-D1, AC-77-E3 and AC-77-F1..... 78

Figure 4.12 Tree-ring width (TRW) for whole tree-ring (whole-wood), early-wood and late-wood for AC-77-A2, AC-77-C3, AC-77-D1, AC-77-E3 and AC-77-F1. 81

Figure 4.13 Comparison of whole (WW) tree-ring width (TRW) versus tree-ring # (age) with whole-ring $\delta^{13}\text{C}_{\text{cellulose}}$ versus tree-ring # for AC-77-A2, AC-77-C3, AC-77-D1, AC-77-E3 and AC-77-F1. 82

Figure 4.14 Comparison of whole (WW) tree-ring width (TRW) versus tree-ring # (age) with whole-ring $\delta^{18}\text{O}_{\text{cellulose}}$ versus tree-ring # for AC-77-A2, AC-77-C3, AC-77-D1, AC-77-E3 and AC-77-F1. 83

List of Appendices

Appendix A Stable carbon- and oxygen-isotope compositions and trees ring widths of all samples.....	101
---	-----

Chapter 1

1 Introduction

Scientists, politicians and the general public are concerned with the current trend of climate change. Today, the warming has already exceeded pre-industrial temperatures by 1.5 °C in many parts of the world (Global Climate Change NASA). Consequently, many ecosystems have been affected by global warming by processes such as biome shifts, fires, extreme weather, droughts, and sea level rise from melting of polar ice sheets. Warmer global temperatures, for example, can disrupt the habitat ranges of many North American species by moving them towards the north and to higher elevations (Groffman et al. 2014). The degree of impact from global warming varies depending on geographic location. Rapid increases in temperature have occurred around the world, but are particularly more evident in northern locations (Global Climate Change NASA).

In Canada, the landscape has cycled through several episodes of glaciation and warming. Over the last 100,000 years, North America, and Ontario, Canada in particular, have experienced two episodes of continental glaciation where ice covered more than half of the continent (Lisiecki and Raymo 2005). Ontario is currently in an interglacial (Marine Isotope Stage (MIS) 1; Table 1.1: kya = thousand years ago). This study aims to investigate the seasonal variations in climate in northern Ontario during one of the previous interglacials (MIS 5a) prior to the second-last glacial (MIS 4) and understand the response of vegetation – tree cellulose in particular – to a natural warming episode. Such information can then be compared with modern proxies such as the isotopic composition of tree-ring cellulose formed during the current interglacial (MIS 1) to better understand the climate information carried by such isotopic signals.

Table 1.1 Marine Isotope Stages (Lisiecki and Raymo 2005).

Marine Isotope Stages	Start interval (kya)	End interval (kya)	Interglacial/glacial
MIS 1	14	0	Interglacial
MIS 2	29	14	Glacial
MIS 3	57	29	Interglacial
MIS 4	71	57	Glacial
MIS 5	130	71	Interglacial
MIS 5a	82 (peak of interglacial sub-stage)		
MIS 5b	87 (peak of glacial sub-stage)		
MIS 5c	96 (peak of interglacial sub-stage)		
MIS 5d	109 (peak of glacial sub-stage)		
MIS 5e	123 (peak of interglacial sub-stage)		
MIS 6	191	130	Glacial
MIS 7	243	191	Interglacial
MIS 8	300	243	Glacial

Current human activities are releasing a large quantity of carbon dioxide (CO₂) to the atmosphere. This increase in greenhouse gases, which also includes methane (CH₄), and nitrous oxide (N₂O), is driving global warming (Stauffer et al. 2002). Atmospheric CO₂ concentration has increased from 277 parts per million (ppm) in 1750, the start of the industrial era to the highest ever recorded of 413 ppm in July 2019 at Mauna Loa observatory. Current levels of atmospheric CO₂ are higher than they have ever been over the last 650 thousand years (Siegenthaler et al. 2005, Joos and Spahni 2008, Scripps 2019).

Large amounts of CO₂ are absorbed by forest growth. Carbon from the atmosphere and oxygen from water are stored and fixed in macromolecules in trees each year through photosynthetic biochemical processes (McCarroll and Loader 2004). The biomass of wood, including cellulose, preserves this carbon and oxygen and studies of cellulose carbon and oxygen isotope ratios allow us to reconstruct both local and regional climate from, both present and past. The isotopic variations observed in tree-rings are caused by changes to the environment each year and provide important climatic information (McCarroll and Loader 2004, Bégin et al. 2015). For example, one might ask, “How does the present temperatures in the boreal forest of James Bay Lowland, Ontario compare with

temperatures in the same region during MIS 5a?”. Unlike modern climate, which is almost certainly affected by anthropogenic activities, changes in paleoclimate during earlier glacial-interglacial oscillations within the Quaternary Period occurred naturally. Glacial – interglacial cycles during the Quaternary largely resulted from variations in the amount of incoming solar radiation from the sun (National Centers for Environmental Information NOAA). Milankovitch cycles describe variations in the Earth’s orbit, wobble and tilt that affect the amount of solar radiation that heats the Earth’s surface. For example, when the Earth has a smaller axial tilt, there is a smaller difference in seasonal temperatures and ice-sheets tend to grow (Hays et al. 1976).

Many previous studies have investigated paleoclimatic conditions using the stable isotopes of tree rings, with stable carbon- and oxygen isotopes receiving the most attention (Johnson and Ingram 2004, Keppler et al. 2007, Bégin et al. 2015, Hook et al. 2015, Bose et al. 2016, Griggs et al. 2017). In this study, the stable carbon- and oxygen-isotope compositions of tree ring cellulose from wood samples of likely MIS 5a age (~82 kya), which were recovered from the James Bay Lowland, are used provide a record of past seasonal and annual variations in precipitation and temperature. These data allow for comparison between the MIS 5a and MIS 1 (current) interglacial intervals.

1.1 Background

Five major “ice ages” occurred over North America during the Quaternary Period, which began at ~2.58 Ma and extends until the present day. The Laurentide Ice Sheet (LIS) covered a large part of North America during a series of advances and retreats across the continent during the Quaternary Period (Dyke and Prest 1987). The climate changed with sequences of cold and warm or glacial and interglacials, lasting thousands of years, also known as marine isotope stages (MIS) (Hays et al. 1976). The last ~130 kya have been divided into 5 MIS based on climate shifts (Lisiecki and Raymo 2005; Table 1.1). The start dates of these isotope stages are: MIS1 (ca. 14 kya), MIS 2 (ca. 29 kya), MIS 3 (ca. 57 kya), MIS 4 (ca. 71 kya), MIS 5 (ca. 130 kya) (Table 1.1); odd numbered MIS are interglacial and even numbers are glacial episodes. The extent of glaciation is less known

for glacial stages prior to Last Glacial Maximum (LGM), which occurred during MIS 2, because records are rare, poorly preserved and difficult to date (Stokes et al. 2015). There is also a paucity of data for interglacials prior to the present time. Previous studies suggest that during MIS 5, most parts of eastern and central North America were ice-free and warmer than or similar to the present interglacial (Allard et al. 2012, Miller and Andrews 2019, Suh et al. 2020). MIS 5 is subdivided into 5 stages of interglacial and glacial sub-stages (MIS 5a – e), 5a, c, and e being warm and b and d cold stages and peaks of substages rather than boundaries are listed in Table 1.1 (Lisiecki and Raymo 2005). This study adds to those data through an examination of MIS 5, likely MIS 5a in particular, in the James Bay Lowland using the stable carbon- and oxygen isotope ratios of tree-ring cellulose from sub-fossil wood as a proxy climate record.

1.2 Sample Location

1.2.1 Site information

In Ontario, to the south and west of James and Hudson Bays, the James Bay Lowland is the northernmost forested region, with an area of $> 325\,000\text{ km}^2$ (Skinner 1973, Nguyen and Hicock 2014, Dalton et al. 2016) (Figure 1.1). It consists mostly of Holocene peatlands that overlie Pleistocene glacial deposits and Palaeozoic and Mesozoic limestone. A variety of habitats, such as marshland (5 %), swamps (13 %), permafrost wetlands (22 %), minerotrophic fens (24 %), and ombrotrophic bogs (36 %) comprise the James Bay Lowland landscape (Riley 2003), and contain sparse, stunted, slow-growing forest dominated by spruce and tamarack.

The ‘subfossil wood’ (defined as partially fossilized and mineralized with silica replacement) samples analyzed in this research were collected from the Missinaibi Formation at Adam Creek, Moose River Basin, Ontario. Currently, a boreal forest comprised of coniferous trees is situated at the Adam Creek site.



Figure 1.1 Adam Creek Site Map (North America), which is located in the James Bay Lowland, Ontario (Modified from Ministry of Natural Resource, 2020).

1.2.2 Stratigraphy of Missinaibi Formation

The Quaternary Missinaibi Formation sediments overlie three older tills (I, II, III) and underlie the Adam till and later units along Adam Creek, Moose River Basin, Ontario (Table 1.2). These sediments were deposited between the retreat and advance of the Laurentide Ice Sheet (LIS) during an interglacial, but their exact age has been debated to be either MIS 3 or MIS 5 – and MIS5a in particular (Skinner 1973, Dalton et al. 2016, Miller and Andrews 2019). Four members have been defined within the Missinaibi Formation, each of which is attributed to a different depositional environment; from oldest to youngest, the environments are: marine, fluvial, forest-peat and lacustrine (Skinner 1973).

Table 1.2 Stratigraphy of Adam Creek, James Bay Lowland, Ontario (Modified from Skinner (1973) and Nguyen and Hicock (2014)).

AGE	FORMATION	SKINNER (1973)	INFERRED EVENTS	AGE C ¹² YEARS B.P.
Holocene	Post-glacial		Proglacial lake is eventually replaced by Tyrell fed Marine and lacustrine silt. Sand beds also common. Glacial retreat	7,800
Late Wisconsin	Upper till	Kippling Till	Deposition by readvancing SW flowing ice. Sandy-silt till, massive, moderate amount of clasts	
Middle-Late Wisconsin	Inter-till	Friday Creek Sediments	Proglacial lake sediments deposited during brief ice retreat. Sand and silt unit up to 1- metres. No organics. Often absent altogether.	
Early Wisconsin	Lower Till	Adam Till	Glacial advance	
Sangamonian	Missinaibi Formation	Lacustrine member <u>Forest-peat member</u> Fluvial member Marine member	Colder interval Warmer interval Colder interval Warmer interval	>54,000
Pre-Missinaibi tills	Glaciation	Till III Intertill-sediments (II-III) Till II Intertill-sediments (I-II) Till I	Glacial advance Glacial retreat Glacial advance Glacial retreat Glacial advance	

The subfossil wood samples used in this study were retrieved from the forest-peat member, which is up to 2 m thick and consists of logs, mosses, sedges, sticks and stumps (Skinner 1973). The wood obtained from this layer has been identified as larch or spruce, but exact differentiation between the two species is difficult since the samples are compressed and partially lignified (Skinner 1973). Skinner (1973) noted that stumps were observed in growth position, in association with the other wood samples, indicating that the samples collected are unlikely to have been transported any great distance from their original location. Skinner (1973) suggested a wet environment of growth for the forest-peat unit, based on the presence of coeval moss and sedge. The implied wet conditions may have resulted in the small diameter of the subfossil wood samples. The lacustrine bed overlying the forest bed provides further evidence of the forest soil conditions being wet as there was flooding during the latter stages of forest-peat unit deposition.

1.3 Isotope Dendrochronology

Tree rings are sensitive bioindicators of local environmental change and the carbon and oxygen-isotope compositions of a wood component like cellulose vary in response to fluctuations of temperature and water availability (McCarroll and Loader 2004). Carbon- and oxygen-isotope ratios are typically reported in δ -notation, as defined in Equations 1.1 ($\delta^{13}\text{C}$) and 1.2 ($\delta^{18}\text{O}$), respectively.

$$\delta^{13}\text{C} = \left(\frac{R_{\text{sample}}}{R_{\text{standard}}} \right) - 1 \quad \text{Eq. 1.1}$$

$$\delta^{18}\text{O} = \left(\frac{R_{\text{sample}}}{R_{\text{standard}}} \right) - 1 \quad \text{Eq. 1.2}$$

Bégin et al. (2015) studied the Canadian northeastern boreal forest, and found that both $\delta^{13}\text{C}$ and $\delta^{18}\text{O}$ of cellulose of black spruce trees in high latitudes are sensitive to summer maximum temperatures, and concluded that during past 200 years, the coldest interval occurred in first half of the 19th century. Furthermore, the $\delta^{18}\text{O}$ of cellulose from spruce tree-rings (*Picea*) from central Switzerland were more strongly correlated to the amount of precipitation, relative humidity, and temperature than tree-ring width when comparing

historical low- and high-frequency climate data (Anderson et al. 1998). For example, lower $\delta^{18}\text{O}_{\text{cellulose}}$ is associated with moist environments and colder temperatures while higher $\delta^{18}\text{O}_{\text{cellulose}}$ results from dry and warm growing conditions (Anderson et al. 2002, Voelker et al. 2015). Glacial advancement causes colder temperatures, which reduces both stomatal conductance and carbon fixation, leading to increasing $\delta^{13}\text{C}$ of cellulose (Leavitt and Kalin 1992). Visible tree rings can be used distinguish annual growth, and can be further divided into seasonal growth through recognition of early-wood and late-wood (Figure 1.2). Therefore, tree rings are ideal proxies to reconstruct past seasonal climate (Barbour et al. 2002).

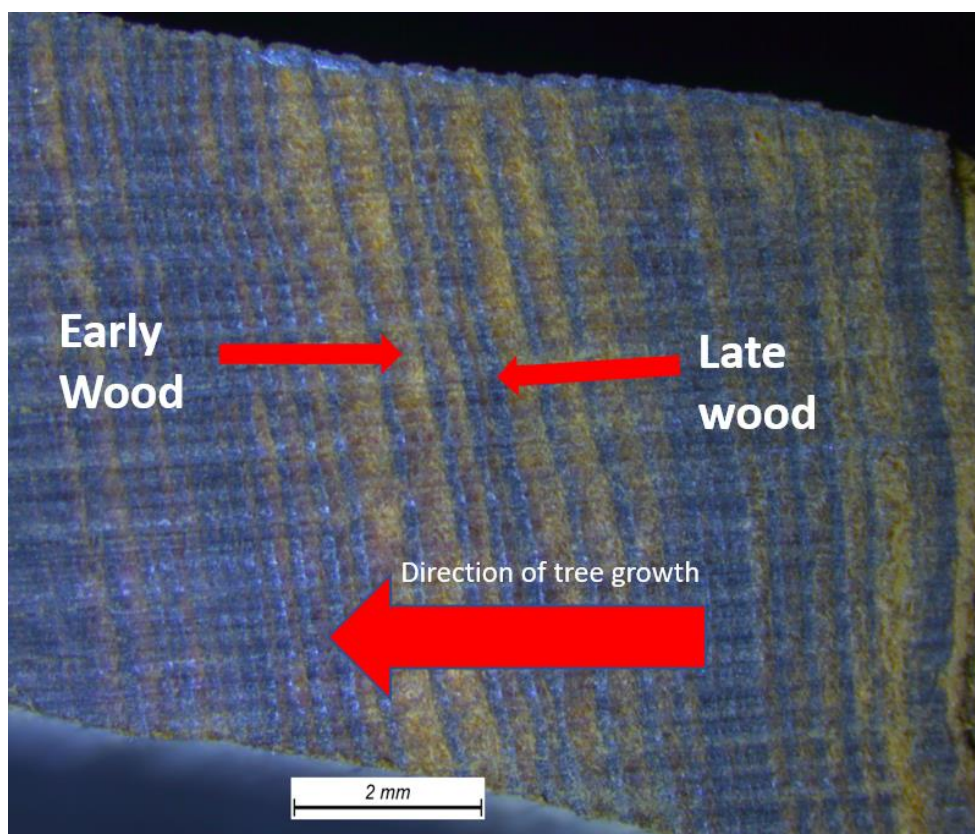


Figure 1.2 Cross-sectioned tree rings of early-wood (light bands) and late-wood (dark bands) of Sample C (AC-77-C3) from Adam Creek, Ontario, Canada.

1.3.1 Wood growth

Both the width and the isotope compositions of tree rings reflect annual and seasonal climate that occurred during tree-ring formation (McCarroll and Loader 2004). Trees grow in both height from bottom to top and width from inside to outside every year through mitosis (cellular division) in the meristem tissue (undifferentiated cells) of the trunk. As the secondary meristem, called the vascular cambium and which is located between the xylem and phloem, undergoes cell division, tree diameter increases. The cells produced in the inner part of cambium are added to the xylem and those that are formed in the outer part are added to the phloem (Stokes & Smiley, 1968).

The xylem is a network of cells that allows a tree to move water and solutes from the soil through the roots to the leaves. The phloem transports glucose and amino acids produced during photosynthetic processes in the leaves around the plant for growth (Schweingruber 2007). The youngest rings are on the outer part of the tree as they grow on top of the previous layers of xylem cells every year. As trees greet a change of season towards colder unfavorable conditions, they suspend xylem cell formations (Stokes and Smiley 1968). Each tree ring is composed of early and late-wood. Typically, early-wood is lighter in colour due to larger and thinner-walled cells (Figure 1.2). Late-wood is formed during the latter part of summer to early fall and typically is darker (Figure 1.2). Furthermore, the formation of late-wood provides an indication of the stalling of tree growth as temperature and amount of sunlight diminish as seasons change (Poole and Bergen 2006).

1.3.2 Stable carbon- and oxygen-isotope compositions of cellulose

Previous studies have found that the stable carbon- and oxygen-isotope compositions of different wood components such as cellulose, lignin and whole-wood vary (Gray and Thompson 1977, Loader et al. 2003). Although there is no significant difference in either $\delta^{18}\text{O}$ or $\delta^{13}\text{C}$ between alpha cellulose and unaltered holocellulose, there is a significant difference when isotopic data for cellulose are compared with untreated whole-wood (Riechelmann et al. 2016). The $\delta^{18}\text{O}$ of cellulose versus whole-wood samples can differ by 5.0 ± 1.2 ‰ (Riechelmann et al. 2016).

Alpha-cellulose $[C_6H_{10}O_5]_n$ is defined as portion of holocellulose (α -cellulose and hemicellulose). Hemicellulose can cause an error in the isotopic signal by having exchangeable carbonyl oxygen (Wright 2008, Hook et al. 2015). In this study, the Brendel method (nitric acid and acetic acid) was used to remove both lignin and hemicellulose. Although there are other macromolecules such as lignin and hemicellulose that make up plant tissues and cell walls of tree rings, cellulose is more resistant to degradation and should better preserve isotope climate signals (Gray and Thompson 1977, Griffith et al. 2008). In fossil tree samples, the isotopic compositions of whole-wood can provide an inaccurate representation of ancient climatic conditions due to degradation of lignin and other components (Gray and Thompson 1977, Loader et al. 2003). Accordingly, McCarroll and Loader (2004) recommended studying cellulose of tree rings to reconstruct seasonal paleoclimate using $\delta^{13}C$ and $\delta^{18}O$. The stable carbon- and oxygen- isotope compositions of tree ring cellulose should display seasonal climatic signals from the early-wood produced during the spring to early summer and the late-wood produced in mid-summer to autumn (Barbour et al. 2002, An et al. 2012, Fu et al. 2017).

1.3.2.1 Oxygen isotopes

The oxygen-isotope composition of tree-ring cellulose provides a record of soil water ($\delta^{18}O_{\text{soil water}}$) taken up by tree roots and leaf water ($\delta^{18}O_{\text{leaf water}}$) that has experienced evaporative ^{18}O enrichment (McCarroll and Loader 2004), as is described in Equation 1.3.

$$\delta^{18}O_{\text{cellulose}} = f_o \cdot (\delta^{18}O_{\text{stem water}}) + (1 - f_o) \cdot (\delta^{18}O_{\text{leaf water}}) + \epsilon_o \quad \text{Eq. 1.3}$$

The parameter f_o is the relative proportion of $\delta^{18}O_{\text{stem water}}$ incorporated into the cellulose. Because there is typically no fractionation when plant roots uptake water (see below), $\delta^{18}O_{\text{stem water}}$ is equivalent to $\delta^{18}O_{\text{soil water}}$, and in temperate regions with abundant rainfall $\delta^{18}O_{\text{soil water}}$ is equivalent to $\delta^{18}O_{\text{precipitation}}$. The parameter ϵ_o is the fractionation between plant water and cellulose during its formation and is ~ 27 ‰ regardless of temperature (McCarroll and Loader 2004).

The primary controls that influence the $\delta^{18}\text{O}_{\text{cellulose}}$ are: (1) the $\delta^{18}\text{O}$ of source water, which varies with temperature, (2) ^{18}O enrichment of leaf water during transpiration, which varies with relative humidity, and (3) biochemical oxygen-isotope fractionation during photosynthesis, which is fairly constant. The $\delta^{18}\text{O}$ of precipitation is higher when temperatures increase and leaf-water $\delta^{18}\text{O}$ is higher when relative humidity decreases (McCarroll and Loader 2004). Hence, the $\delta^{18}\text{O}_{\text{cellulose}}$ helps us to understand the climate and hydrological cycle of a region (Gray and Thompson 1977, Edwards and Fritz 1986a, Roden and Ehleringer 1999).

Leaf water becomes enriched in ^{18}O by transpiration due to evaporation at the stomata. More evaporation in a drier environment leads to higher $\delta^{18}\text{O}_{\text{leaf water}}$ and ultimately an increase in $\delta^{18}\text{O}_{\text{cellulose}}$ (Epstein et al. 1977). An increase in $\delta^{18}\text{O}_{\text{stem water}}$ is caused by increase in $\delta^{18}\text{O}$ of source water since there is generally agreed that there is no fractionation during take-up of water by tree roots (Ehleringer and Dawson 1992). Precipitation is usually the main water source to plants. The $\delta^{18}\text{O}$ of precipitation decreases as a moisture mass moves northward and inland in the northern hemisphere because ^{18}O is preferentially precipitated relative to ^{16}O as the moisture mass moves along its northern / inland trajectory (Craig 1961, Dansgaard 1964, Galewsky et al. 2016). As a result, $\delta^{18}\text{O}_{\text{cellulose}}$ of a tree grown in a higher latitude and/or colder region will be lower than a tree grown in a lower latitude and/or warmer region.

Trees with deep roots may get replenished from both precipitation and ground water (Waterhouse et al. 2002). Therefore, $\delta^{18}\text{O}_{\text{cellulose}}$ may reflect a mixture of recent precipitation and groundwater. Waterhouse et al. (2002), for example, found the ratio of ca. 40:60 of ground water and precipitation in $\delta^{18}\text{O}_{\text{cellulose}}$ of an oak tree over an eight month interval. However, the wet surface environment forest-peat layer of the Missinaibi formation at Adam Creek suggests that the ground water was near or at the surface and its $\delta^{18}\text{O}$ likely closely resembled that of precipitation.

1.3.2.2 Carbon isotopes

Most trees, and especially those of the northern forests, use the C₃ photosynthetic pathway where three carbon atoms are contained in the first photosynthetic byproduct. The $\delta^{13}\text{C}$ of atmospheric carbon dioxide ($\delta^{13}\text{C}_{\text{atm}}$) is incorporated into the $\delta^{13}\text{C}$ of wood component. Currently, $\delta^{13}\text{C}_{\text{atm}}$ is ~ -8.2 ‰ (VPDB) (Keeling et al. 2010), but during pre-industrial era, the values was ~ -6.4 ‰ (VPDB) (McCarroll and Loader 2004). The $\delta^{13}\text{C}$ of modern tree rings can be corrected to the pre-industrial standard value using equation 1.4 (Schubert and Jahren 2015):

$$\delta^{13}\text{C}_{\text{Cor}} = \delta^{13}\text{C}_{\text{plant}} - (\delta^{13}\text{C}_{\text{atm}} + 6.4) \quad \text{Eq. 1.4}$$

As a result of isotopic fractionation during the transportation and transition of carbon in the process of cellulose production, $\delta^{13}\text{C}_{\text{cellulose}}$ has much lower values (-27 to -21 ‰) than atmospheric CO₂. For example, the $\delta^{13}\text{C}_{\text{cellulose}}$ of modern tree-ring cellulose along a precipitation transect in Oregon, United States, varied from -26.3 to -22.1 ‰ (Roden et al. 2005). Two main fractionations take place as the CO₂ molecule is fixed into the wood component. The CO₂ molecules with lighter isotope (¹²C) of carbon diffuse more easily into the stomata than those with heavier isotope (¹³C) with a fractionation (a) of 4.4 ‰ as air diffuses through the pores of the plant (Francey and Farquhar 1982). The second fractionation ($b = 27$ ‰) occurs with the discrimination against ¹³C during gaseous diffusion and photosynthesis called carboxylation. This process is driven by an enzyme called Rubisco. These two main controls on the $\delta^{13}\text{C}$ of plant material can be expressed as:

$$\delta^{13}\text{C}_{\text{plant}} = \delta^{13}\text{C}_{\text{air}} - a - (b - a) (c_i/c_a) \quad \text{Eq. 1.5}$$

where a is the fractionation against ¹³CO₂ that results from diffusion, b is the net discrimination from carboxylation as a result of Rubisco, and c_i and c_a are intercellular and ambient CO₂ concentrations (Farquhar et al. 1982). The ratio of c_i/c_a is related to a plant's water use efficiency (iWUE) (Eq. 1.6) (McCarroll and Loader 2004).

$$\text{iWUE} = A/g = c_a [1 - (c_i/c_a)] (0.625) \quad \text{Eq. 1.6}$$

where A is the rate of CO_2 assimilation and g is stomatal conductance. Low water use efficiency typically results if a plant experiences high stomatal conductance in a high humidity environment (Leavitt 2002). Therefore, variations in $\delta^{13}\text{C}_{\text{cellulose}}$ are affected by changes in environmental factors that control the rate of stomatal conductance and the rate of photosynthesis. Temperature, water availability and amount of solar radiation are the main environmental variables that cause changes in $\delta^{13}\text{C}_{\text{cellulose}}$. Under warmer and drier conditions, the opening of the stomata decreases in order to reduce water loss. This limits the preferential diffusion of ^{12}C into the plant and as a result, $\delta^{13}\text{C}_{\text{cellulose}}$ will increase. Temperature further affects $\delta^{13}\text{C}$ signal in plants because the plant's enzymes do not function properly when the temperature is too cold, CO_2 uptake is reduced and $\delta^{13}\text{C}$ decrease (Tieszen 1991). Since most plants grow in areas where the temperature is favourable to their growth, this is not always important. In high latitude areas, however, boreal forest tree-ring $\delta^{13}\text{C}$ has been shown to vary with temperature (Tardif et al. 2008, Loader et al. 2013a, Bégin et al. 2015).

In the modern boreal forests of northern Ontario and subarctic Manitoba, Canada, summer temperature (July to September) has been shown to be a stronger control on $\delta^{13}\text{C}_{\text{cellulose}}$ than other environmental variables (Tardif et al. 2008, Holzkämper et al. 2012, Bégin et al. 2015). For example, Porter et al. (2009) found that $\delta^{13}\text{C}_{\text{cellulose}}$ of white spruce from northern Canada was most strongly associated with mean maximum temperatures in June and July, which influenced stomatal conductance. In contrast, Voelker et al. (2019) studied both $\delta^{13}\text{C}$ and $\delta^{18}\text{O}$ of cellulose in the early-wood portion of tree rings formed from spring to early summer in white spruce trees located near Lake Superior, Canada and found that isotopic signatures were related to the conditions of the previous winter such as winter minimum temperature, Lake Superior ice cover, and regional and continental-scale atmospheric winter pressure variability in response to lake effect climate. In short, the isotopic signals of tree-rings can be influenced by multiple environmental parameters.

1.3.3 Examples of tree ring isotope studies of fossil wood in Ontario

Relative to modern tree studies, there are significantly fewer studies of stable isotopes in fossil wood from the boreal forest in northern Canada, especially prior to LGM (Naulier et

al. 2014). That said, previous stable isotope studies of modern and fossil wood within MIS 1 in North American boreal forest collectively showed that conditions such as the summer temperature and relative humidity that affect $\delta^{13}\text{C}_{\text{cellulose}}$ were similar among various boreal forests over a wide geographic area (Leavitt and Kalin 1992, Hunter et al. 2006, Naulier et al. 2014, Bégin et al. 2015). Similarly, studies investigating seasonal and annual climate of $\delta^{18}\text{O}_{\text{cellulose}}$ in modern trees in boreal forests are far more common compared to those of ancient trees. Those few studies of ancient boreal forest trees, however, demonstrate that the $\delta^{18}\text{O}_{\text{cellulose}}$ decreases with increasing latitude and decreasing temperatures (Edwards and Fritz 1986a, Hunter et al. 2006, Sensula and Pazdur 2013). Furthermore, using subfossil wood remains of black spruce trees from boreal lakes, Naulier et al. (2014) found that both $\delta^{13}\text{C}_{\text{cellulose}}$ and $\delta^{18}\text{O}_{\text{cellulose}}$ tree-ring series were reliable for climatic reconstruction. Variations in $\delta^{18}\text{O}_{\text{cellulose}}$ over a time series provided an indication of changes in boreal forest climate, with cold and wet conditions reflected in low $\delta^{18}\text{O}_{\text{cellulose}}$ (+19.2 to +22.6 ‰) of black spruce trees. Bégin et al. (2015) demonstrated that $\delta^{13}\text{C}_{\text{cellulose}}$ from boreal forest modern spruce trees formed a stronger correlation with temperature than with precipitation amount in northeastern Canada.

1.4 Objectives

The purpose of this study is to assess interglacial (likely MIS 5a) climate and seasonality at Adam Creek, Ontario to determine if this area experienced similar growing-season temperature and precipitation as today. To achieve this goal, we have analyzed the stable carbon- and oxygen-isotope compositions of both early- and late-wood tree-ring cellulose from five subfossil trees collected from Missinaibi Formation at Adam Creek, Ontario. Furthermore, a comparison between the isotopic compositions of early-wood and late-wood of each year has also been used to interpret variations in growing-season conditions among five different samples. Finally, comparisons of results for the study area and the isotopic compositions of modern and ancient tree-rings from different areas of North America were made in order to enhance understanding of the interglacial climate during this time of forest growth (likely MIS 5a).

Chapter 2

2 Methods

2.1 Sample Location and Samples

The five ancient wood samples analyzed were collected from the Missinaibi Formation at Adam Creek, Ontario (50.23780428, -82.10114966) by Owen L. White (1979) of the Ontario Geological Survey and stored by Paul Karrow (University of Waterloo), prior to being provided to Fred J. Longstaffe (The University of Western Ontario). Adam Creek is a tributary of the Moose River, which flows towards James Bay in Ontario (Figure 1.1). The Missinaibi Formation is a non-glacial deposit, formed as a result of the retreat of the Laurentide Ice Sheet, likely during the MIS 5a interglacial. The wood samples were found in a submerged forest-peat unit overlain by lacustrine beds and underlain by glacial, marine, and fluvial sediments (Skinner 1973). It has been debated whether Missinaibi beds are interstadial or interglacial (Skinner 1973, Dalton et al. 2016). Skinner (1973) suggested a wet environment during formation of the forest peat because of existence of moss and sedge. The forest-peat is described by Skinner (1973) as consisting mosses, sedges, sticks, logs and stumps. By comparison, the current vegetation in this area is a boreal forest with wetlands. Today, the Adam Creek region receives ~732 mm and ~238 mm of rainfall annually and in summer, respectively and summer mean temperature is 15.1 °C (Climate Atlas of Canada 2019).

The wood samples were photographed using a high definition Cannon DSLR camera (Figures 2.1 to 2.5). Three out of five samples had been radially compressed asymmetrically during burial (Figures 2.2, 2.4 and 2.5). Each wood sample was cut to into 2.5 - 5 cm blocks ('cookies'), using a band saw. The sample blocks were smoothed using 400 grit sandpaper in preparation for tree-ring subsampling and thin sectioning. Individual tree rings were numbered with the assistance of a Nikon SMZ800 stereomicroscope. For each wood cross-section (cookie), the early and late-wood were numbered, and their thickness measured in μm using the built-in scalar of the stereomicroscope. The densities (kg/m^3) of each samples were calculated by measuring the weight (in grams) and the amount of water displaced (volume; $1000\text{L} = 1\text{m}^3$).

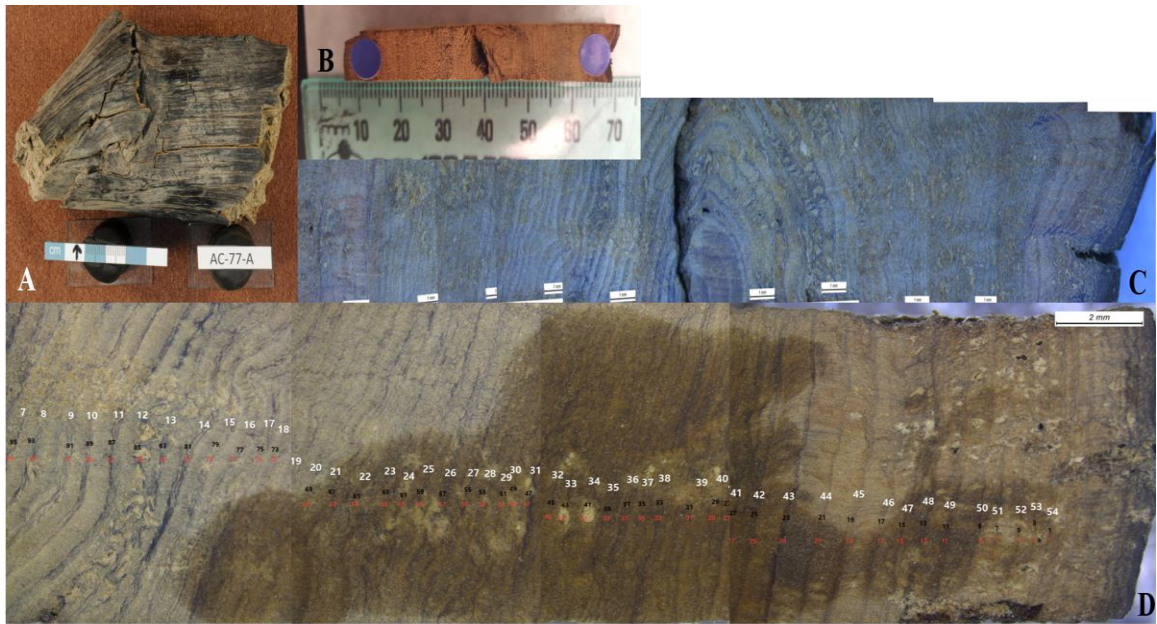


Figure 2.1 Wood sample A (AC-77-A2). Tree-rings are symmetrical. (A) Bird's-eye view of the wood; (B) Cross-section of the tree rings; (C) and (D) Photomicrographs of the tree rings.

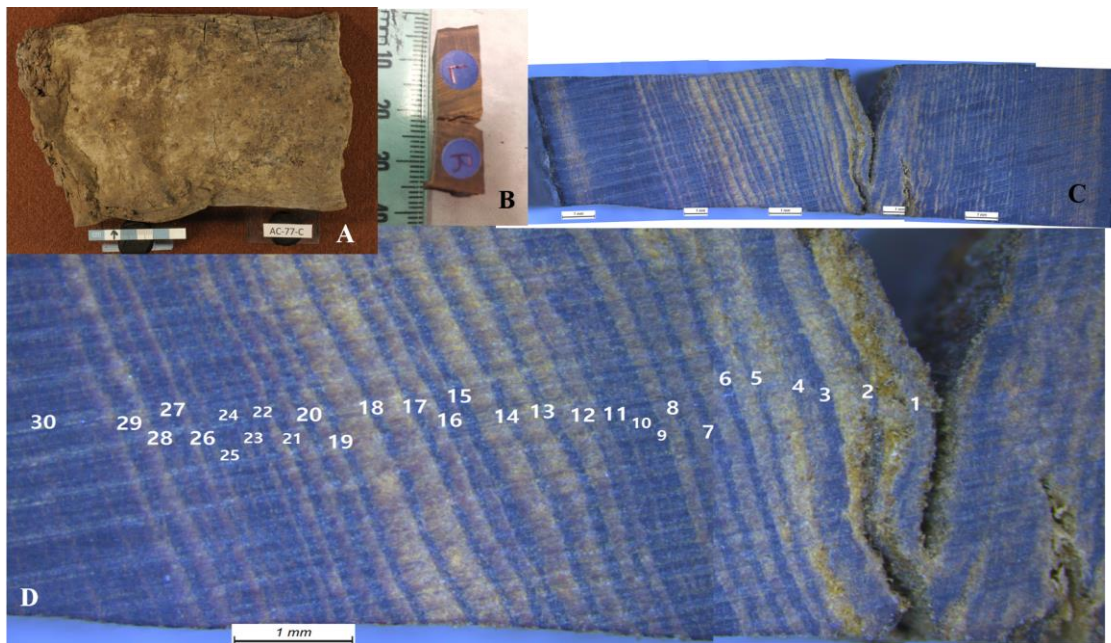


Figure 2.2 Wood sample C (AC-77-C3). Tree-rings are radially asymmetric. (A) Bird's-eye view of the wood; (B) Cross-section of the tree rings; (C) and (D) Photomicrographs of the tree rings.

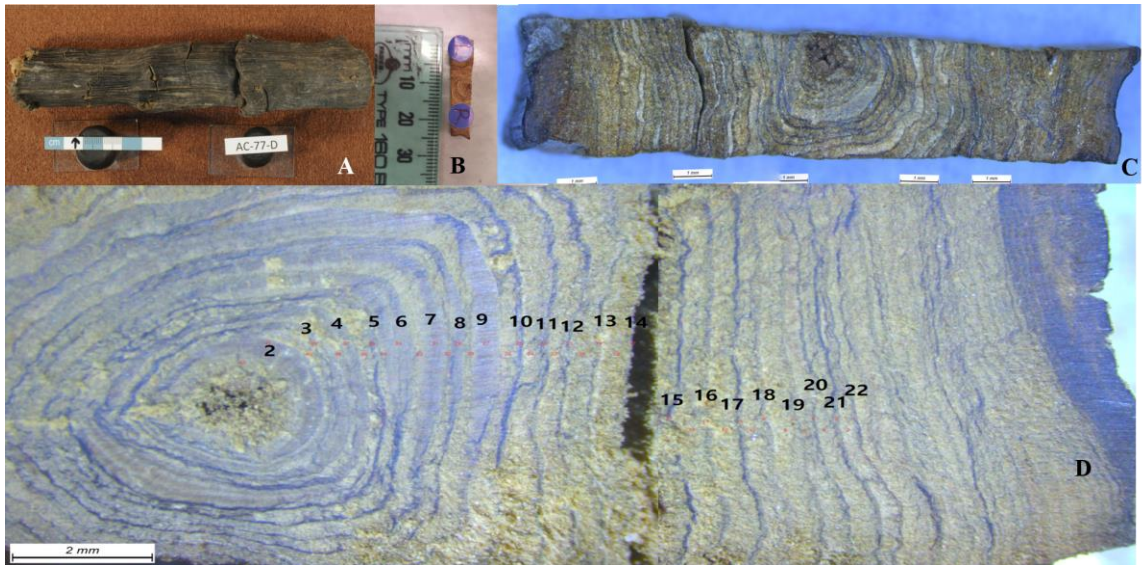


Figure 2.3 Wood sample D (AC-77-D1). Tree-rings are symmetrical. (Z) Bird's-eye view of the wood; (B) Cross-section of the tree rings; (C) and (D) Photomicrographs of the tree rings.

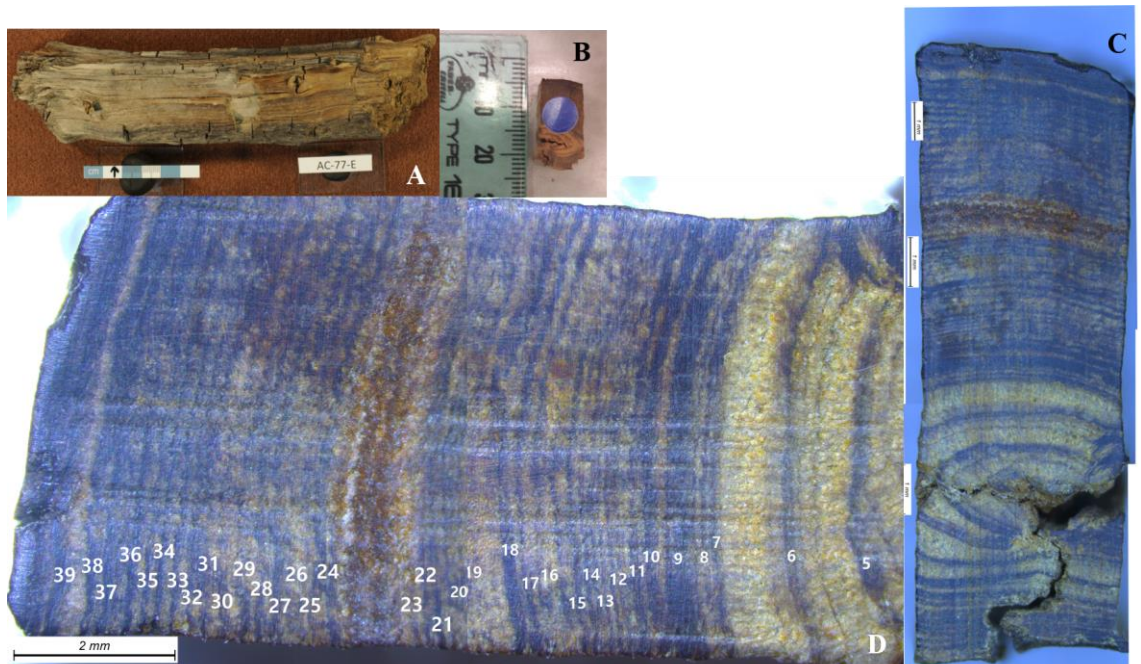


Figure 2.4 Wood sample E (AC-77-E3). Tree-rings are radially asymmetric. (A) Bird's-eye view of the wood; (b) Cross-section of the tree rings: (C) and (D) Photomicrographs of the tree rings.

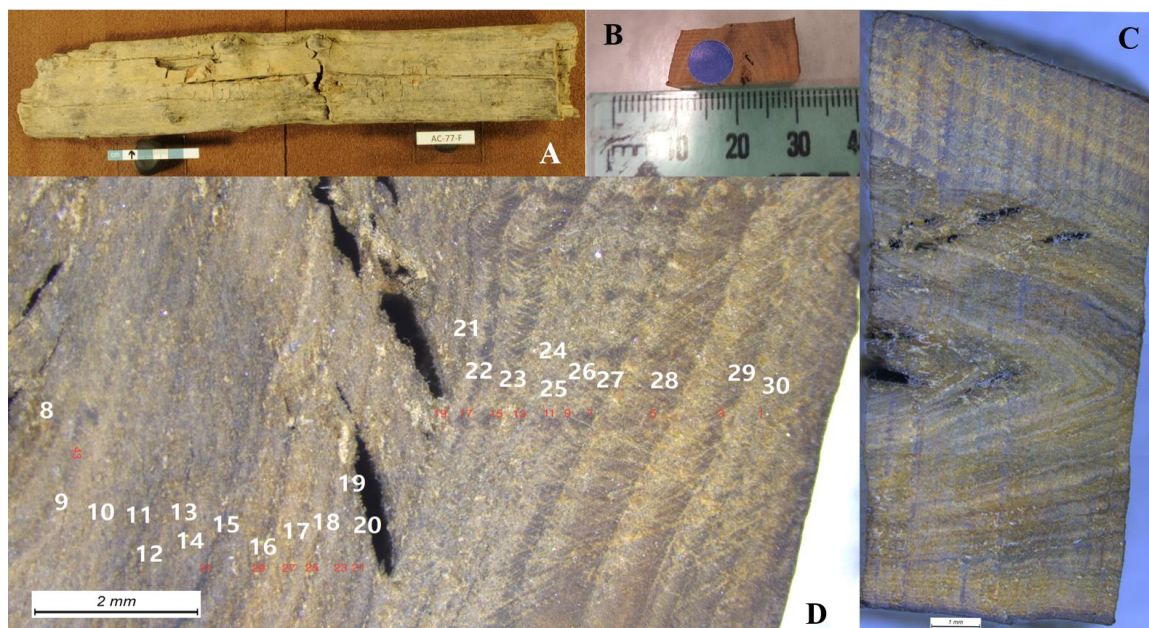


Figure 2.5 Wood sample F (AC-77-F1). Tree-rings are radial asymmetric. (A) Bird's-eye view of the wood; (B) Cross-section of the tree rings; (C) and (D) Photomicrographs of the tree rings.

In addition, 30 μm -thick thin sections were obtained for each wood sample from Spectrum Petrographics, Inc. Vancouver, WA, USA. Thin sections were obtained for both the transverse and tangential tree ring orientations. These sections were used in an effort to identify the tree species, as guided by the dendrochronology wood library (Schweingruber 2007) and a dichotomous key to wood anatomy described by Esau (1960).

There are some basic differences in wood anatomy between softwood (conifers, *Coniferopsida*) and hardwood (deciduous, angiosperm) trees. In angiosperm trees, cells have larger diameter vessels in early-wood compared to late-wood. In coniferous trees, cells in early-wood have thin walls, a large diameter, and are light in colour, whereas cells in late-wood have thick walls, a small diameter, and are dark in colour (Schweingruber 2007). Furthermore, the cell type known as tracheae are absent in conifers, which allow them to survive in cool temperate regions. Specific wood anatomical structures (e.g., axial

resin ducts, epithelial cells of resin ducts, ray tracheids) were attempted to identify in order to narrow the choice of appropriate species (Esau 1960).

Subsampling of the tree-rings was performed on the least compressed portion of the wood cross-section. The sub-samples of late-wood and early-wood were removed by hand using a scalpel, with the aid of a standard binocular microscope to ensure proper separation of the two components. Each wood sample was then weighed and stored in a labeled sample tube for cellulose extraction.

2.2 Cellulose Extraction

The Brendel method (Brendel et al. 2000), as modified by Evans and Schrag (2004), was used to extract alpha-cellulose. Nitric acid (120 μ L, 69 %) and acetic acid (12 μ L, 80 %) was added to ~ 1 mg of powdered wood sample, which was then maintained at 120 °C in a sand bath for 30 minutes to remove both lignin and hemicellulose. Then, 90 % ethanol was added to the samples to further rinse and remove hemicellulose, lignin and ethanol-extractives. This was followed by rinsing with distilled water to remove all traces of acid. Lastly, an ethanol wash followed by an acetone rinse were performed to further clean and then quickly dehydrate the samples. After all acid, ethanol, distilled water and acetone rinses were completed, the samples were centrifuged (12 min at 12,000 rpm), any supernatant was removed, and the samples were then dried and stored at room temperature.

2.3 Isotopic Analyses of Cellulose

2.3.1 Oxygen isotopes

About 0.07 mg of each cellulose sample was placed in silver capsule and stored in a desiccator until analysis. The oxygen-isotope compositions of cellulose samples were determined using a Thermo Scientific TC-EA (High Temperature Conversion-Elemental Analyzer) coupled to a Thermo Scientific Delta Plus^{XL} mass spectrometer in continuous

flow mode. The oxygen in cellulose samples was converted to CO by pyrolysis in a glassy carbon reactor of the TC-EA at 1350 °C. Then the CO was separated from N₂ in a gas chromatograph on a flow of He gas and introduced to the mass spectrometer through a Thermo Scientific ConFlo 3 interface. The oxygen-isotope composition of all samples is reported in the standard δ -notation (see Chapter 1, Eqn. 1.2, $R = {}^{18}\text{O}/{}^{16}\text{O}$) relative to VSMOW in per mil (‰).

Secondary standards used to make calibration curve to the VSMOW-SLAP scale were IAEA C-6 (formerly ANU sucrose) (accepted value = +36.4 ‰; Loader and Buhay 1999) and H₂O VSMOW (defined as 0 ‰ exactly; United States Geological Survey 2020). The reproducibility of IAEA C-6 and H₂O VSMOW during the course of this project were ± 0.3 ‰ (n = 23) and ± 0.3 ‰ (n = 15), respectively. Benzoic acid (IAEA-601) and IAEA C3 (cellulose) were used to independently test the precision and accuracy of the calibration curve, for which the following values were obtained: $+26.0 \pm 0.8$ ‰ (n = 15) and $+31.2 \pm 0.4$ ‰ (n = 12). These results can be compared with the accepted values for benzoic acid (IAEA-601) and IAEA C3, which are +23.1 ‰ and +31.3 to +32.7 ‰, respectively. The average reproducibility of replicated cellulose samples was ± 0.3 ‰ (n = 34 pairs).

2.3.2 Stable carbon isotopes

Cellulose samples were weighed to ~0.100 mg and placed in a tin capsule and stored in a desiccator until analysis. Their carbon-isotope compositions were determined using a Costech EA (Elemental Analyzer) coupled to a Thermo Scientific Delta V Plus mass spectrometer in continuous flow mode. The carbon-isotope compositions of all samples are expressed in standard δ -notation (see Chapter 1, Eqn. 1.1, $R = {}^{13}\text{C}/{}^{12}\text{C}$) relative to VPDB in per mil (‰).

Secondary standards used to make the calibration curve to VPDB were USGS 41a (accepted value = +36.55 ‰) and USGS 40 (accepted value = -26.39 ‰). The precision of USGS 41a and USGS 40 during the course of this project was ± 0.3 ‰ (n = 18) and ± 0.1 ‰ (n = 17). Laboratory keratin (-24.1 ± 0.1 ‰, n = 24) and IAEA-CH-6 (sucrose) (-

10.5 ± 0.1 ‰, $n = 10$) were also used to evaluate both the accuracy of the calibration curve as well as to provide additional information concerning accuracy. The accepted values for keratin and IAEA-CH-6 are -24.04 ‰, and -10.45 ‰ respectively (United States Geological Survey 2020). The average precision of replicated samples was ± 0.1 ‰ ($n = 30$ pairs).

The isotopic compositions of whole tree-ring samples were calculated from weighted values from early- and late-wood. For example, weighted values for whole tree-rings were calculated by adding early- and late-wood isotopic values proportion to the tree-ring width of early- and late-wood.

2.4 Radiocarbon Dating

Wood samples were sent to A.E. Lalonde AMS Laboratory at the University of Ottawa for radiocarbon dating. The sample preparation and accelerator mass spectrometry (AMS) methods used there are described in Crann et al. (2017). Calibration of radiocarbon dates was performed using OxCal v. 4.3 (Ramsey 2009) and the IntCal13 calibration curve (Reimer et al. 2013). The radiocarbon detection limits at the Lalonde AMS laboratory corresponds to ~ 50 kya, after which only infinite ages are reported.

2.5 Statistical Methods

Tests for correlation between cellulose $\delta^{18}\text{O}$ and $\delta^{13}\text{C}$ were considered significant if $p < 0.05$ by performing two-tailed t-test using Excel and SPSS (IBM 2016). Statistical comparisons for both stable carbon- and oxygen-isotope compositions were made between: (i) early and late-wood, (ii) early-wood from earlier years of growth versus later years of growth, and (iii) late-wood from earlier years of growth versus later years of growth. Linear correlations, r^2 and Pearson R values were also generated for $\delta^{13}\text{C}$ and $\delta^{18}\text{O}$ in early-wood, late-wood, and whole tree-ring data using Excel and SPSS.

Chapter 3

3 Results

3.1 Physical Properties of Samples

The physical properties of the five subfossil wood samples (weight and density) are listed in Table 3.1. All samples had a density greater than 1g/cm^3 , with samples AC-77-C3 and AC-77-F1 having the highest densities (3.76 g/cm^3 and 5.41 g/cm^3 , respectively). The densities of this subfossil wood are higher than normal wood ($0.2 - 1\text{ g/cm}^3$) (Gartner and Meinzer 2005), likely because of mineralization. Mustoe (2016), for example, found that the densities of wood mineralized by quartz or chalcedony were $2.3 - 2.1\text{ g/cm}^3$ in opalized wood.

Table 3.1 Physical properties of samples.

Samples	Volume (cm^3) ¹	Density (g/cm^3)	Diameter (cm) ¹	Total # of rings ²
AC-77-A2	220	1.04	6.5	54
AC-77-C3	127	3.76	3.5	30
AC-77-D1	50	1.43	3.5	22
AC-77-E3	90	1.31	3	39
AC-77-F1	40	5.41	2	30

¹ Data obtained from 2.5 - 5 cm blocks ('cookies') of a sample

² Total number of tree-rings obtained for analyses

Typically, the cross-section of a trunk or branch is close to circular. The cross-sections of these subfossil wood samples, however, are sometimes asymmetrical (Figures 2.2, 2.4 and 2.5), likely because of lateral compression during burial.

All five tree samples at the Adam Creek site were identified as softwood (conifers, *Coniferopsida*) (Figure 3.1 - 3.5). Since some, not all of these samples were compressed

during burial, however, the wood structure was not always well preserved (Figures 3.2, 3.4 and 3.5).

Specific species could not be identified, however, because wood preservation was inadequate to observe specific wood anatomical structures such as epithelial cells of resin ducts and difficult to identify species. Skinner (1973) suggested that that the trees are spruce or larch. Farley-Gill (1980) found that black and white spruce are the dominant trees growing at James Bay Lowland today.

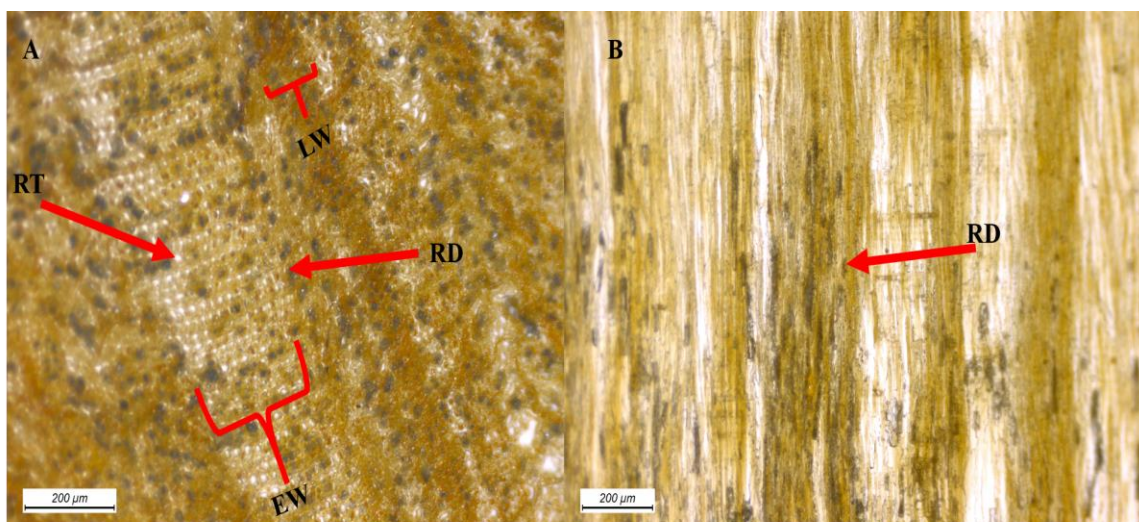


Figure 3.1 Wood sample A (AC-77-A2). Wood not compressed. (A) Transverse thin-section of tree rings, showing prominent growth rings with a sharp transition from large early-wood cells to late-wood cells; and (B) Radial thin-section of tree rings. EW = early-wood; LW= late-wood; RD = resin duct; RT = ray tracheid.

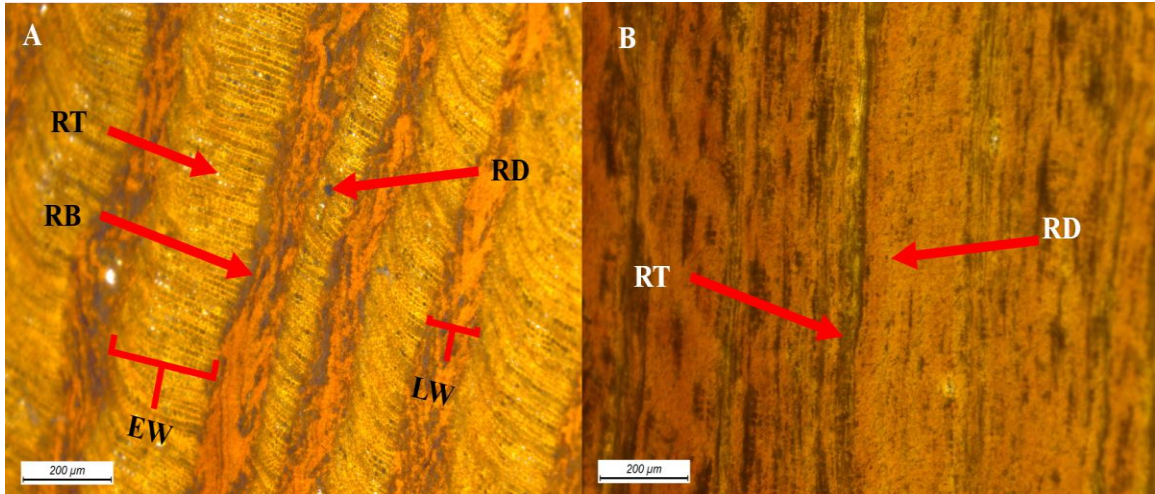


Figure 3.2 Wood sample C (AC-77-C3). Wood compressed. (A) Transverse thin-section of tree-rings, showing prominent growth rings with a sharp transition from large earlywood cells to latewood cells; and (B) Tangential thin-section of tree-rings. EW = early-wood; LW = late-wood; RB = ring boundary; RD = resin duct; RT = ray tracheid.

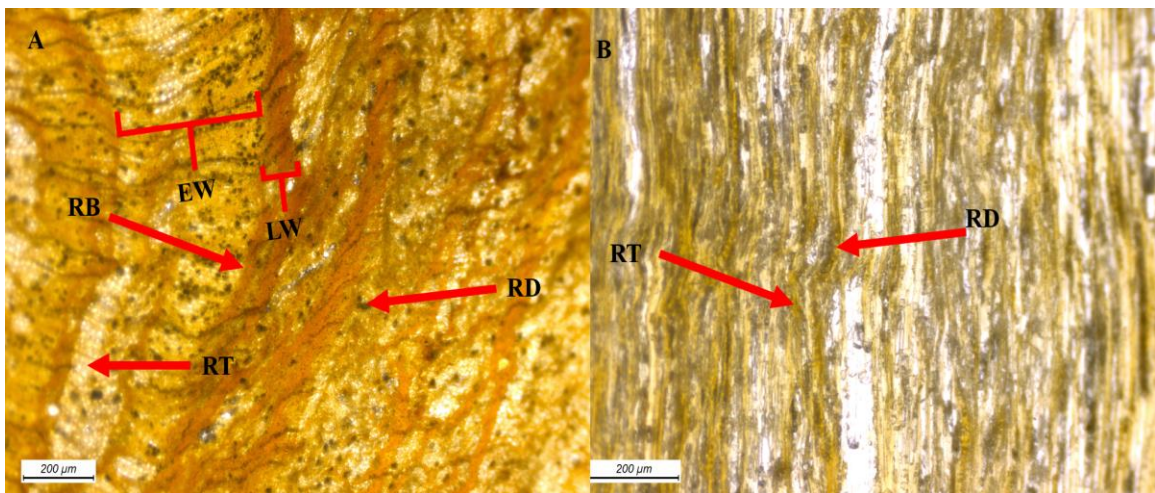


Figure 3.3 Wood sample D (AC-77-D1). Wood not compressed. (A) Transverse thin-section of tree-rings, showing prominent growth rings with a sharp transition from large early-wood cells to late-wood cells; and (B) Tangential thin-section of tree rings. EW = early-wood; LW = latewood; RB = ring boundary; RD = resin duct.

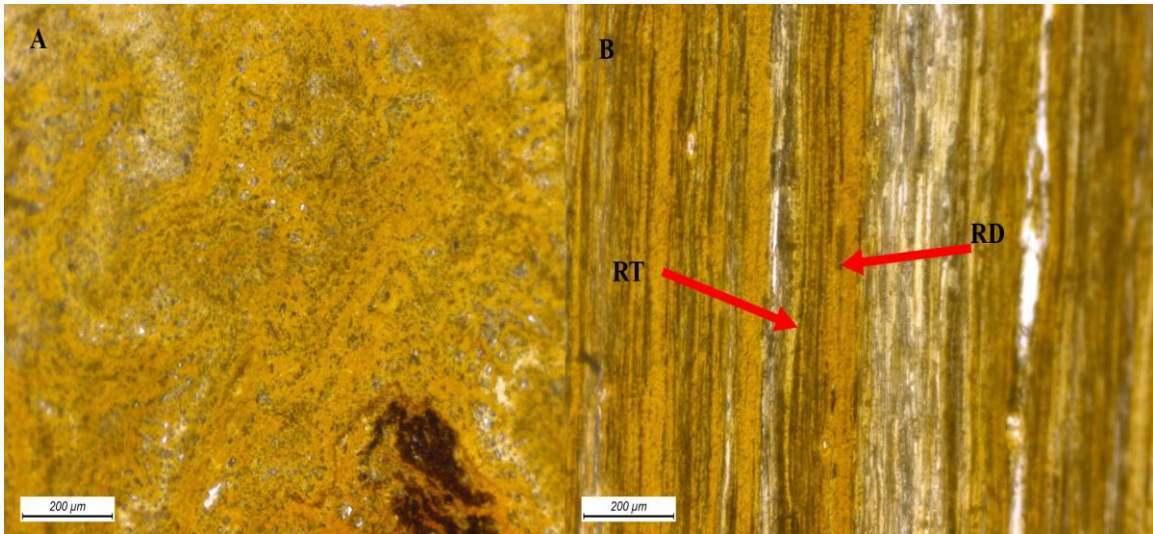


Figure 3.4 Wood sample E (AC-77-E3). Wood compressed. (A) Transverse thin-section tree-rings, not showing prominent growth rings with no sharp transition from large early-wood cells to late-wood cells; and (B) Tangential thin-section of tree-rings. RT = ray tracheid; RD = resin ducts.

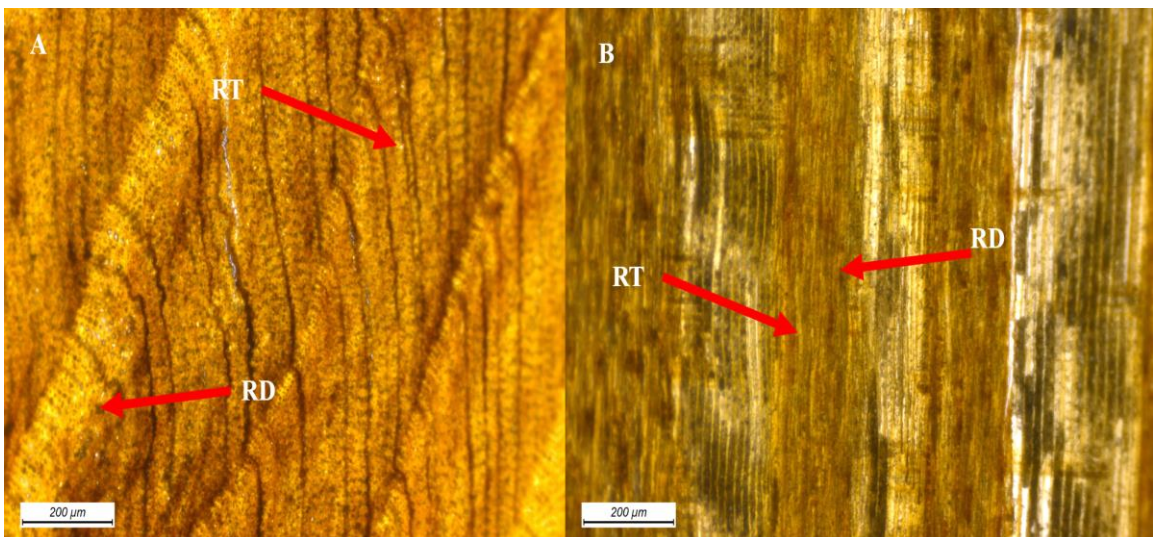


Figure 3.5 Wood sample F (AC-77-F1). Wood compressed. (A) Transverse thin-section tree-rings, inadequate to show prominent growth rings with no sharp transition from large early-wood cells to late-wood cells; and (B) Radial thin-section of tree-rings. RD = resin duct; RT = ray tracheid.

3.2 Tree-ring Widths, Stable Isotope and Radiocarbon Results

The tree ring widths (TRWs) and average $\delta^{18}\text{O}$ and $\delta^{13}\text{C}$ of early-wood and late-wood for all samples are reported in Appendix A. The radiocarbon dates for all samples are reported in Table 3.2.; all dates were infinite (^{14}C yr BP > 46,500).

Table 3.2 Radiocarbon dates for wood samples¹.

AA Lab #	Sample ID	Material	Radiocarbon age (^{14}C -year)	Calibrated age (cal year BP)
UOC-7090	AC-77-A-2	wood	>46500	n/a ²
UOC-7092	AC-77-C-3	wood	>46500	n/a ²
UOC-7093	AC-77-D-1	wood	>46500	n/a ²
UOC-7094	AC-77-E-3	wood	>46500	n/a ²
UOC-7095	AC-77-F-1	wood	>46500	n/a ²

¹Dates obtained at the University of Ottawa A.E. Lalonde AMS Laboratory in Ottawa, ON, Canada.

²Infinite age

3.2.1 Sample AC-77-A2

A total of 96 sub-samples of early (48) and late (48) wood were collected from this sample (Appendix A). The tree-ring widths (TRW) of early-wood and late-wood ranged from 120-684 μm and 20-185 μm , respectively. The TRW of the full tree-ring ranged from 191-771 μm .

Cellulose was extracted from a subset of 26 early-wood and 25 late-wood tree-ring sub-samples. The other sub-samples were too small (<0.5 mg) for cellulose extraction. The $\delta^{18}\text{O}$ and $\delta^{13}\text{C}$ of early-wood cellulose ranged from +22.8 to +27.6 ‰ (average = +25.6 ‰) and -23.0 to -21.2 ‰ (average = -22.4 ‰), respectively (Table 3.3). The $\delta^{18}\text{O}$ and $\delta^{13}\text{C}$ of late-wood cellulose ranged from +23.7 to +27.8 ‰ (average = +25.8 ‰) and -23.2 to -21.9 ‰ (average = -22.6 ‰) (Table 3.3). The calculated, weighted values of $\delta^{18}\text{O}$ and $\delta^{13}\text{C}$ for whole-ring cellulose ranged from +23.0 to +27.4 ‰ (average = +25.6 ‰) and -23.0 to -21.4 ‰ (average = -22.4 ‰) (Table 3.3).

The results of all statistical comparisons are summarized in Table 3.5, with significance defined as $p \leq 0.05$. The $\delta^{18}\text{O}$ and $\delta^{13}\text{C}$ of early-wood cellulose were not significantly different from late-wood cellulose ($p = 0.45$ and $p = 0.16$, respectively). Next, we compared ‘young’ (represented by ring # ≤ 20) versus ‘old’ (represented by ring # > 20) in order to detect any significant difference in isotopic compositions between growth age of the tree-ring. The $\delta^{18}\text{O}$ of cellulose from rings formed earlier in life (‘young’; ring # ≤ 20) of early and late-wood were not significantly different from cellulose from older rings (ring # > 20) of early and late-wood ($p = 0.06$, $p = 0.06$, respectively). The $\delta^{13}\text{C}$ of young late-wood cellulose was not significantly different ($p = 0.08$) from older late-wood cellulose. The $\delta^{13}\text{C}$ of young early-wood cellulose, however, was significantly higher ($p = 0.0004$) than older early-wood cellulose.

Annual, 3-year and 5-year running averages of the isotopic results for each of early, late, and whole tree-ring cellulose sub-samples are illustrated in Figures 3.1 ($\delta^{18}\text{O}$) and 3.2 ($\delta^{13}\text{C}$). The $\delta^{18}\text{O}$ of the cellulose increased at first as the tree grew, but for tree-rings formed later in life $\delta^{18}\text{O}$ began to decrease (Figure 3.6). The 5-year running average of $\delta^{18}\text{O}$ for all tree-rings increased from young rings (#12), peaked at ring #25 and then decreased thereafter. By comparison, the $\delta^{13}\text{C}$ of all tree-ring cellulose (early, late, calculated whole ring) trended to lower values from earliest to latest growth (Figure 3.7). Of all comparisons, the 5-year running averages of $\delta^{13}\text{C}$ in early-wood cellulose showed the most linear response and produced the strongest coefficient of determination ($r^2 = 0.94$). There were no significant correlations between $\delta^{18}\text{O}$ and $\delta^{13}\text{C}$ for early-wood, late-wood or calculated whole-ring cellulose (Figure 3.8).

Table 3.3 Minimum, maximum and mean values of subfossil wood stable carbon- and oxygen-isotope compositions.

Sample ID	$\delta^{18}\text{O}$ (‰) minimum	$\delta^{18}\text{O}$ (‰) maximum	average (‰)	$\Delta^{18}\text{O}_{\text{maximum-}}minimum$ (‰)	$\delta^{13}\text{C}$ (‰) minimum	$\delta^{13}\text{C}$ (‰) maximum	average (‰)	$\Delta^{13}\text{C}_{\text{maximum-}}minimum$ (‰)
AC-77-A2 EW ¹	+22.8	+27.6	+25.6	4.8	-23.0	-21.2	-22.4	1.8
AC-77-A2 LW	+23.7	+27.8	+25.8	4.1	-23.2	-21.9	-22.6	1.3
AC-77-A2 WR	+23.0	+27.4	+25.6	4.4	-23.0	-21.4	-22.4	1.6
AC-77-C3 EW	+23.3	+26.7	+25.0	3.4	-22.9	-21.1	-22.0	1.9
AC-77-C3 LW	+21.4	+26.7	+24.9	5.3	-23.3	-21.4	-22.3	1.9
AC-77-C3 WR	+23.4	+26.6	+24.9	3.1	-23.1	-21.4	-22.1	1.7
AC-77-D1 EW	+23.9	+26.6	+25.0	2.7	-22.6	-21.7	-22.2	0.9
AC-77-D1 LW	+23.2	+27.1	+24.7	3.8	-22.9	-21.3	-22.1	1.6
AC-77-D1 WR	+23.8	+26.8	+25.0	2.9	-22.6	-21.7	-22.1	0.9
AC-77-E3 EW	+24.6	+29.5	+26.3	4.9	-23.8	-20.6	-22.5	3.2
AC-77-E3 LW	+24.4	+29.2	+26.1	4.8	-23.5	-19.9	-22.2	3.6
AC-77-E3 WR	+25.0	+29.3	+26.4	4.4	-23.6	-20.9	-22.4	2.7
AC-77-F1 EW	+22.4	+27.0	+25.1	4.6	-25.1	-22.9	-24.0	2.2
AC-77-F1 LW	+23.1	+26.2	+24.9	3.0	-25.2	-23.2	-24.1	2.0
AC-77-F1 WR	+24.4	+26.8	+25.2	2.4	-25.0	-23.0	-23.9	2.0

¹ EW = early-wood; LW = late-wood; WR = whole-ring

Table 3.4 Summary of p-values (t-test) for tree-ring cellulose stable carbon- and oxygen-isotope compositions. Values of $p \leq 0.05$ are shown in bold font.

Sample:	AC-77-A2		AC-77-C3		AC-77-D1		AC-77-E3		AC-77-F1	
Analyses	p values for $\delta^{18}\text{O}$	p values for $\delta^{13}\text{C}$	p values for $\delta^{18}\text{O}$	p values for $\delta^{13}\text{C}$	p values for $\delta^{18}\text{O}$	p values for $\delta^{13}\text{C}$	p values for $\delta^{18}\text{O}$	p values for $\delta^{13}\text{C}$	p values for $\delta^{18}\text{O}$	p values for $\delta^{13}\text{C}$
¹ EW vs LW	0.45	0.16	0.54	0.18	0.29	0.67	0.61	0.47	0.39	0.84
EW _(young) vs EW _(old)	0.06	0.001	0.006	0.001	0.92	0.06	0.04	< 0.001	0.12	0.002
LW _(young) vs LW _(old)	0.06	0.08	0.55	0.02	0.97	0.09	0.02	< 0.001	0.07	< 0.001

¹ EW = early-wood; LW = late-wood

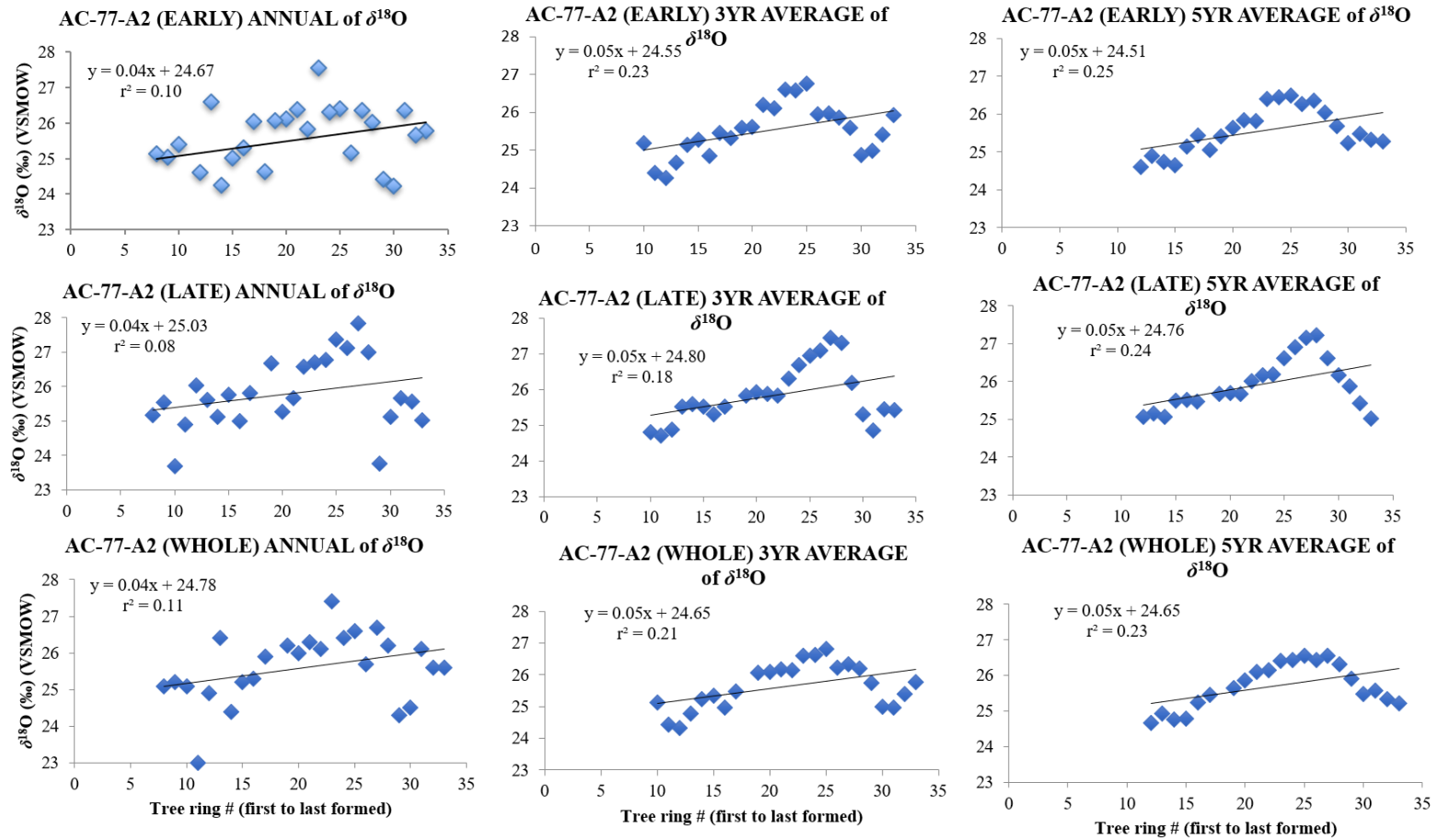


Figure 3.6 $\delta^{18}\text{O}$ versus tree-ring number for sample AC-77-A2 for early-, late-, and whole-ring cellulose, as calculated annually, and for 3-year and 5-year running averages.

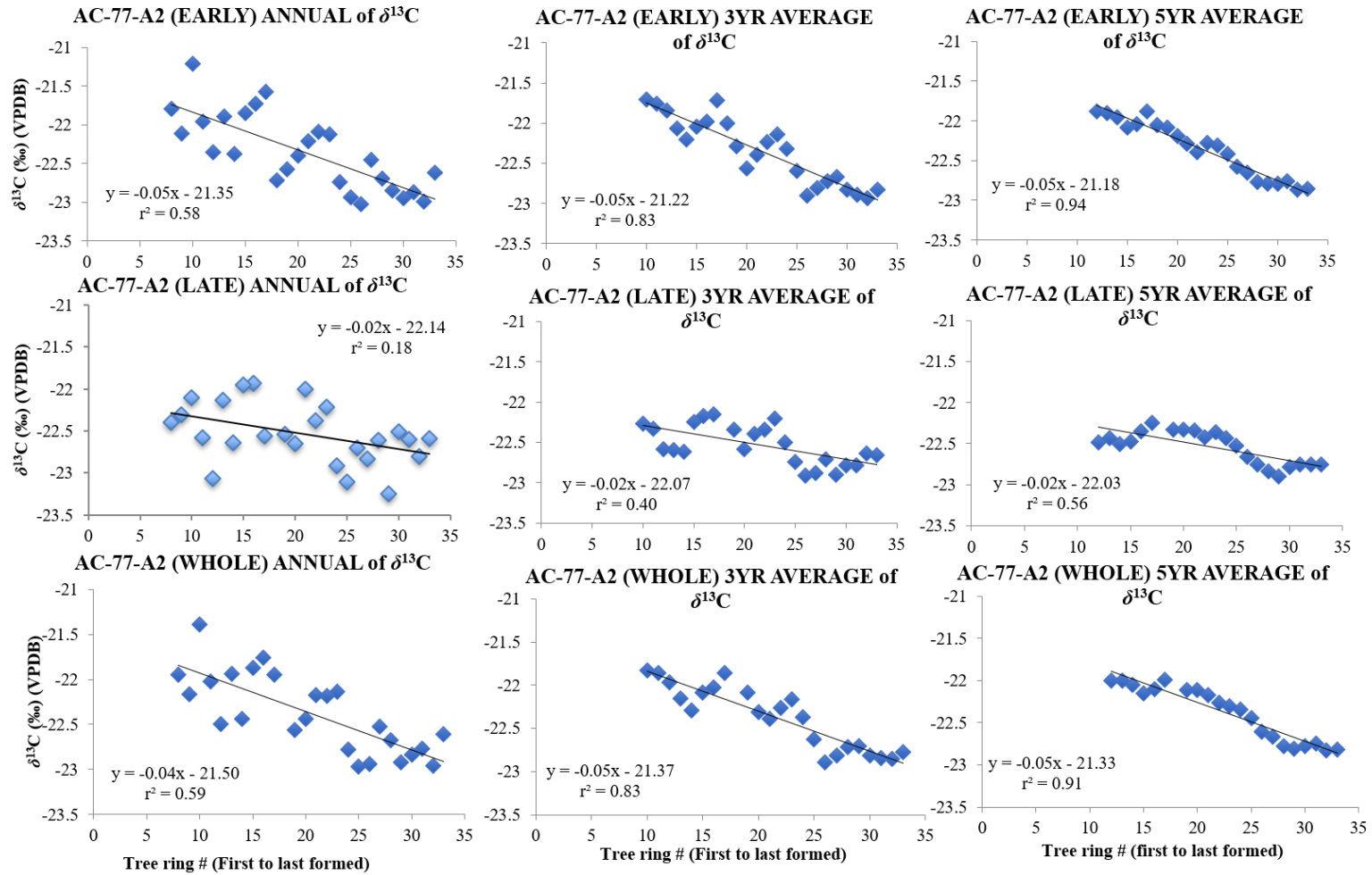


Figure 3.7 $\delta^{13}\text{C}$ versus tree-ring number for sample AC-77-A2 for early-, late-, and whole-ring cellulose, as calculated annually, and for 3-year and 5-year running averages.

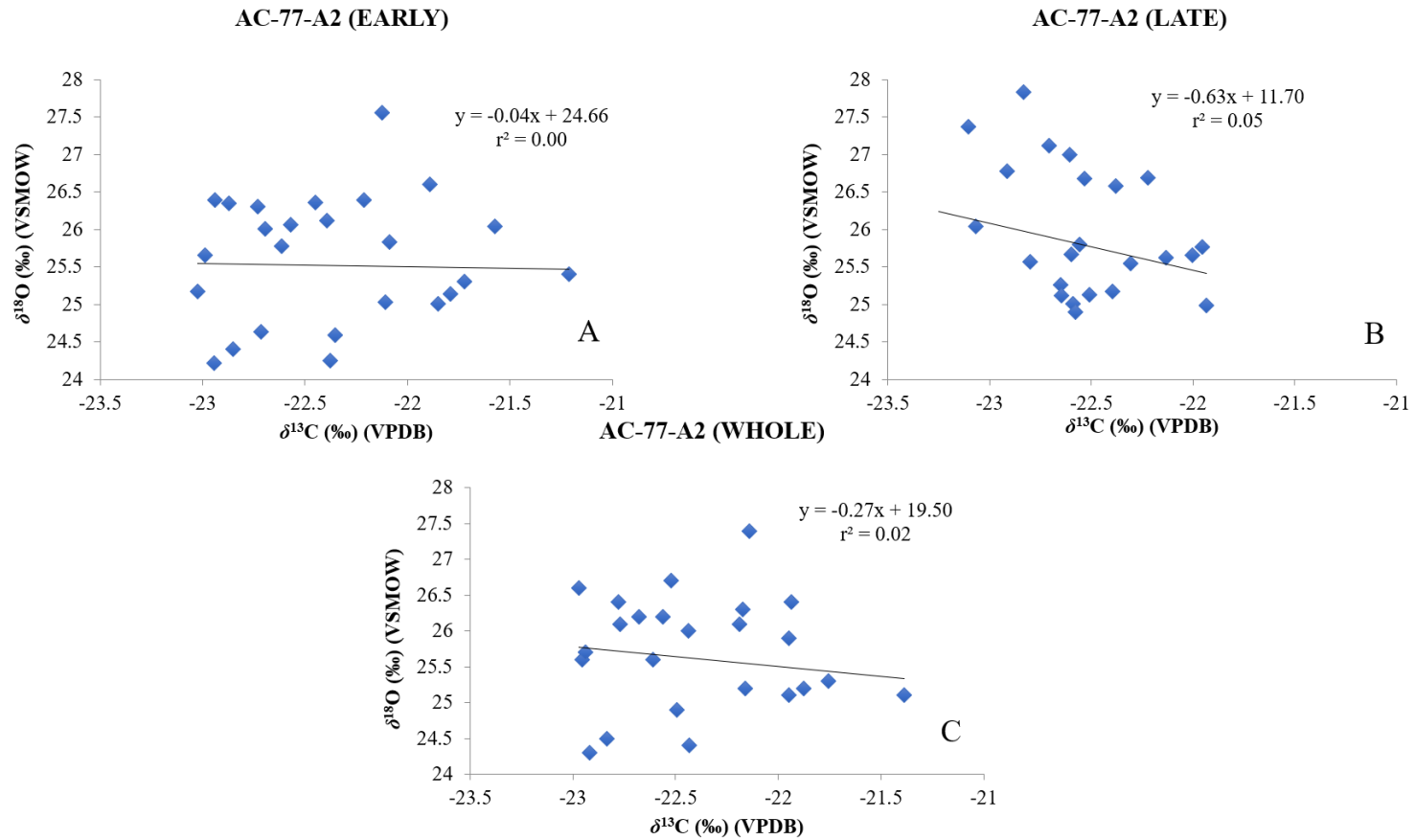


Figure 3.8 Correlation between $\delta^{18}\text{O}$ (‰) (VSMOW) and $\delta^{13}\text{C}$ (‰) (VPDB) for: (A) early-wood cellulose, (B) late-wood cellulose, and (C) calculated whole-wood cellulose for sample AC-77-A2.

3.2.2 Sample AC-77-C3

A total of 58 sub-samples of early (29) and late (29) wood were collected from this sample (Appendix A). The TRW of early-wood and late-wood ranged from 15-295 μm and 30-138 μm , respectively (Appendix A). The TRW of the full tree-ring ranged from 74-395 μm (Appendix A).

Because of sample amount limitations, cellulose was only extracted from a subset of 17 early-wood and 20 late-wood tree-ring sub-samples. The $\delta^{18}\text{O}$ and $\delta^{13}\text{C}$ of early-wood cellulose ranged from +23.3 to +26.7 ‰ (average = +25.0 ‰) and -22.9 to -21.1 ‰ (average = -22.0 ‰), respectively (Table 3.3). The $\delta^{18}\text{O}$ and $\delta^{13}\text{C}$ of late-wood cellulose ranged from +21.4 to +26.7 ‰ (average = +24.9 ‰) and -23.3 to -21.4 ‰ (average = -22.3 ‰), respectively (Table 3.3). The calculated, weighted $\delta^{18}\text{O}$ and $\delta^{13}\text{C}$ for whole-ring cellulose ranged from +23.4 to +26.6 ‰ (average = +24.9 ‰) and -23.1 to -21.4 ‰ (average = -22.1 ‰), respectively (Table 3.3).

The $\delta^{18}\text{O}$ and $\delta^{13}\text{C}$ of early-wood cellulose were not significantly different from late-wood cellulose ($p = 0.54$ and $p = 0.18$, respectively; Table 3.4). The $\delta^{18}\text{O}$ of young, late-wood cellulose (ring # ≤ 10) was not significantly different from that of cellulose in rings formed at a later time (ring # > 10) ($p = 0.55$; Table 3.4). The $\delta^{18}\text{O}$ of young rings from early-wood cellulose, however, were significantly lower than for rings formed at a later time ($p = 0.006$) (Table 3.4). The $\delta^{13}\text{C}$ of young rings (ring # ≤ 10) from early-wood cellulose and from late-wood cellulose were significantly higher than for rings formed at a later time (ring # > 12) ($p = 0.001$ and $p = 0.02$, respectively; Table 3.4).

Early-wood cellulose $\delta^{18}\text{O}$ increased (Figure 3.9) and both early-wood and late-wood $\delta^{13}\text{C}$ (Figure 3.10) decreased with continued growth of the tree. The 5-year running averages of both $\delta^{18}\text{O}$ and $\delta^{13}\text{C}$ for early-wood cellulose produced higher correlations with year of growth ($r^2 = 0.78$ and $r^2 = 0.89$, respectively) than annual or 3-year running averages. Late-wood cellulose $\delta^{18}\text{O}$ showed little correlation with year of tree-ring formation (Figure 3.11). Late-wood cellulose $\delta^{13}\text{C}$ decreased sharply beginning at about tree-ring #15.

Overall, there were no statistically significant correlations between $\delta^{18}\text{O}$ and $\delta^{13}\text{C}$ for early-wood, late-wood or calculated whole-ring cellulose (Figure 3.11).

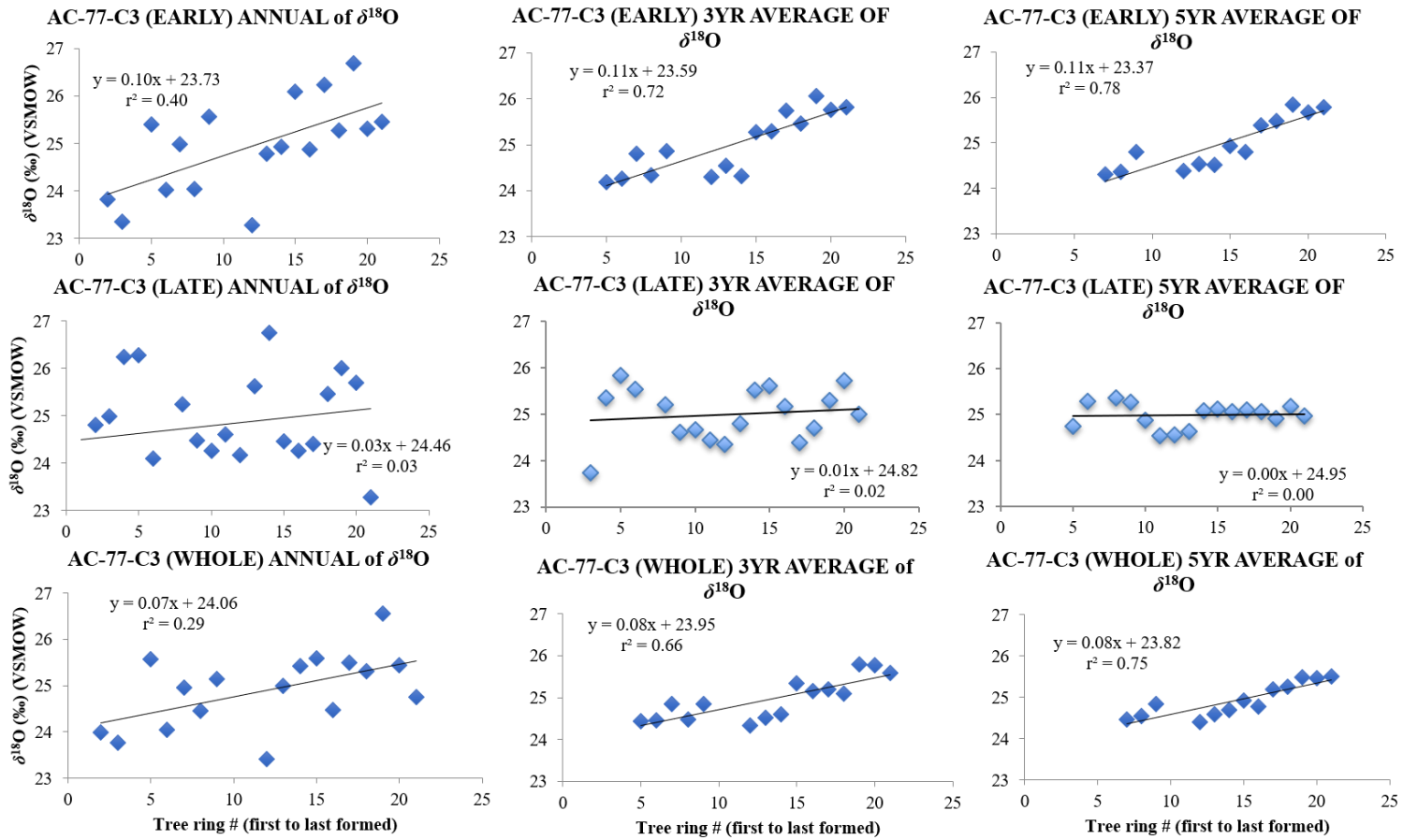


Figure 3.9 $\delta^{18}\text{O}$ versus tree-ring number for sample AC-77-C3 for early-, late-, and whole-ring cellulose, as calculated annually, and for 3-year and 5-year running averages.

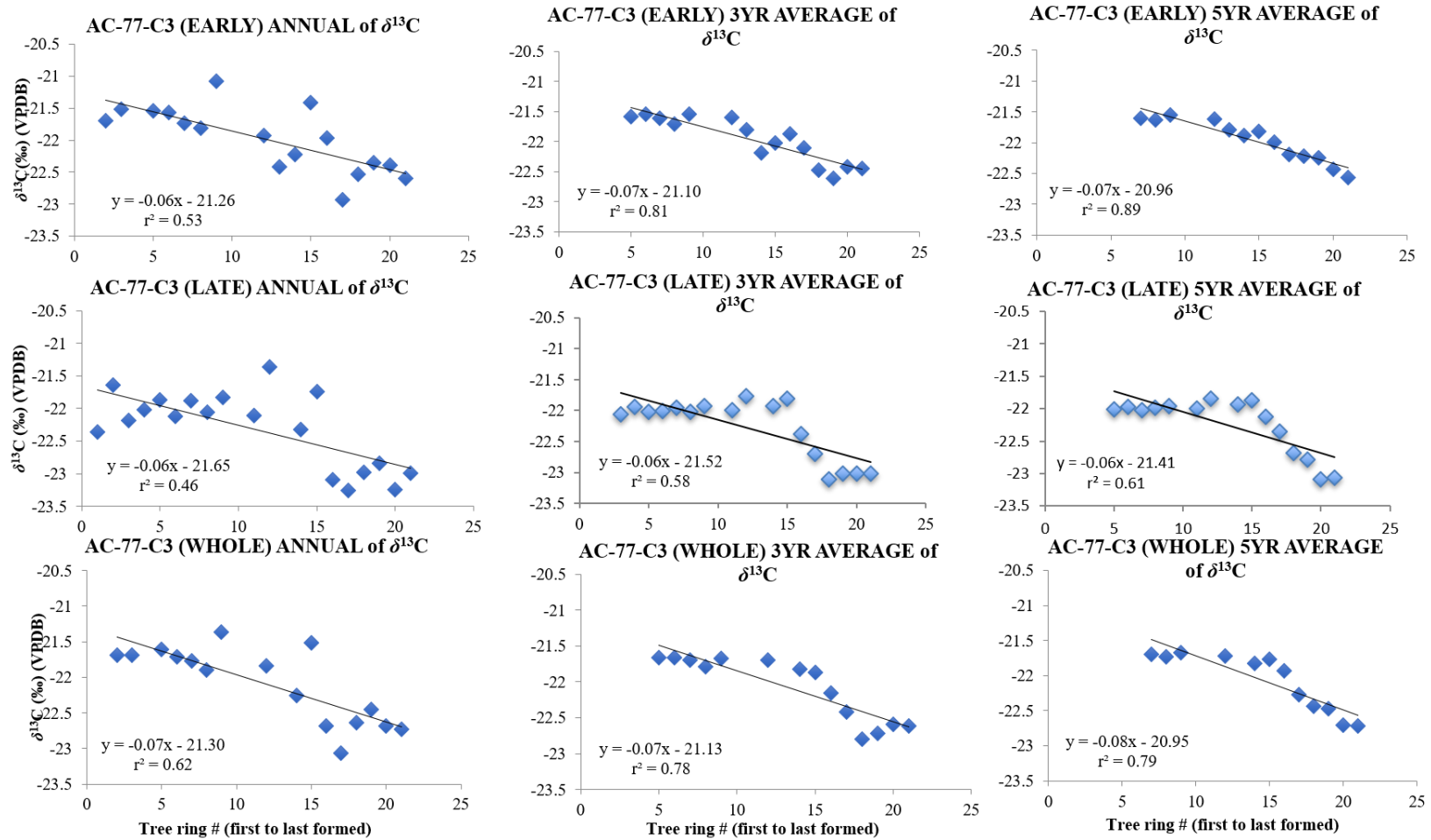


Figure 3.10 $\delta^{13}\text{C}$ versus tree ring-number for sample AC-77-C3 for early-, late-, and whole-ring cellulose, as calculated annually, and for 3-year and 5-year running averages.

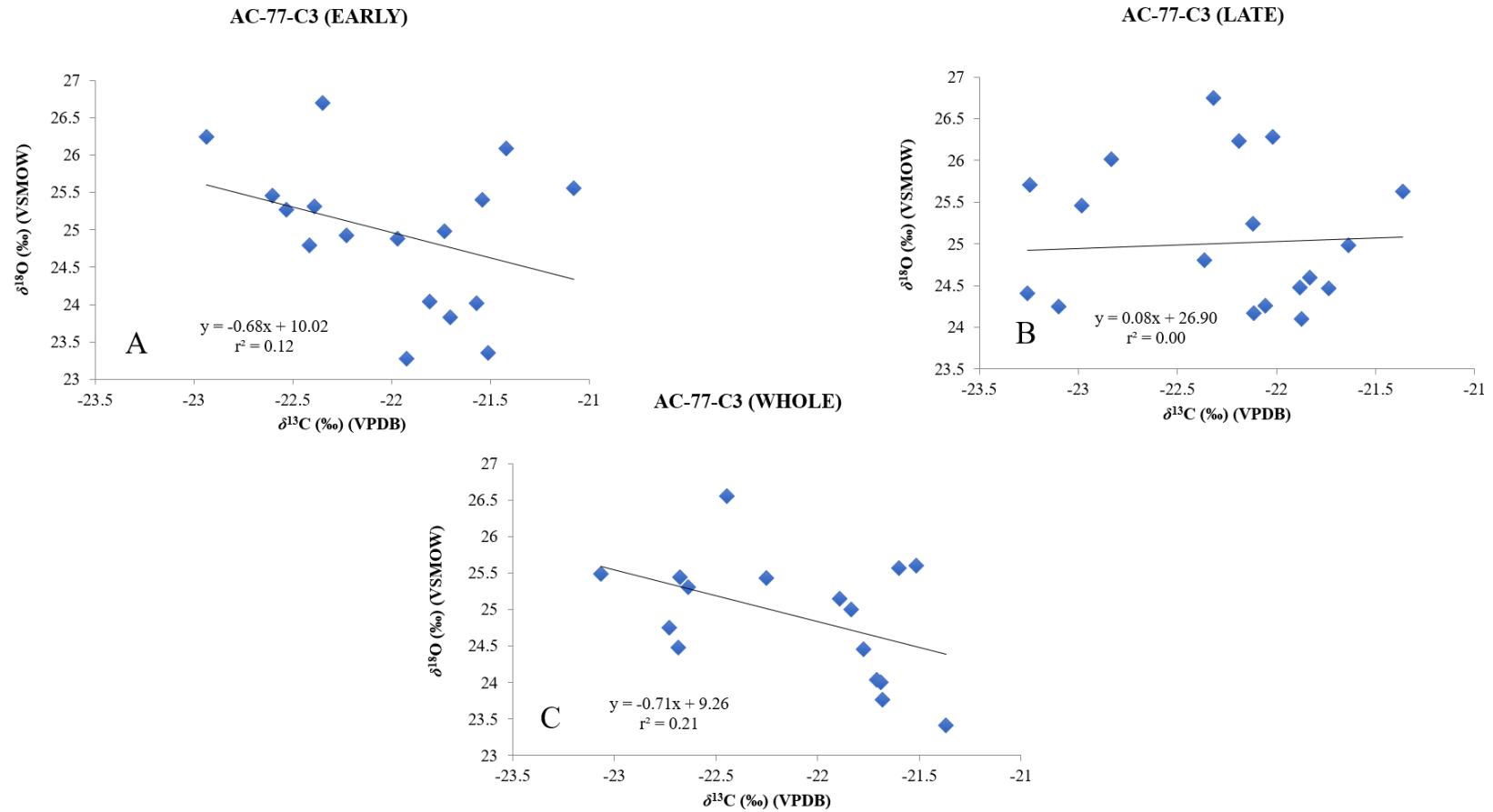


Figure 3.11 Correlation between $\delta^{18}\text{O}$ (‰) (VSMOW) and $\delta^{13}\text{C}$ (‰) (VPDB) for: (A) early-wood cellulose, (B) late-wood cellulose, and (C) calculated whole-wood cellulose for sample AC-77-C3.

3.2.3 Sample AC-77-D1

A total of 42 sub-samples of early (21) and late-wood (21) were collected from this sample (Appendix A). The TRW of early-wood and late-wood ranged from 45-343 μm and 5-189 μm , respectively (Appendix A). The TRW of the full tree ring ranged from 128 -377 μm (Appendix A).

Because of sample amount limitations, cellulose was only extracted from a subset of 16 early-wood and 18 late-wood tree-ring sub-samples. The $\delta^{18}\text{O}$ and $\delta^{13}\text{C}$ of early-wood cellulose ranged from +23.9 to +26.6 ‰ (average = +25.0 ‰) and -22.6 to -21.7 ‰ (average = -22.2 ‰), respectively (Table 3.3). The $\delta^{18}\text{O}$ and $\delta^{13}\text{C}$ of late-wood cellulose ranged from +23.2 to +27.1 ‰ (average = +24.7 ‰) and -22.9 to -21.3 ‰ (average = -22.1 ‰), respectively (Table 3.3). The calculated, weighted $\delta^{18}\text{O}$ and $\delta^{13}\text{C}$ for whole tree-ring cellulose ranged from +23.8 to +26.8 ‰ (average = +25.0 ‰) and -22.6 to -21.7 ‰ (average -22.1 ‰), respectively (Table 3.3).

The $\delta^{18}\text{O}$ and $\delta^{13}\text{C}$ of early-wood cellulose were not significantly different from late-wood cellulose ($p = 0.29$ and $p = 0.67$, respectively; Table 3.4). The $\delta^{18}\text{O}$ of young, early-wood and late-wood cellulose (ring # ≤ 10) were also not significantly different from that of cellulose in rings formed at a later time (ring # > 10) ($p = 0.92$ and $p = 0.97$, respectively; Table 3.4), as was also the case for $\delta^{13}\text{C}$ ($p = 0.06$ and $p = 0.09$ respectively; Table 3.4).

None of the annual, 3-year or 5-year running averages for cellulose $\delta^{18}\text{O}$ produced a linear coefficient of determination of note (Figure 3.12). Instead, a sinusoidal pattern is evident in all plots of $\delta^{18}\text{O}$ versus ring number. It is best expressed in the 5-year running average for early-wood, late-wood and full-ring, with a minimum beginning at ring #8 being followed by a maximum at ring #13 and then followed by a minimum at ring #19 (Figure 3.12). An overall weak trend towards lower $\delta^{13}\text{C}$ of tree-ring cellulose with increasing tree age is apparent in all diagrams shown on Figure 3.13, with the 5-year running average of $\delta^{13}\text{C}$ for full-ring cellulose producing the highest linear coefficient of determination ($r^2 = 0.59$). That said, this trend clearly resolves into a sinusoidal (rather than linear) pattern in the 3-year, and to a lesser extent, 5-year running averages (Figure 3.13). Overall, however,

there were no significant correlations between $\delta^{18}\text{O}$ and $\delta^{13}\text{C}$ for early-wood, late-wood or calculated whole tree-ring cellulose (Figure 3.14).

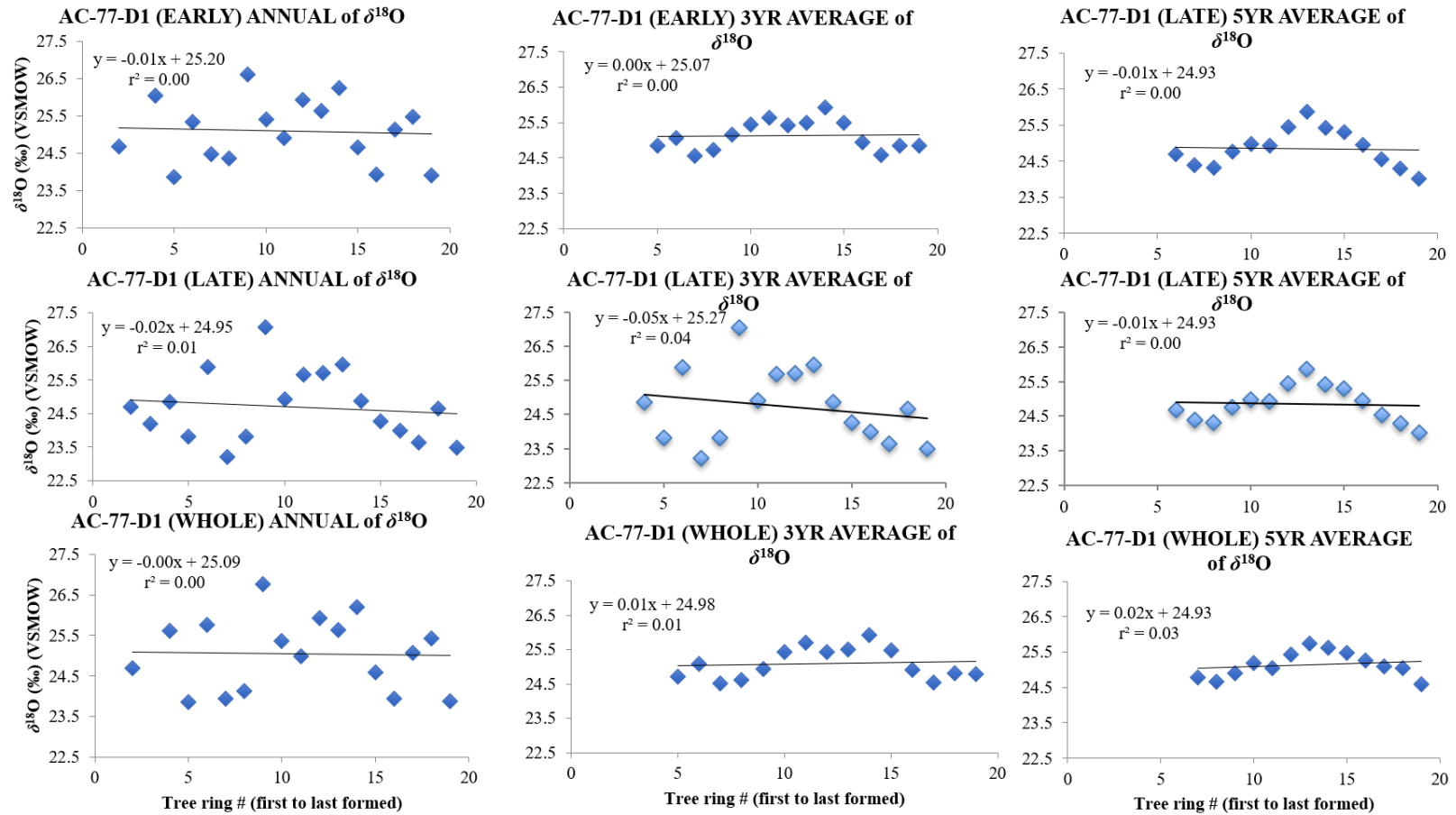


Figure 3.12 $\delta^{18}\text{O}$ versus tree-ring number for sample AC-77-D1 for early-, late-, and whole-ring cellulose, as calculated annually, and for 3-year and 5-year running averages.

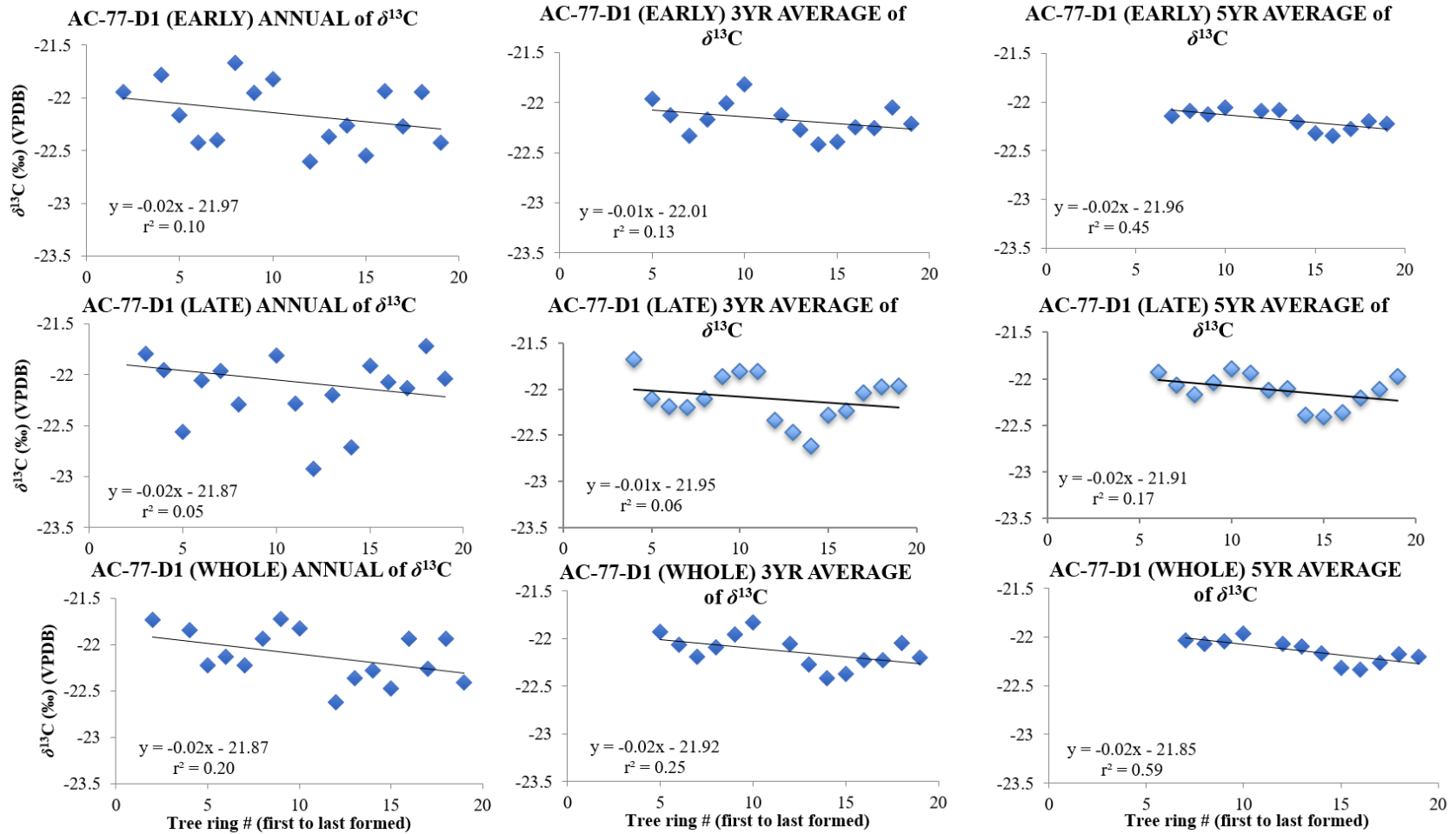


Figure 3.13 $\delta^{13}\text{C}$ versus tree-ring number for sample AC-77-D1 for early-, late-, and whole-ring cellulose, as calculated annually, and for 3-year and 5-year running averages.

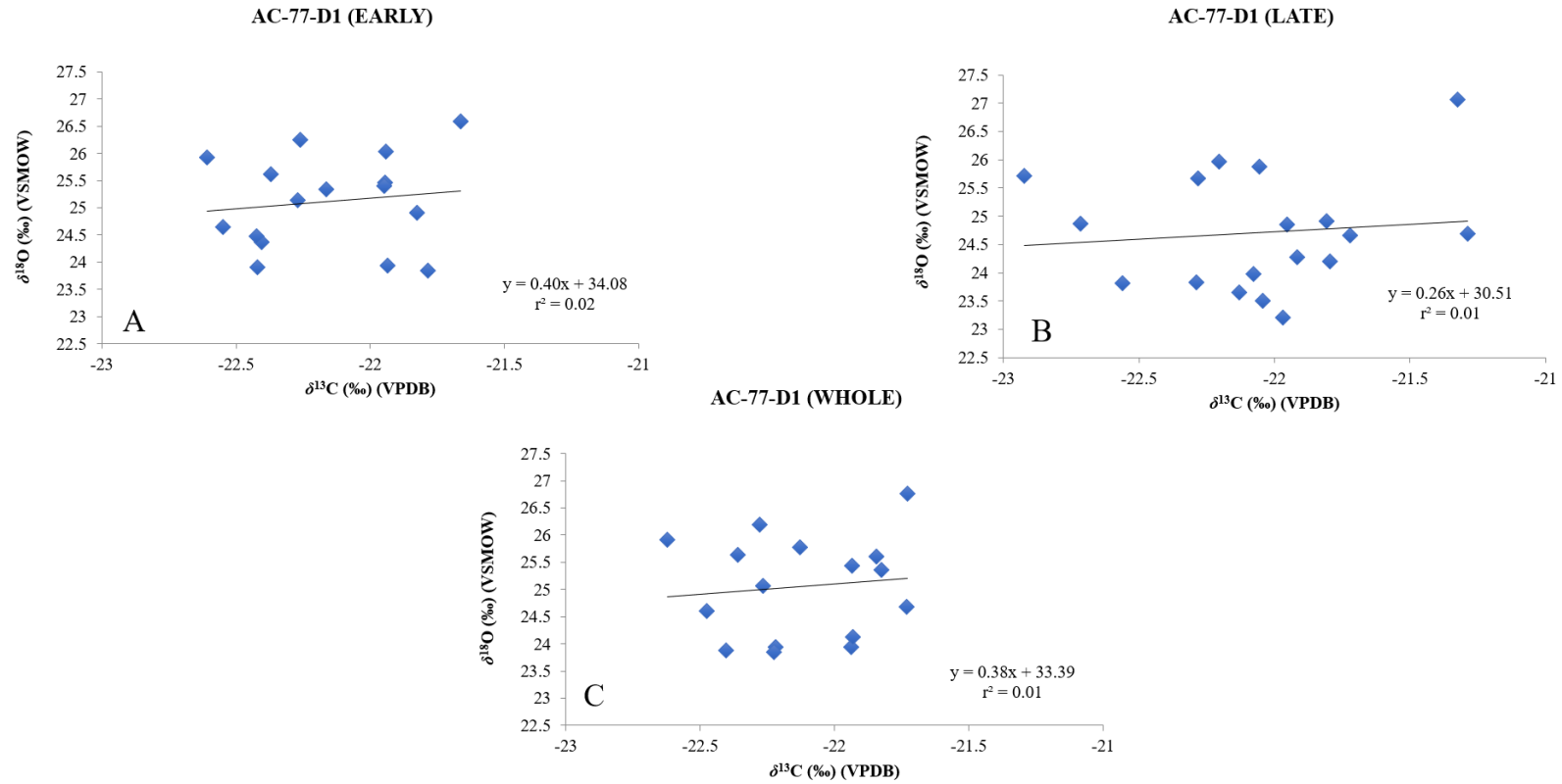


Figure 3.14 Correlation between $\delta^{18}\text{O}$ (‰) (VSMOW) and $\delta^{13}\text{C}$ (‰) (VPDB) for: (A) early-wood cellulose, (B) late-wood cellulose, and (C) calculated whole-wood cellulose for sample AC-77-D1.

3.2.4 Sample AC-77-E3

A total of 71 sub-samples of early (35) and late-wood (36) were collected from this sample (Appendix A). The TRW of early and late-wood ranged from 41-937 μm and 11-206 μm , respectively (Appendix A). The TRW of the full tree-ring ranged from 92-1022 μm (Appendix A).

Because of sample amount limitations, cellulose was only extracted from a subset of 12 early-wood and 17 late-wood tree-ring sub-samples. The $\delta^{18}\text{O}$ and $\delta^{13}\text{C}$ of early-wood cellulose ranged from +24.6 to +29.5 ‰ (average = +26.3 ‰) and -23.8 to -20.6 ‰ (average = -22.5 ‰), respectively (Table 3.3). The $\delta^{18}\text{O}$ and $\delta^{13}\text{C}$ of late-wood cellulose ranged from +24.4 to +29.2 ‰ (average = +26.1 ‰) and -23.5 ‰ to -19.9 ‰ (average = -22.2 ‰), respectively (Table 3.3). The calculated, weighted $\delta^{18}\text{O}$ and $\delta^{13}\text{C}$ for whole tree-ring cellulose ranged from +25.0 to +29.3 ‰ (average = +26.4 ‰) and -23.6 to -20.9 ‰ (average = -22.4 ‰), respectively (Table 3.3).

The $\delta^{18}\text{O}$ and $\delta^{13}\text{C}$ of early-wood cellulose were not significantly different from late-wood cellulose ($p = 0.61$ and $p = 0.47$, respectively; Table 3.4). Both early-wood and late-wood cellulose $\delta^{18}\text{O}$ of younger rings (ring # ≤ 12) were significantly higher than cellulose in rings formed at a later time (ring # > 12) ($p = 0.04$ and $p = 0.02$, respectively; Table 3.4). The result was similar for cellulose $\delta^{13}\text{C}$ ($p = 0.0004$ and $p = 0.00002$, respectively; Table 3.4).

The annual, 3-year and 5-year running averages for early-wood, late-wood and calculated whole tree-ring cellulose $\delta^{18}\text{O}$ all trend towards lower values with increasing age of the tree, with the 5-year running average producing the highest linear coefficient of determination ($r^2 = 0.71$ -0.83; Figure 3.15). The pattern is the same for cellulose $\delta^{13}\text{C}$ ($r^2 = 0.79$ -0.90 for 5-year running average; Figure 3.16). The $\delta^{18}\text{O}$ and $\delta^{13}\text{C}$ of both early-wood and late-wood cellulose showed a weak positive linear correlation ($r^2 = 0.43$ and $r^2 = 0.53$, respectively), with a stronger, positive correlation produced for the calculated whole tree-ring data ($r^2 = 0.81$) (Figure 3.17).

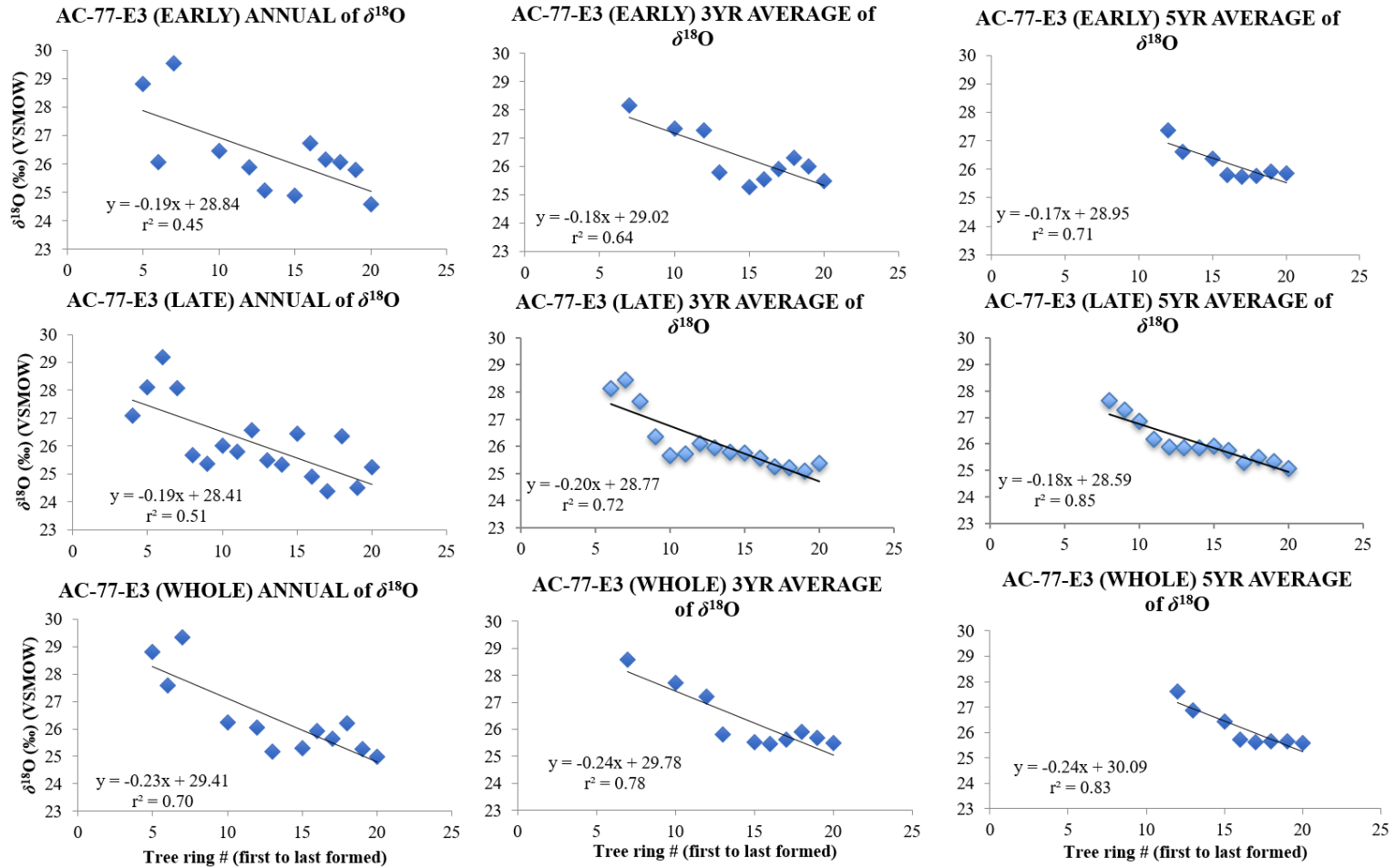


Figure 3.15 $\delta^{18}\text{O}$ versus tree-ring number for sample AC-77-E3 for early-, late-, and whole-ring cellulose, as calculated annually, and for 3-year and 5-year running averages.

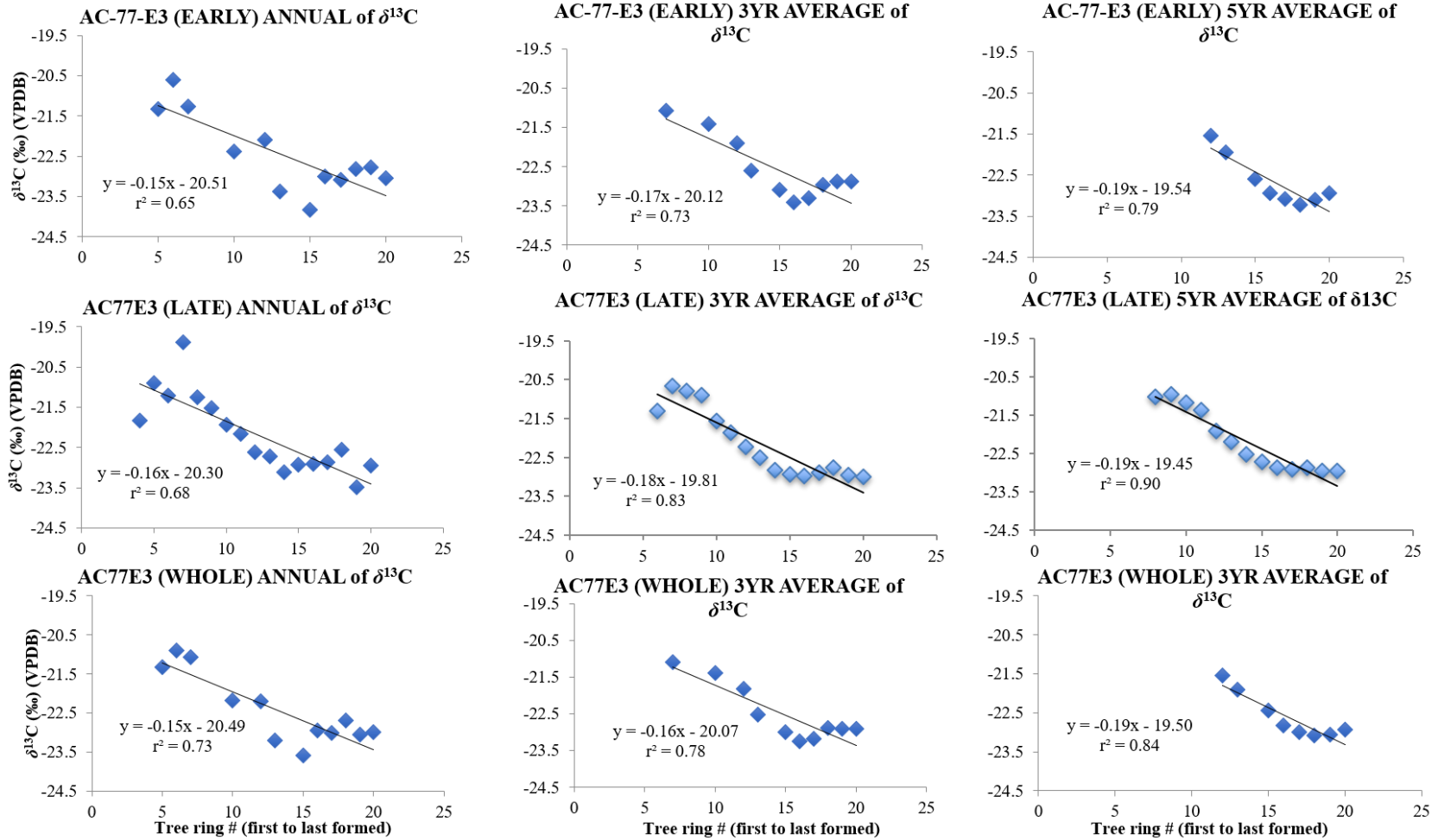


Figure 3.16 $\delta^{13}\text{C}$ versus tree-ring number for sample AC-77-E3 for early-, late-, and whole-ring cellulose, as calculated annually, and for 3-year and 5-year running averages.

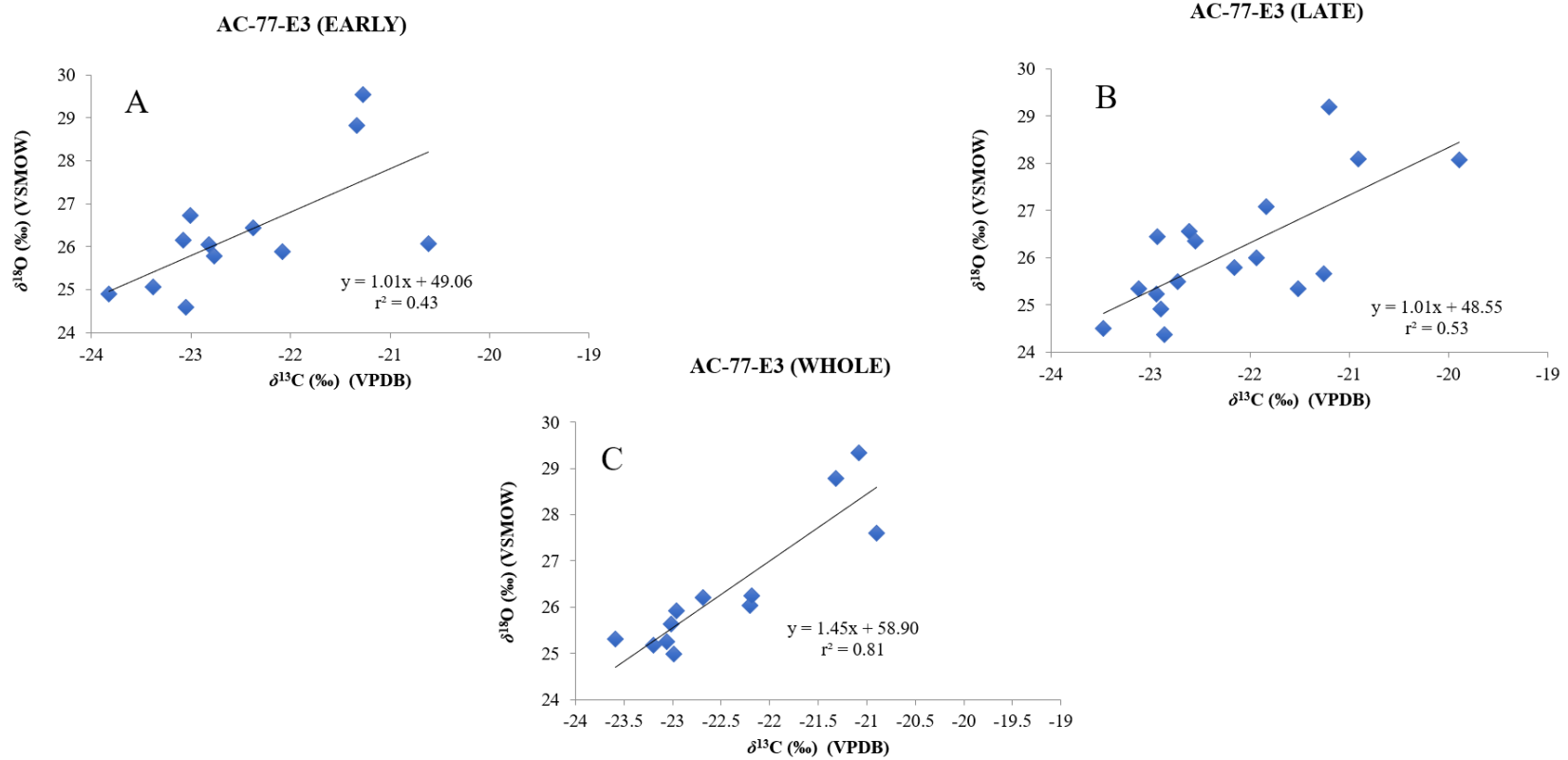


Figure 3.17 Correlation between $\delta^{18}\text{O}$ (‰) (VSMOW) and $\delta^{13}\text{C}$ (‰) (VPDB) for: (A) early-wood cellulose, (B) late-wood cellulose, and (C) calculated whole-wood cellulose for sample AC-77-E3.

3.2.5 Sample AC-77-F1

A total of 45 sub-samples of early (22) and late (23) wood were collected from this sample (Appendix A). The TRW of early-wood and late-wood ranged from 110-545 μm and 42-310 μm , respectively (Appendix A). The TRW of the full tree-ring ranged from 170-733 μm (Appendix A).

Because of sample amount limitations, cellulose was only extracted from a consecutive subset of 8 early-wood and 7 late-wood sub-samples. The $\delta^{18}\text{O}$ and $\delta^{13}\text{C}$ of early-wood cellulose ranged from +22.4 to +27.0 ‰ (average = +25.1 ‰) and -25.1 to -22.9 ‰ (average = -24.0 ‰), respectively (Table 3.3). The $\delta^{18}\text{O}$ and $\delta^{13}\text{C}$ of late-wood cellulose ranged from +23.1 to +26.2 ‰ (average = +24.9 ‰) and -25.2 ‰ to -23.2 ‰ (average = -24.1 ‰), respectively (Table 3.3). The calculated, weighted $\delta^{18}\text{O}$ and $\delta^{13}\text{C}$ for whole-ring cellulose ranged from +24.4 to +26.8 ‰ (average = +25.2 ‰) and -23.9 to -23.0 ‰ (average = -23.9 ‰), respectively (Table 3.3).

The $\delta^{18}\text{O}$ and $\delta^{13}\text{C}$ of early-wood cellulose were not significantly different from the late-wood cellulose ($p = 0.39$ and $p = 0.84$, respectively; Table 3.4). Both early-wood and late-wood cellulose $\delta^{18}\text{O}$ of younger rings (ring # ≤ 14) were not significantly different than later rings (ring # > 14) ($p = 0.12$ and $p = 0.07$, respectively; Table 3.4). The $\delta^{13}\text{C}$ of both young early-wood and young late-wood cellulose (ring # ≤ 14), however, were significantly lower than later-formed cellulose (ring # > 12) ($p = 0.002$ and $p = 0.00001$, respectively; Table 3.4).

The annual, 3-year and 5-year running averages for early-wood, late-wood and calculated whole-ring cellulose $\delta^{18}\text{O}$ and $\delta^{13}\text{C}$ all trend towards higher values with increasing age of the tree (Figures 3.18 and 3.19); the limited data, however, make the 3- and 5-year running averages increasingly unreliable. While the $\delta^{18}\text{O}$ and $\delta^{13}\text{C}$ of both early-wood and late-wood cellulose showed a weak positive linear coefficient of determination ($r^2 = 0.38$ and $r^2 = 0.43$, respectively), the small sample size and the clustering of data points makes this putative relationship unreliable. A somewhat stronger, positive linear coefficient of

determination is evident for the calculated whole tree-ring data ($r^2 = 0.62$), but still does not provide a good fit to the limited number of data points (Figure 3.20).

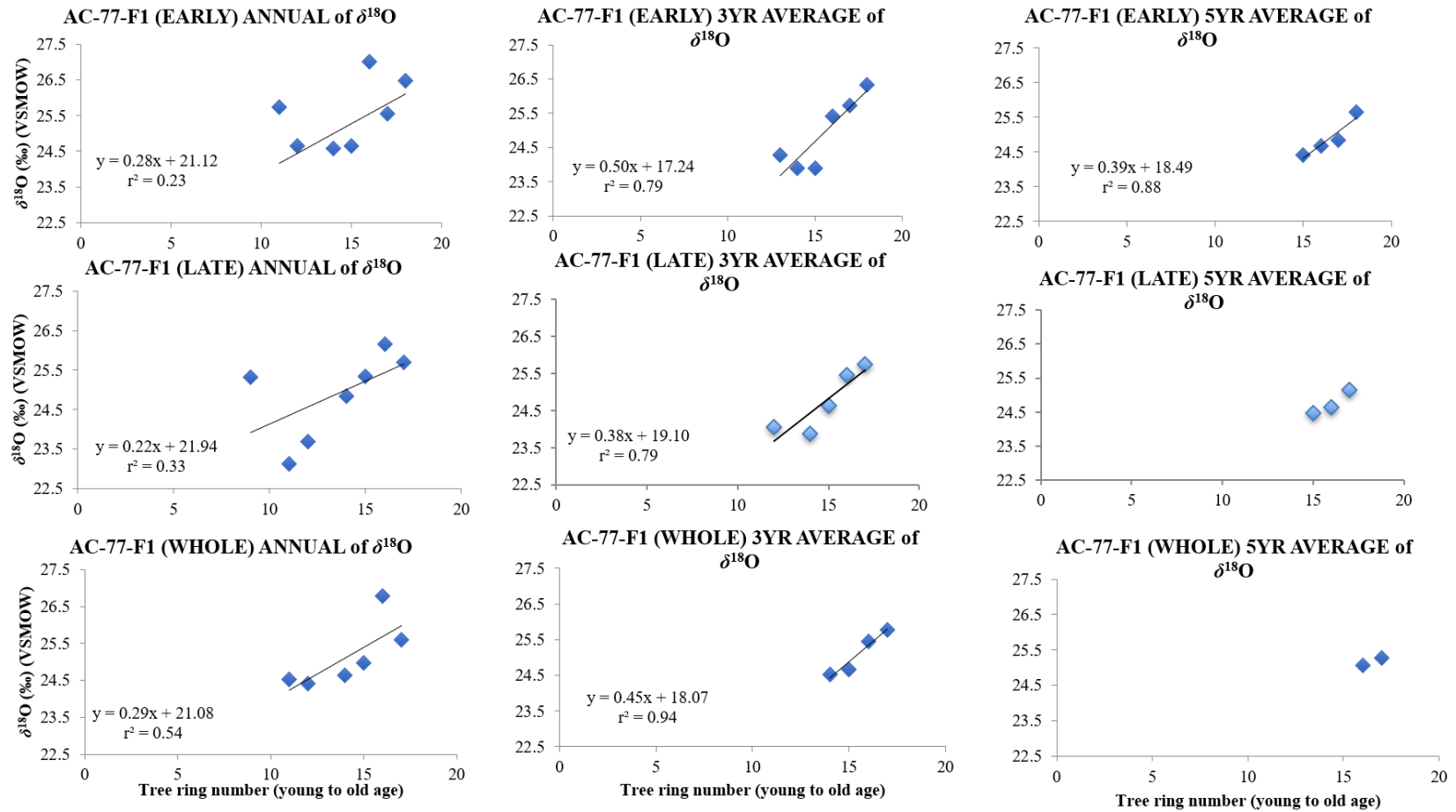


Figure 3.18 $\delta^{18}\text{O}$ versus tree-ring number for sample AC-77-F1 for early-, late-, and whole-ring cellulose, as calculated annually, and for 3-year and 5-year running averages.

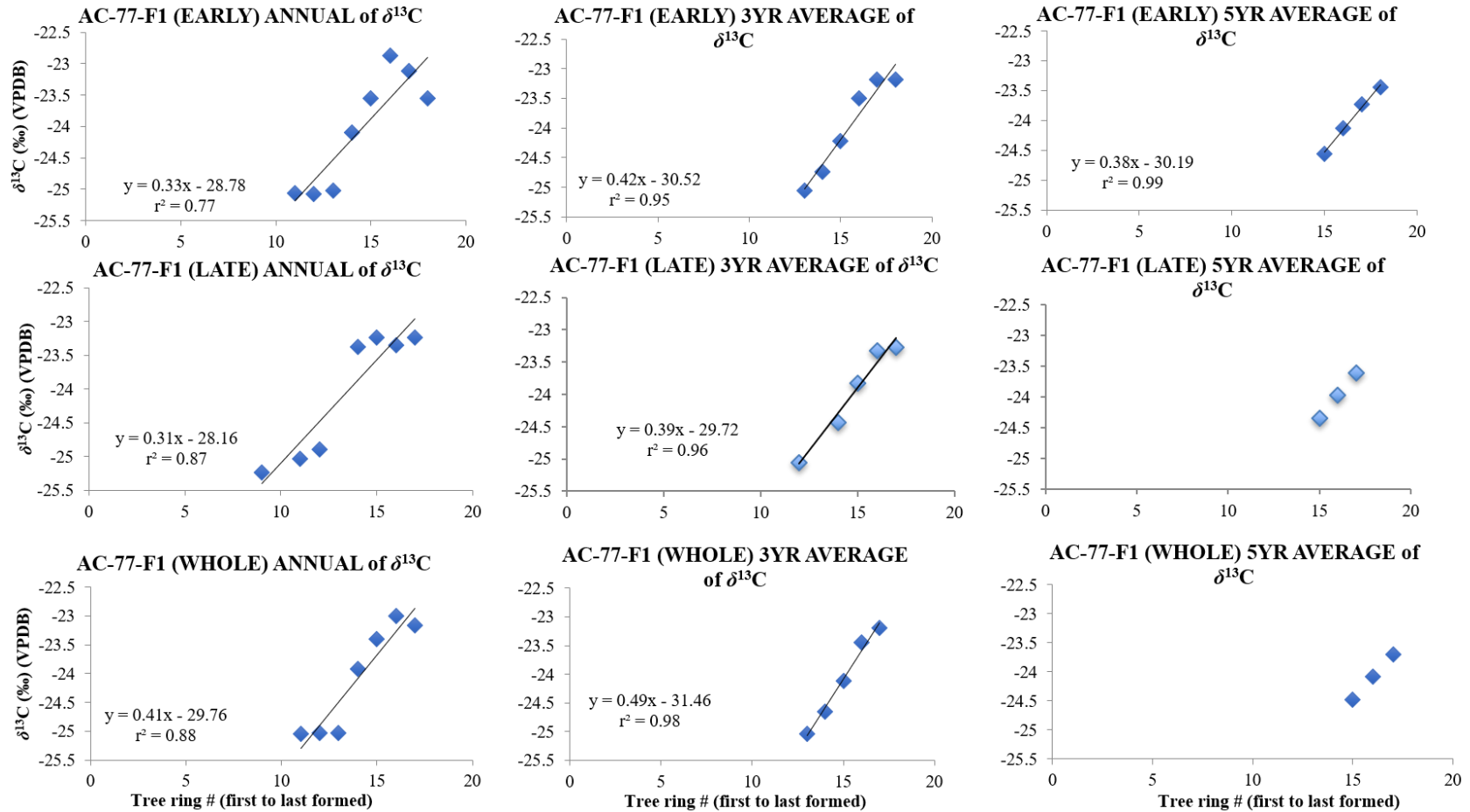


Figure 3.19 $\delta^{13}\text{C}$ versus tree-ring number for sample AC-77-F1 for early-, late-, and whole-ring cellulose, as calculated annually, and for 3-year and 5-year running averages.

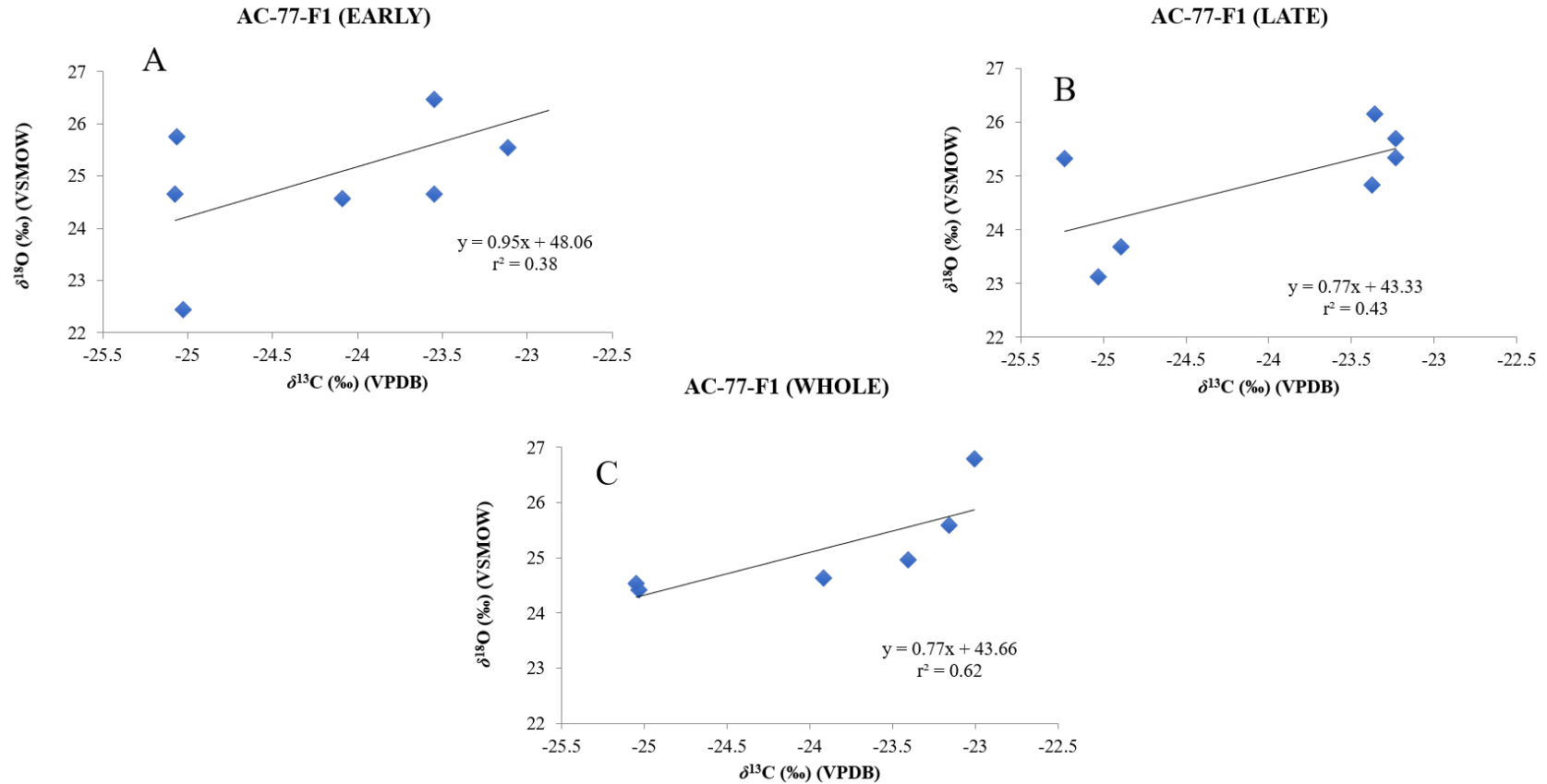


Figure 3.20 Correlation between $\delta^{18}\text{O}$ (‰) (VSMOW) and $\delta^{13}\text{C}$ (‰) (VPDB) for: (A) early-wood cellulose, (B) late-wood cellulose, and (C) calculated whole-wood cellulose for sample AC-77-F1.

Chapter 4

4 Discussion

The purpose of this study is to assess Quaternary interglacial or interstadial climate in an area that appears to have had similar vegetation as northern Ontario does today. To achieve this, we analyzed the stable carbon- and oxygen-isotope compositions of both early- and late-wood tree-ring cellulose from five sub-fossil tree samples collected from the Missinaibi Formation at Adam Creek, Ontario.

The samples produced infinite radiocarbon dates, which means that they are older than 46,500 radiocarbon years (^{14}C BP). As such, these samples could have grown during early Marine Isotope Stage (MIS) 3 (~57,000-29,000 ^{14}C BP) or MIS 5 (~130,000-71,000 ^{14}C BP) (Allard et al. 2012, Dalton et al. 2016, 2017, Miller and Andrews 2019), or perhaps even earlier. According to Miller and Andrews (2019), however, the Missinaibi Formation most likely developed during MIS 5a (peak of this interglacial substage occurred at ~82 kya; Lisiecki and Raymo 2005) because the James Bay Lowland, and hence the Adam Creek area, was not ice-free during MIS 3. Allard et al. (2012) also obtained U-Th dates for fossil wood from Missinaibi Formation in the Hudson Bay Lowland that are consistent with a MIS 5 rather than MIS 3 time-frame.

Whether the five tree samples examined in this thesis grew contemporaneously is not known. Skinner (1973), however, previously reported being able to collect wood only from the forest peat layer of the Missinaibi Formation at the Adam Creek site. Some trees observed were still in their growth position (Skinner 1973), indicating that this was a forest ecosystem and that the subfossil wood had not been transported from its original location. The samples available for analysis in the present study, however, were not in growth position, as demonstrated by radial, asymmetric compression of some trunks. A lack of detailed field notes for these samples, which were collected in 1977, makes it impossible to confirm that they were located together with *in situ* (growth position) sub-fossil wood or had been locally transported by water to their current position. The peat layer containing the sub-fossil wood is situated above fluvial sediments and below a lacustrine sediment. It

is also not possible to know whether the trees represented by these five samples grew at exactly the same time, but it is apparent that they grew in the same forest ecosystem because they were found together in the same formation.

Variations in the cellulose stable carbon- ($\delta^{13}\text{C}_{\text{cellulose}}$) and oxygen- ($\delta^{18}\text{O}_{\text{cellulose}}$) isotope compositions of the tree rings were commonly observed between early- and late-wood of the same tree ring, across the transect from the first to last formed tree-rings in the same sample, and among each of the five subfossil wood samples. These differences are attributed to variations in temperature, water availability, water source and micro-environment, as is discussed below.

4.1 Juvenile Effect

The $\delta^{13}\text{C}_{\text{cellulose}}$ formed during early life of a tree may be 1-2 ‰ lower than later in life (Freyer 1979, Anderson et al. 1998, Gagen et al. 2008). This feature is believed to occur because younger, shorter trees in a forested environment can experience what is known as the “canopy effect”. The CO_2 in the understory of a forest can have lower $\delta^{13}\text{C}$ because of the contribution from respired CO_2 , which is enriched in ^{12}C ; trees growing beneath the canopy can also have lower $\delta^{13}\text{C}$ because of reduced irradiance (Francey and Farquhar 1982, France 1996, Anderson et al. 1998). In addition, as a tree gains height, hydraulic conductivity in the trunk is reduced (McCarroll and Loader 2004, Gagen et al. 2007). This change causes reduction in stomatal conductivity, which leads to increases the $\delta^{13}\text{C}$ of cellulose in rings formed in more mature trees (Anderson et al. 1998).

Some researchers have reported a juvenile effect in the $\delta^{13}\text{C}_{\text{cellulose}}$ of tree-rings formed during the first 50 years of growth in coniferous trees (Freyer 1979, Anderson et al. 1998, Gagen et al. 2008, Daux et al. 2011, Duffy et al. 2017). Hence, care should be taken when making hydroclimatic interpretations of $\delta^{13}\text{C}_{\text{cellulose}}$ based on increases from juvenile to mature tree-rings. There is no known juvenile effect on the $\delta^{18}\text{O}$ of tree-ring cellulose, however (Anderson et al. 1998, Treydte et al. 2006, Liu et al. 2008, Xu et al. 2016, Duffy et al. 2017, Cai et al. 2018).

In this investigation, carbon isotope analysis was performed beginning at tree-ring # 2 to 11, depending on the sample. For samples AC-77-A2, AC-77-C3, AC-77-D1 and AC-77-E3, the calculated $\delta^{13}\text{C}$ of whole-ring cellulose decreased by 0.6 to 1.7 ‰ from the inner to the outer tree-rings (Table 4.1, Figure 4.1). The juvenile effect, however, might be masked in the calculated whole-ring $\delta^{13}\text{C}_{\text{cellulose}}$ because early-wood $\delta^{13}\text{C}_{\text{cellulose}}$ can reflect carbon from starches stored in the previous fall (Hill et al. 1995, Vaganov et al. 2009). Examination of late-wood $\delta^{13}\text{C}_{\text{cellulose}}$, however, also shows a pattern of decreasing values by 0.2 to 1.1 ‰ from inner to the outer tree-rings (Table 4.2). Hence, a juvenile effect is not apparent in these four samples. These samples varied in age from 23 to 54 years based on tree-ring accounts. Hence it is possible that a juvenile effect may not be apparent because these trees were still quite young. Alternatively, the samples may have been branches from taller trees.

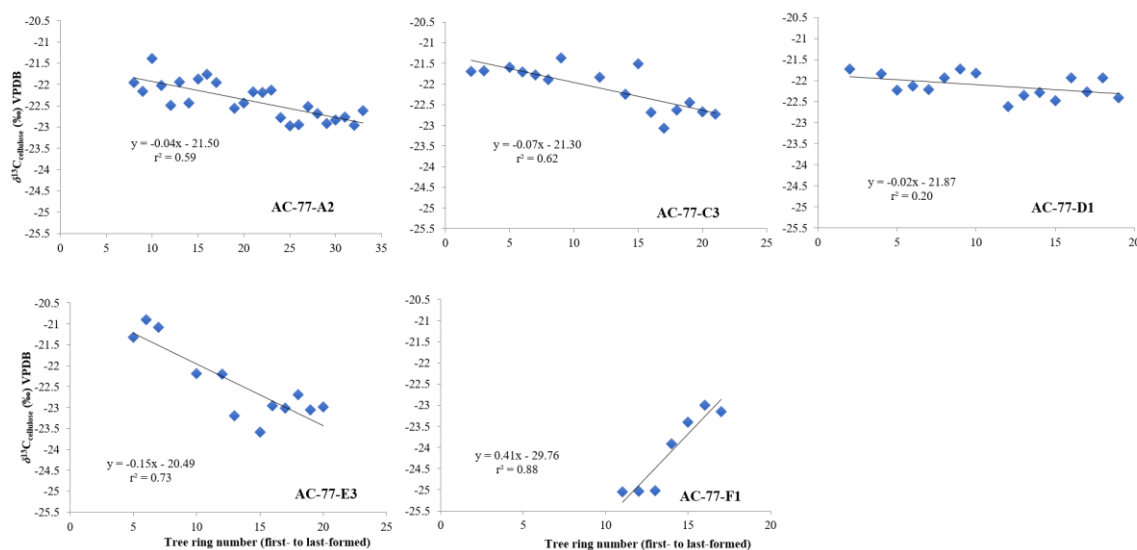


Figure 4.1 Calculated $\delta^{13}\text{C}_{\text{cellulose}}$ of whole tree-rings on an annual basis.

Table 4.1 Calculated carbon-isotope composition and tree-ring # for whole tree-ring cellulose.

Sample	Number of sub-samples	First tree-ring # analyzed	First tree-ring $\delta^{13}\text{C}$ (‰, VPDB)	Last tree-ring # analyzed	Last tree-ring $\delta^{13}\text{C}$ (‰, VPDB)	Minimum $\delta^{13}\text{C}$ (‰, VPDB)	Maximum $\delta^{13}\text{C}$ (‰, VPDB)	$\Delta^{13}\text{C}_{\text{max-min}}$ (‰)	Average $\delta^{13}\text{C}$ (‰, VPDB)
AC-77-A2	25	8	-22.0	33	-22.6	-23.0	-21.4	1.6	-22.4
AC-77-C3	16	2	-21.7	21	-22.7	-23.1	-21.4	1.7	-22.3
AC-77-D1	16	2	-21.7	19	-22.4	-22.6	-21.7	0.9	-22.1
AC-77-E3	12	5	-21.3	20	-23.0	-23.6	-20.9	2.7	-22.4
AC-77-F1	7	11	-25.0	17	-23.2	-25.0	-23.0	0.9	-24.1

Table 4.2 Carbon-isotope composition and tree-ring # of late-wood cellulose.

Sample	Number of sub-samples	First tree-ring # analyzed	First tree-ring $\delta^{13}\text{C}$ (‰, VPDB)	Last tree-ring # sampled	Last tree-ring $\delta^{13}\text{C}$ (‰, VPDB)	Minimum $\delta^{13}\text{C}$ (‰, VPDB)	Maximum $\delta^{13}\text{C}$ (‰, VPDB)	$\Delta^{13}\text{C}_{\text{max-min}}$ (‰)	Average $\delta^{13}\text{C}$ (‰, VPDB)
AC-77-A2	25	8	-22.4	33	-22.6	-23.2	-21.9	1.3	-22.6
AC-77-C3	19	1	-22.4	21	-23.0	-23.3	-21.4	1.9	-22.3
AC-77-D1	18	2	-21.3	19	-22.0	-22.9	-21.3	1.6	-22.1
AC-77-E3	17	4	-21.8	20	-22.9	-23.5	-19.9	3.6	-22.2
AC-77-F1	7	9	-23.3	17	-23.2	-25.2	-23.2	0.1	-24.1

The $\delta^{13}\text{C}_{\text{cellulose}}$ of whole tree-rings from sample AC-77-F1 increased by 1.8 ‰ from ring # 11 to #17 (Table 4.1, Figure 4.1). The small diameter (2 cm) of this sample and its limited number of rings (45) suggest that it was either a young tree or a branch. The increase in $\delta^{13}\text{C}_{\text{cellulose}}$ could result from a juvenile effect, but the data are too few to be certain. An increase in $\delta^{13}\text{C}_{\text{cellulose}}$ may also result from the stress of excess water caused by flooding of the area, (Anderson et al. 2005, Buhay et al. 2008), which is a likely risk for this peat forest growing above fluvial sediments and overlain by lacustrine sediments. But because we cannot rule out a juvenile effect, the $\delta^{13}\text{C}_{\text{cellulose}}$ of AC-77-F1 are not considered further as proxies of hydroclimatic conditions.

4.2 Climate

Each year, both early- and late-wood are produced in a tree-ring. Early-wood and late-wood represent beginning of spring and early summer, and mid-summer to autumn growth, respectively. Tree-rings obtain values of $\delta^{13}\text{C}_{\text{cellulose}}$ and $\delta^{18}\text{O}_{\text{cellulose}}$ that are related to humidity, temperature, and precipitation amount and isotopic composition at the time of cellulose formation. Some studies have also shown that early-wood produced in the spring may use starch stored from the previous year to produce new cell walls (Roden et al. 2000, Kagawa et al. 2006, Dodd et al. 2008). Kagawa et al. (2006), for example, showed that ~43% of the early-wood $\delta^{13}\text{C}_{\text{cellulose}}$ of *Larix gemlinii* (larch) saplings was derived from the tree's previous year carbohydrate reserves. As a result, early-wood can have $\delta^{13}\text{C}_{\text{cellulose}}$ that does not correspond with spring and early summer growth conditions (Hill et al. 1995, Vaganov et al. 2009, Fu et al. 2017). The potential impact on $\delta^{18}\text{O}_{\text{cellulose}}$ is more muted. While starch molecules also contain oxygen, there is 30-40% isotopic exchange of starch oxygen with plant water during later cellulose formation, which means that early-wood $\delta^{18}\text{O}_{\text{cellulose}}$ continues to be largely representative of spring and early summer climate and water sources (Anderson et al. 1998, Roden and Ehleringer 1999, Roden et al. 2000). At high latitude sites, such as in this study, it is also common to observe large seasonal variation in the $\delta^{18}\text{O}$ of source water. This variation arises from the wide ranges in seasonal temperature and precipitation $\delta^{18}\text{O}$, and the propensity of plants to obtain water at different

soil depths or from ground water at different times in the growing season (Anderson et al. 2002, Barbour et al. 2002). Generally, these results have prompted most researchers to examine only the $\delta^{13}\text{C}_{\text{cellulose}}$ and $\delta^{18}\text{O}_{\text{cellulose}}$ of late-wood, which entirely reflect conditions during the year of growth (Kozłowski 1992). Hence, our discussion of the interannual variations in $\delta^{13}\text{C}$ or $\delta^{18}\text{O}$ of cellulose at Adam Creek will be restricted to late-wood or whole tree-ring isotope data. Comparisons of early-wood and late-wood will be used to assess differences in spring-early summer versus mid-summer-autumn climate affecting $\delta^{13}\text{C}$ and $\delta^{18}\text{O}$.

4.2.1 $\delta^{13}\text{C}_{\text{cellulose}}$ and isotope dendrochronology

The $\delta^{13}\text{C}_{\text{cellulose}}$ of tree-rings are known to correlate with growth conditions. Increases in $\delta^{13}\text{C}_{\text{cellulose}}$ indicate either decreased rates of carbon fixation or decreased rate of stomatal conductance (Francey and Farquhar 1982). More specifically, $\delta^{13}\text{C}_{\text{cellulose}}$ will increase when the tree experiences stress from limited water availability, excessive water input or higher temperatures (Tieszen 1991, McCarroll and Loader 2004, Anderson et al. 2005, Buhay et al. 2008, Porter et al. 2009). Bégin et al. (2015) showed that tree-ring cellulose $\delta^{13}\text{C}$ in the boreal forest from northeastern Canada was more strongly related to changes in summer temperature than water availability (precipitation and relative humidity). Tardif et al. (2008) observed that $\delta^{13}\text{C}_{\text{cellulose}}$ of tree-rings was related to ambient temperature controlled by ice cover over Hudson Bay in subarctic Manitoba, Canada. They suggested that the $\delta^{13}\text{C}_{\text{cellulose}}$ increased during longer ice-free seasons (early break-up, late freeze-up). Although trees at different locations might experience different amounts of water stress, Loader et al. (2013) showed that in northern boreal forests stomatal conductance was more controlled by solar radiation/ temperature than water stress.

For the conifer samples from Adam's Creek the main influences on $\delta^{13}\text{C}_{\text{cellulose}}$ likely were: (1) water use efficiency and related water availability (Buhay et al. 2008), (2) temperature, and (3) solar radiation. Increases in solar radiation will enhance the rate of photosynthetic activity in trees, which results in an increase in $\delta^{13}\text{C}_{\text{cellulose}}$. Unfortunately, data to test the effects of changes of solar radiation/cloud cover are not available. Because the forest grew

in a generally wet environment (e.g. the forest peat layer is situated between fluvial sediments below and lacustrine sediments above), there is high possibility that flooding ultimately caused destruction of the forest. The possible effects of flooding on the isotopic compositions of the tree-ring cellulose will also be considered.

For the five trees sampled, the $\delta^{13}\text{C}_{\text{cellulose}}$ of late-wood cellulose ranges from -23.5 to -19.9 ‰; averages for samples AC-77-A2, AC-77-C3, AC-77-D1 and AC-77-E3 range from -22.6 to -22.1 ‰ whereas the average for sample AC-77-F1 is lower (-24.1 ‰) (Table 4.2, Figure 4.2). Based on these averages, it appears that samples AC-77-A2, AC-77-C3, AC-77-D1, and AC-77-E3 grew under similar conditions. As noted earlier, the lower $\delta^{13}\text{C}_{\text{cellulose}}$ for sample AC-77-F1 may reflect a juvenile effect.

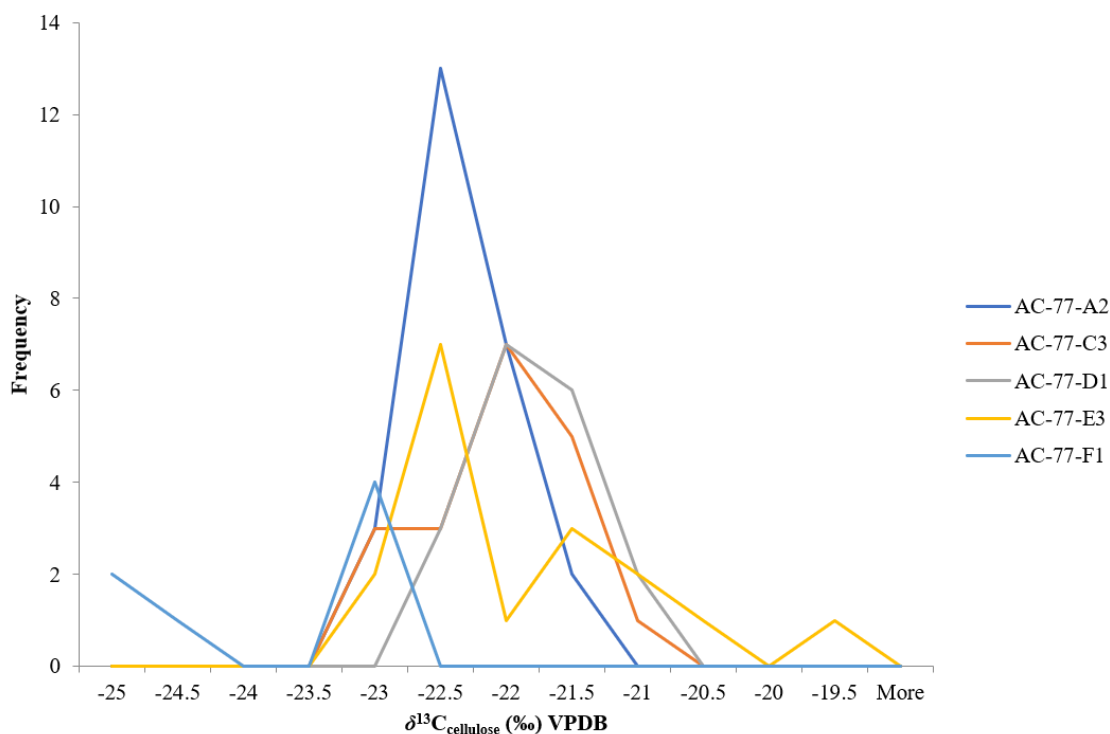


Figure 4.2 Frequency of $\delta^{13}\text{C}_{\text{cellulose}}$ obtained for late-wood.

For samples AC-77-A2, AC-77-C3, AC-77-D1, and AC-77-E3, the average $\delta^{13}\text{C}_{\text{cellulose}}$ of late-wood was -22.3 ‰. Coincidentally, the average $\delta^{13}\text{C}_{\text{cellulose}}$ for calculated whole tree-rings of these 4 samples is also -22.3 ‰, which is ~ 4 ‰ higher than observed for the average whole tree-ring $\delta^{13}\text{C}_{\text{cellulose}}$ formed at the Two Creeks area in northern Wisconsin during the latest Pleistocene ($\sim 11,900$ - $11,640$ ^{14}C BP) (Leavitt and Kalin 1992), right at the start of MIS 1. The tree species at the Two Creeks site, recognized as an “interglacial forest bed”, are *Picea glauca* (white spruce) and/or *Picea mariana* (black spruce), both of which were identified in that site’s pollen. It has been shown for samples in the French Alps that variations in $\delta^{13}\text{C}_{\text{cellulose}}$ resulting from different species are less than within the same species (Gagen et al. 2004). This suggests that variations $\delta^{13}\text{C}_{\text{cellulose}}$ of tree-rings can be compared among different species because they are more controlled by growth conditions than species of conifer (Gagen et al. 2004, Li et al. 2015).

The difference in $\delta^{13}\text{C}_{\text{cellulose}}$ between these two sites and time intervals suggest that the trees at Adam Creek experienced more water stress and/or warmer temperatures during MIS 5a than the Two Creeks location during the Pleistocene-Holocene transition. The Two Creeks trees experienced a transition interval between a glacial and interglacial episodes, where they might have experienced cooler temperatures than typical of the full interglacial stage (Leavitt and Kalin 1992). Overall, these results suggest that the MIS 5 climate at the Adam Creek site was warmer and/or drier than early Holocene climate in Wisconsin. Alternately, the Adam Creek forest from Missinaibi Formation might have experienced excessive water supply from flooding or snow melt at the time of growth and this produced higher $\delta^{13}\text{C}_{\text{cellulose}}$ than measured for the Two Creeks trees (Buhay et al. 2008). This scenario is unlikely, however, since Leavitt and Kalin (1992) also reported that the trees growing at Two Creeks were growing in saturated sediments, which should result in elevated $\delta^{13}\text{C}_{\text{cellulose}}$. Hence, the higher $\delta^{13}\text{C}_{\text{cellulose}}$ at Adam Creek during MIS 5a most likely reflects warmer temperatures than during terminal Pleistocene in Wisconsin.

In Figure 4.3, we compare the Adam Creek $\delta^{13}\text{C}_{\text{cellulose}}$ to modern tree-ring $\delta^{13}\text{C}_{\text{cellulose}}$ from a variety of modern boreal forest locations. The results for modern samples were corrected for the lowering of the $\delta^{13}\text{C}$ of modern atmospheric CO_2 resulting from fossil-fuel burning, otherwise known as the Suess effect (Suess 1955). The Adam Creek samples have similar

(alpha) $\delta^{13}\text{C}_{\text{cellulose}}$ to modern (alpha) cellulose from the Columbia Ice Field B.C. ($\delta^{13}\text{C} = -21.7\text{‰}$; Edwards et al. 2008) and holocellulose from a 7,600-year-old submerged forest found in Lake Huron (average $\delta^{13}\text{C} = -23.4\text{‰}$; Hunter et al. 2006). As noted in the Introduction, there should be no significant difference in the $\delta^{13}\text{C}_{\text{cellulose}}$ and $\delta^{18}\text{O}_{\text{cellulose}}$ between holocellulose and alpha cellulose (Riechelmann et al. 2016). The $\delta^{13}\text{C}_{\text{cellulose}}$ of modern whole tree-rings from Churchill Manitoba, are about 1.7 ‰ lower than the Adam Creek samples. For modern boreal forests at five sites ranging across Finland, north-eastern USA, Quebec, Manitoba and British Columbia (McCarroll and Pawellek 2001, Hunter et al. 2006, Edwards et al. 2008, Tardif et al. 2008, Bégin et al. 2015), the average $\delta^{13}\text{C}_{\text{cellulose}}$ lies between -24.0 and -21.7‰ . The average $\delta^{13}\text{C}_{\text{cellulose}}$ of late-wood (and whole tree-rings) for Adam Creek samples AC-77-A2, -C3, -D1 and -E3 is $-22.3 \pm 0.2\text{‰}$, placing it in the middle of this range.

The above results suggests that the conditions that affect the $\delta^{13}\text{C}_{\text{cellulose}}$ of tree-rings are similar among various boreal forests, which is not surprising as the geographic distribution of the Boreal forest ecosystem is a function of water availability and temperature (Tardif et al. 2008, Loader et al. 2013b, Bégin et al. 2015). At this point we cannot assess in more detail the effects of multiple climate factors on $\delta^{13}\text{C}_{\text{cellulose}}$ for the Adam's Creek samples. For example, lower temperatures may cause a lowering of $\delta^{13}\text{C}_{\text{cellulose}}$ while flooding stress could increase $\delta^{13}\text{C}_{\text{cellulose}}$. If cooler temperatures occurred concurrently with flooding these two effects may counteract each other and produce $\delta^{13}\text{C}_{\text{cellulose}}$ in the range that we observe for modern boreal forests. Likewise, the $\delta^{13}\text{C}_{\text{cellulose}}$ of the Adam Creek samples might appear similar to modern boreal forests if this location had higher temperatures during MIS 5a than today (causing $\delta^{13}\text{C}_{\text{cellulose}}$ to increase), but the trees we sampled had relatively lower $\delta^{13}\text{C}_{\text{cellulose}}$ because they are all <50 years old and experiencing a juvenile effect. The simplest explanation, however, is that the trees at Adam Creek during MIS 5a did not experience any unusual water stress, extreme temperatures or lack of sunshine that would have caused $\delta^{13}\text{C}_{\text{cellulose}}$ to vary significantly from the range observed for modern boreal forest ecosystems.

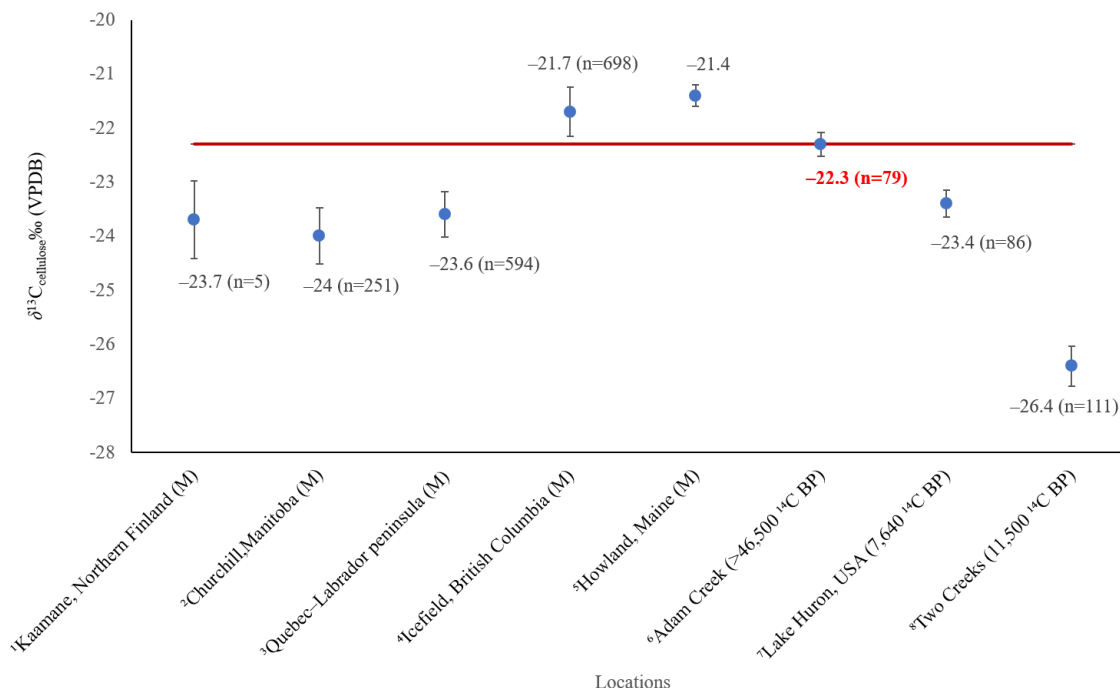


Figure 4.3 Tree-ring $\delta^{13}\text{C}_{\text{cellulose}}$ for boreal conifers from various locations. The red line indicates the average whole tree-ring and late-wood $\delta^{13}\text{C}_{\text{cellulose}}$ of Adam Creek samples AC-77-A2, -C3, -D1 and -E3. M = modern (¹McCarroll and Pawellek 2001, ²Tardif et al. 2008, ³Bégin et al. 2015, ⁴Edwards et al. 2008, ⁵Guerrieri et al. 2017, ⁶this thesis, ⁷Hunter et al. 2006, ⁸Leavitt and Kalin 1992). Late-wood cellulose: references 1 and 6; whole-ring cellulose: references 2-5 and 7-8.

4.2.1.1 Interannual $\delta^{13}\text{C}_{\text{cellulose}}$ variability

The average late-wood $\delta^{13}\text{C}_{\text{cellulose}}$ for the Adam Creek samples (excepting AC-77-F1) was tightly constrained around -22.3‰ . Each tree, however, exhibited a 1.3 to 3.6 ‰ range between maximum and minimum late-wood $\delta^{13}\text{C}_{\text{cellulose}}$ ($\Delta^{13}\text{C}_{\text{max-min}}$) (Table 4.2). All samples displayed some annual variation in late-wood $\delta^{13}\text{C}_{\text{cellulose}}$. This suggests that these trees experienced changes in water availability and growing season temperature throughout their lives (Brooks et al. 1998, McCarroll and Loader 2004, Bégin et al. 2015), which varied with a periodicity of 1-4 years (Figure 4.4). Such variations are typical of boreal forest, for example a 2 to 3 ‰ range in $\delta^{13}\text{C}_{\text{cellulose}}$ has been observed within individual trees grown

in boreal forests in North Italy, Central Germany, North Sweden, and central Canadian boreal forest (Brooks et al. 1998, Vaganov et al. 2009).

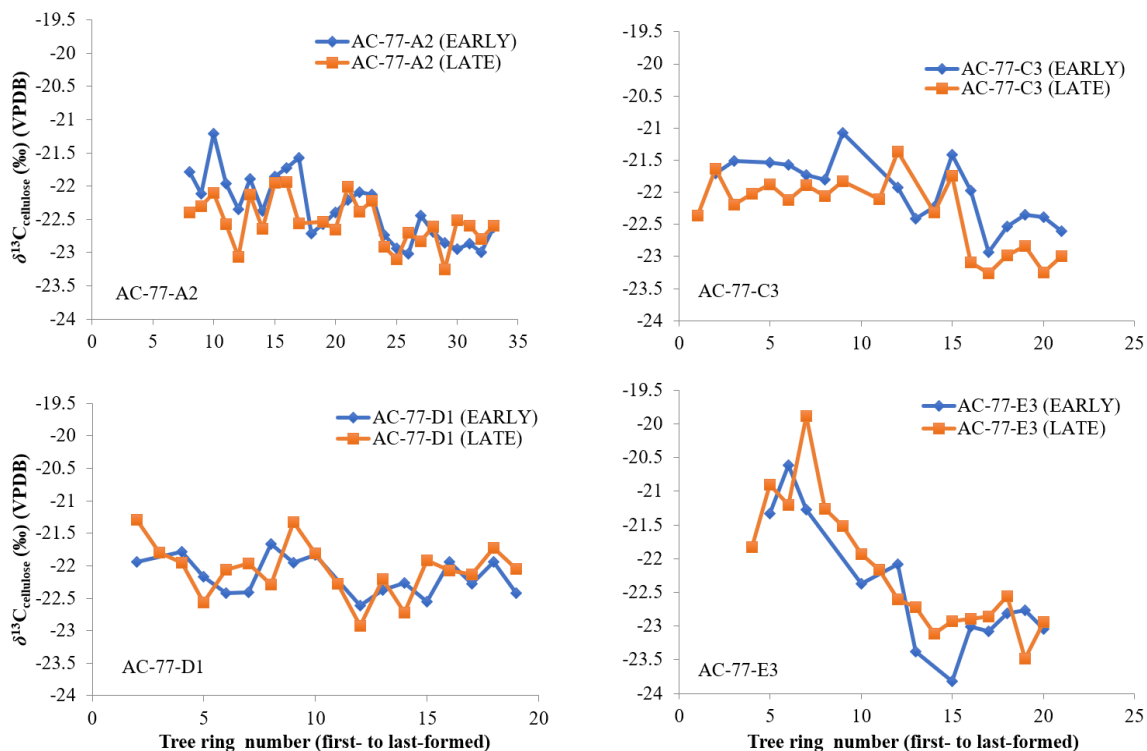


Figure 4.4 The $\delta^{13}\text{C}_{\text{cellulose}}$ of early-wood (blue) and late-wood (orange) for AC-77-A2, AC-77-C3, AC-77-D1 and AC-77-E3.

All samples showed an overall pattern of lower $\delta^{13}\text{C}_{\text{cellulose}}$ with increasing age of the tree. This change is most pronounced for AC-77-E3, which exhibits a large decline in $\delta^{13}\text{C}_{\text{cellulose}}$ from years 7 to 14 and very little fluctuation in $\delta^{13}\text{C}$ from year to year after this interval (Figure 4.4). The overall downward trend in all four samples is suggestive of increasing water availability (Saurer et al. 1995, McCarroll and Loader 2004), perhaps reflecting hydrological transitions in the forest-peat ecosystem in which the samples grew. The forest-peat accumulation overlies fluvial sediments, which is suggestive of proximity to a riparian zone, and underlies lacustrine sediments, which is indicative of a rise in water table that

led to periodic and then constant flooding of the forest. As noted earlier, decreasing $\delta^{13}\text{C}_{\text{cellulose}}$ is commonly associated with reduced (or the absence of) moisture-deficit stress on a tree. As Anderson et al. (2005) and Buhay et al. (2008) have noted, however, moisture-excess associated with periodic flooding can also lead to growth stress on a tree, which is reflected in an increase in $\delta^{13}\text{C}_{\text{cellulose}}$. Such moisture-excess stress was not apparent in the $\delta^{13}\text{C}_{\text{cellulose}}$ of AC-77-A2, -C3, -D1 and -E3. That said, the large and steady decrease of cellulose $\delta^{13}\text{C}$ during the last years of life of AC-77-E3 could indicate an ever-increasing water availability associated with a rising water table, but not yet to the point of moisture-excess stress. The $\delta^{13}\text{C}_{\text{cellulose}}$ pattern in AC-77-F1 (Figure 4.1), which has been set aside because of possible juvenile effects, nonetheless could also potentially indicate a shift to waterlogged conditions associated with flooding.

4.2.2 $\delta^{18}\text{O}_{\text{cellulose}}$, source water and temperature

Values of $\delta^{18}\text{O}_{\text{cellulose}}$ vary with that of precipitation and the extent of ^{18}O enrichment during evapotranspiration (McCarroll and Loader 2004). At any given location, these factors can be correlated with air temperature and relative humidity, respectively. The $\delta^{18}\text{O}$ of precipitation is typically higher when temperatures increase and leaf-water $\delta^{18}\text{O}$ is higher when relative humidity decreases (McCarroll and Loader 2004). A study of modern, black spruce trees situated along a lakeshore in a boreal forest from northeastern Canada, for example, showed that low $\delta^{18}\text{O}_{\text{cellulose}}$ of whole tree-rings was related to cold and wet conditions (Naulier et al. 2014).

Within individual tree samples, $\Delta^{18}\text{O}_{\text{max-min}}$ for early-wood cellulose ranges from 2.7 to 4.9 ‰ (Table 4.3) and for late-wood, from 3.1 to 5.3 ‰ (Table 4.4). All tree samples displayed annual variation both in early-wood and late-wood $\delta^{18}\text{O}_{\text{cellulose}}$ (Figure 4.5). Some samples displayed a strong trend towards higher $\delta^{18}\text{O}_{\text{cellulose}}$ (e.g., AC-77-A2, AC-77-F1) with increasing age, others an overall decrease in $\delta^{18}\text{O}_{\text{cellulose}}$ (AC-77-E3) with increasing age, and still others, shorter term variability, but no overall trend towards higher or lower $\delta^{18}\text{O}_{\text{cellulose}}$ (AC-77-C3, AC-77-D1). This variability in $\delta^{18}\text{O}_{\text{cellulose}}$ among samples is larger than typically expected from local environmental effects within or at the edge of a forest.

Instead, it probably reflects different ages of the samples within the overall lifespan of this forest from the time of its establishment until its death, probably by drowning. In any particular sample, the $\delta^{18}\text{O}_{\text{cellulose}}$ of early versus late-wood generally tracked each other (Figure 4.5), albeit typically with a lag reflecting seasonal differences in the oxygen-isotope compositions of water during the growing season.

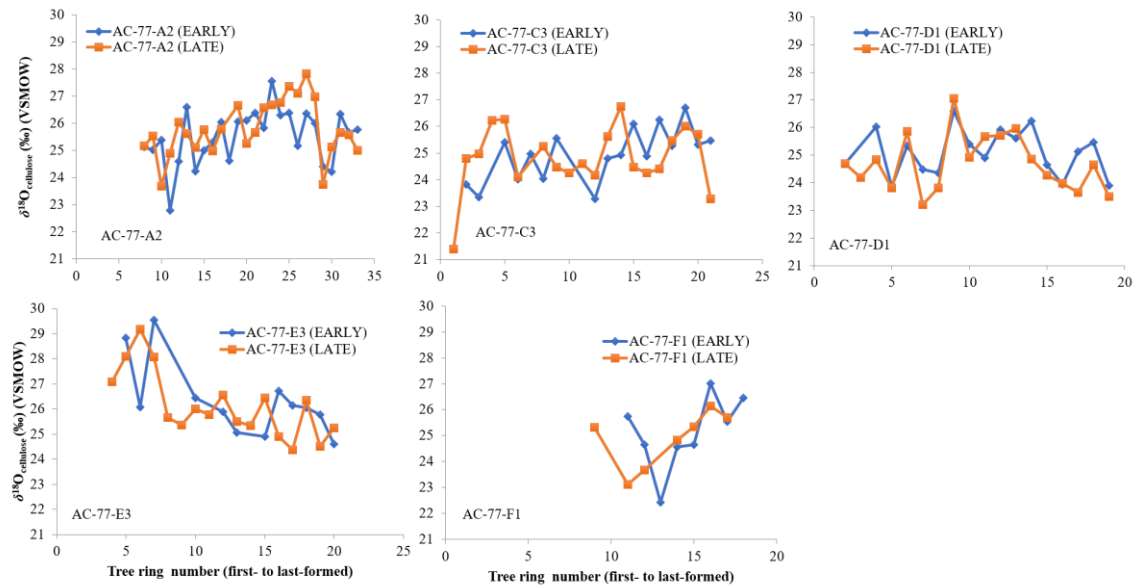


Figure 4.5 The $\delta^{18}\text{O}_{\text{cellulose}}$ of early-wood (blue) and late-wood (orange) for AC-77-A2, AC-77-C3, AC-77-D1, AC-77-E3 and AC-77-F1.

Table 4.3 Oxygen-isotope composition and tree ring # of early-wood cellulose.

Sample	Number of samples	First tree-ring # analyzed	First tree-ring $\delta^{18}\text{O}$ (‰, VSMOW)	Last tree-ring # analyzed	Last tree-ring $\delta^{18}\text{O}$ (‰, VSMOW)	Minimum $\delta^{18}\text{O}$ (‰, VSMOW)	Maximum $\delta^{18}\text{O}$ (‰, VSMOW)	$\Delta^{18}\text{O}_{\text{max-min}}$ (‰)	Average $\delta^{18}\text{O}$ (‰, VSMOW)
AC-77-A2	26	8	+25.1	33	+25.8	+22.8	+27.6	4.8	+25.6
AC-77-C3	17	2	+23.8	21	+25.5	+23.3	+26.7	3.4	+24.9
AC-77-D1	17	2	+24.7	19	+23.9	+23.9	+26.6	2.7	+25.1
AC-77-E3	12	5	+28.8	20	+24.6	+24.6	+29.5	4.9	+26.3
AC-77-F1	8	11	+25.7	18	+26.5	+22.4	+27.0	4.6	+25.1

Table 4.4 Oxygen-isotope composition and tree-ring # of late-wood cellulose.

Sample	Number of samples	First tree-ring # analyzed	First tree-ring $\delta^{18}\text{O}$ (‰, VSMOW)	Last tree-ring # analyzed	Last tree-ring $\delta^{18}\text{O}$ (‰, VSMOW)	Minimum $\delta^{18}\text{O}$ (‰, VSMOW)	Maximum $\delta^{18}\text{O}$ (‰, VSMOW)	$\Delta^{18}\text{O}_{\text{max-min}}$ (‰)	Average $\delta^{18}\text{O}$ (‰, VSMOW)
AC-77-A2	25	8	+25.2	33	+25.0	+23.7	+27.8	4.1	+25.8
AC-77-C3	20	1	+21.4	21	+23.3	+21.4	+26.7	5.3	+24.9
AC-77-D1	18	2	+24.7	19	+23.5	+23.2	+27.1	3.9	+24.7
AC-77-E3	16	4	+27.1	20	+25.2	+24.4	+29.2	4.8	+26.1
AC-77-F1	7	9	+25.3	17	+25.7	+23.1	+26.2	3.1	+24.9

For the five trees sampled, the $\delta^{18}\text{O}_{\text{cellulose}}$ of late-wood ranged from +21.4 to +29.2 ‰ with an average value of +25.3 ‰ (Table 4.4). Sample AC-77-F1 was included because the juvenile effect should not significantly affect $\delta^{18}\text{O}_{\text{cellulose}}$. Based on the small difference in their average, late-wood $\delta^{18}\text{O}_{\text{cellulose}}$ (± 0.6 ‰), all samples likely grew under similar conditions (Figure 4.6). Among the samples, AC-77-C3 and AC-77-D1 might have grown under a slightly cooler conditions (lower $\delta^{18}\text{O}$ precipitation) and/or higher relative humidity (lower $\delta^{18}\text{O}$ leaf water), whereas AC-77-A2, AC-77-E3 and AC-77-F1 reflect slightly warmer and/or drier conditions. For AC-77-E3 in particular, the average, slightly higher late-wood $\delta^{18}\text{O}_{\text{cellulose}}$ (+26.1 ‰, Table 4.4) is consistent with warmer conditions and higher stomatal conductance, but this average is skewed by particularly high late-wood $\delta^{18}\text{O}_{\text{cellulose}}$ during the first four years sampled (Fig. 4.5). The $\delta^{18}\text{O}_{\text{cellulose}}$ of its late-wood in later tree-rings (8 to 20; $\delta^{18}\text{O}_{\text{cellulose}} = +25.5$ ‰) is similar to the average $\delta^{18}\text{O}_{\text{cellulose}}$ for the other four samples (Table 4.4), suggesting a similar water source at that time. Those later conditions might have included an increasingly saturated soil water column and/or an unconfined, very shallow water table associated with increased precipitation and perhaps also cooling associated with periodic or gradual inundation of the forest.

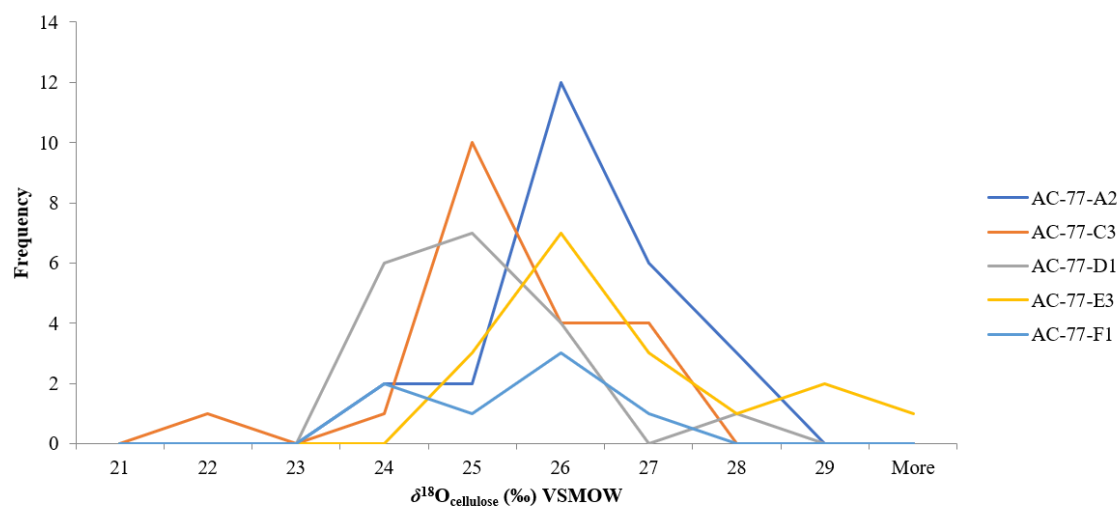


Figure 4.6 Frequency of $\delta^{18}\text{O}_{\text{cellulose}}$ obtained for late-wood for samples AC-77-A2, AC-77-C3, AC-77-D1, AC-77-E3 and AC-77-F1.

The average $\delta^{18}\text{O}_{\text{cellulose}}$ for all 5 samples calculated for whole tree-rings (+25.4 ‰) is very similar to the average obtained for late-wood only (Table 3.3). Figure 4.7 compares the average $\delta^{18}\text{O}_{\text{cellulose}}$ for the Adam Creek whole tree-ring samples to the $\delta^{18}\text{O}_{\text{cellulose}}$ of conifers from other sites and time intervals (data from Edwards and Fritz 1986, Kerr-Lawson et al. 1992, Hunter et al. 2006, Edwards et al. 2008, Bégin et al. 2015, Guerrieri et al. 2017). As shown in Figure 4.7, modern whole tree-ring $\delta^{18}\text{O}_{\text{cellulose}}$ from conifer trees collected over a wide geographic area decreases with increasing latitude. The range of average $\delta^{18}\text{O}_{\text{cellulose}}$ of whole tree-ring for the five Adam Creek tree samples (+24.9 to +26.4 ‰; Table 3.3) is similar to the range (+24.1 to +27.2 ‰) for whole tree-ring samples from Brampton, Ontario – located 770 km southeast of Adam Creek – which range in age from 11,450 ^{14}C BP to modern (Edwards and Fritz 1986). Edwards and Fritz (1986) noted that the $\delta^{18}\text{O}_{\text{cellulose}}$ became progressively lower towards the present day, suggesting that the climate was becoming cooler and moister.

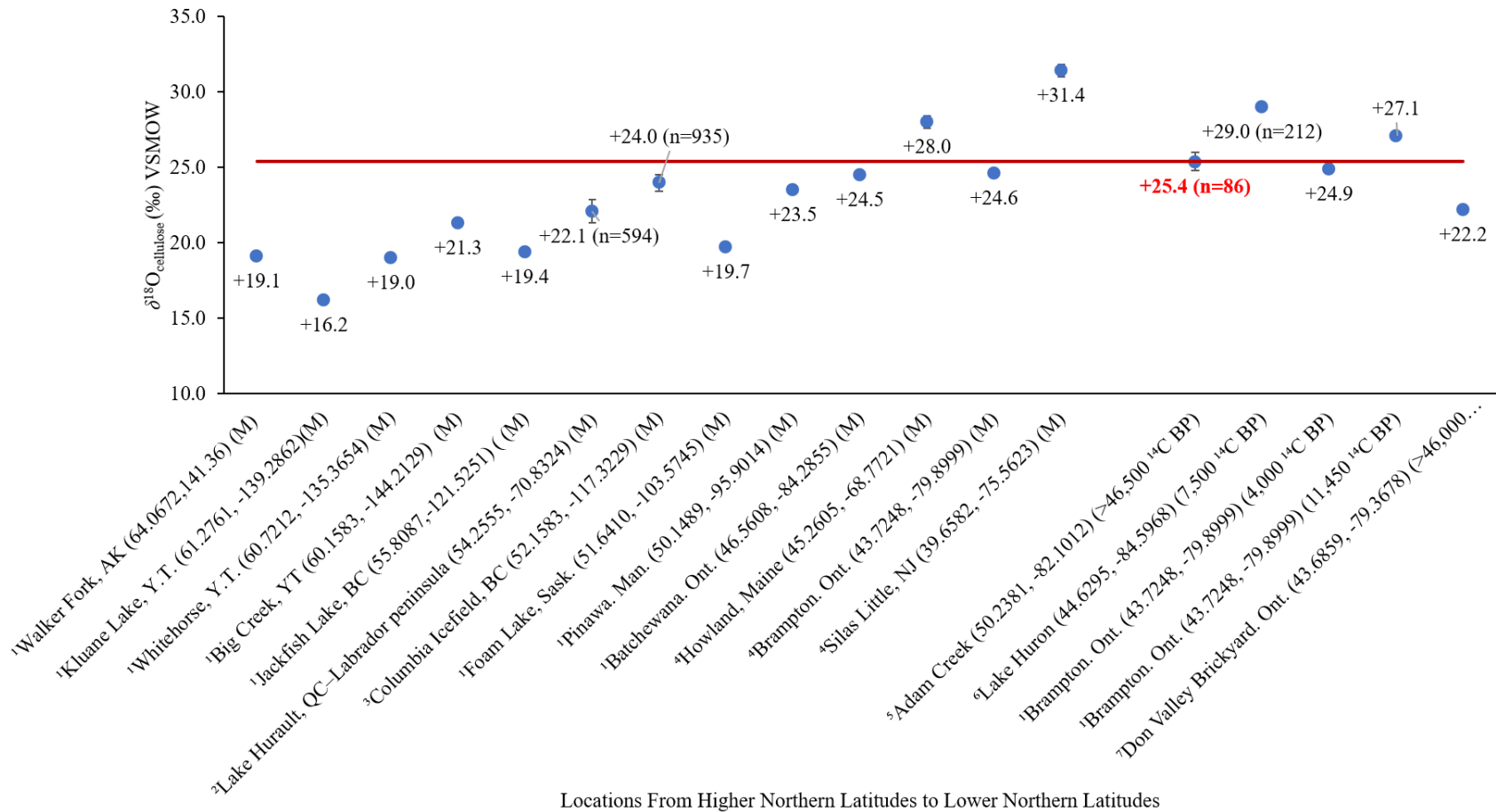


Figure 4.7 $\delta^{18}\text{O}_{\text{cellulose}}$ from different locations. Red line displays Adam Creek oxygen-isotope compositions. M = modern. ¹Edwards and Fritz 1986, ²Edwards et al. 2008, ³Bégin et al. 2015, ⁴Guerrieri et al. 2017, ⁵thesis, ⁶Hunter et al. 2006, ⁷Kerr-Lawson et al. 1992. All data are for whole-wood except 6 (late-wood).

For the modern samples illustrated in Figure 4.7, the $\delta^{18}\text{O}$ of annual precipitation was calculated using the model of Bowen and Revenaugh (2003) based on the latitude, altitude and elevation of those sites. The $\delta^{18}\text{O}$ of annual precipitation is plotted versus $\delta^{18}\text{O}_{\text{cellulose}}$ for samples of modern boreal forests in Figure 4.8 to obtain the relationship:

$$\delta^{18}\text{O}_{\text{precipitation}} = 1.03 \delta^{18}\text{O}_{\text{cellulose}} - 38.84 \quad (\text{Equation 4.1})$$

Equation 4.1 was used with the average $\delta^{18}\text{O}$ for whole-ring cellulose of the Adam Creek samples to calculate a $\delta^{18}\text{O}$ of -12.7‰ for annual precipitation at this site during MIS 5a. The modern annual $\delta^{18}\text{O}_{\text{precipitation}}$ calculated with the Bowen and Revenaugh (2003) model is -13.8‰ . This result suggests that the Adam Creek samples grew under a precipitation regime that was $\sim 1\text{‰}$ higher than today. This suggests that during MIS 5a, the Adam Creek area was slightly warmer and/or less humid than at present where summer mean temperature is 15.1 °C (Climate Atlas of Canada, 2019) with modern relative humidity of 63% in month of July 2020 (Environment Canada 2014).

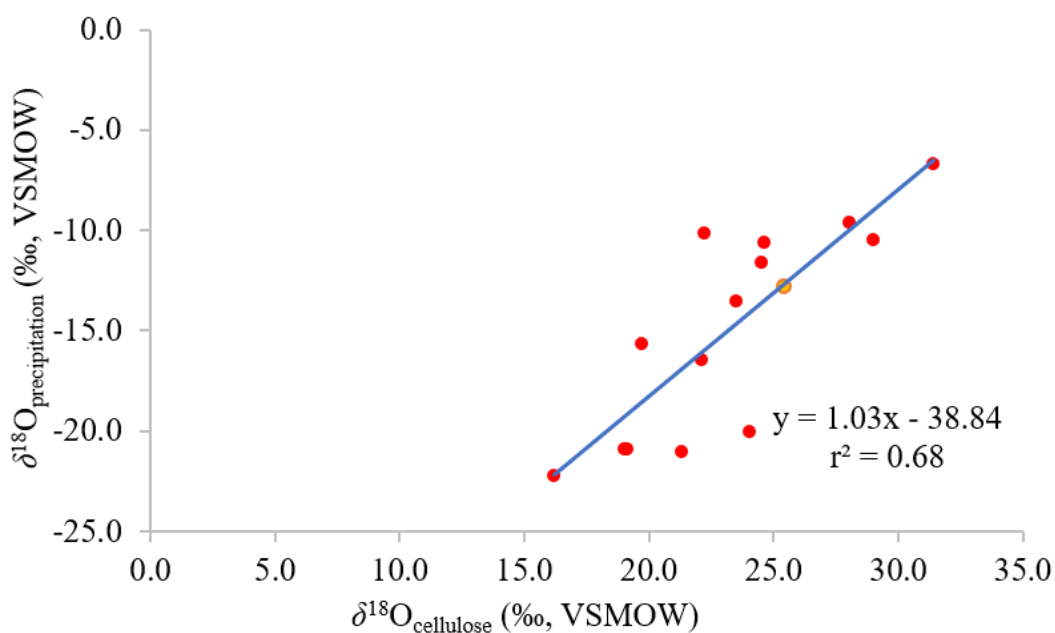


Figure 4.8 $\delta^{18}\text{O}_{\text{precipitation}}$ versus $\delta^{18}\text{O}_{\text{cellulose}}$ for localities shown in Figure 4.7.

4.2.3 Covariation between $\delta^{18}\text{O}_{\text{cellulose}}$ and $\delta^{13}\text{C}_{\text{cellulose}}$

Testing for covariation between $\delta^{13}\text{C}_{\text{cellulose}}$ and $\delta^{18}\text{O}_{\text{cellulose}}$ provides an opportunity to learn more about the water resources available during tree growth. Under warm and dry conditions both $\delta^{13}\text{C}_{\text{cellulose}}$ and $\delta^{18}\text{O}_{\text{cellulose}}$ should increase (Seftigen et al. 2011, Bégin et al. 2015). For the late-wood sub-samples examined in this study, however, values of the coefficient of determination (r^2) were low except for AC-77-E3 (Table 4.5, Figure 4.9). For this sample, there was a positive correlation between $\delta^{13}\text{C}_{\text{cellulose}}$ and $\delta^{18}\text{O}_{\text{cellulose}}$ ($r^2 = 0.53$). This value, however, is driven by data for the first 4 years of growth analyzed; when those data are omitted, this correlation disappears (Table 4.5, Figure 4.9).

Table 4.5 Correlation between late-wood $\delta^{18}\text{O}_{\text{cellulose}}$ and $\delta^{13}\text{C}_{\text{cellulose}}$.

Sample	slope of trendline	Coefficient of Determination (r^2)
AC-77-A2	0.6	0.05
AC-77-C3	0.08	< 0.01
AC-77-D1	0.3	0.01
AC-77-E3	1	0.53
AC-77-E3 (first 4 years omitted)	0.3	0.10
AC-77-F1	0.8	0.43

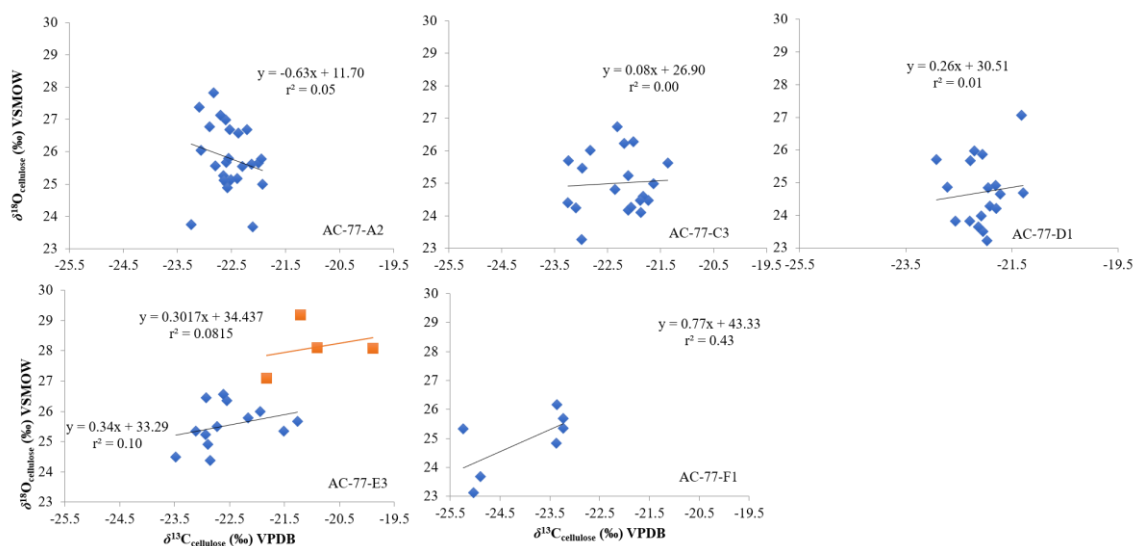


Figure 4.9 Correlations between late-wood $\delta^{18}\text{O}_{\text{cellulose}}$ and $\delta^{13}\text{C}_{\text{cellulose}}$ for samples AC-77-A2, AC-77-C3, AC-77-D1, AC-77-E3 and AC-77-F1. Data and trend-line shown in orange for AC-77-E3 represent the first four tree-ring sub-samples analyzed.

The paleoclimate at Adam Creek should have had similar subarctic characteristics as today such as warm-dry or cold-wet conditions during growing season. As such, both $\delta^{13}\text{C}_{\text{cellulose}}$ and $\delta^{18}\text{O}_{\text{cellulose}}$ should covary and have been sensitive to moisture limitations (Naulier et al. 2014, 2015, Bégin et al. 2015, Alvarez et al. 2018). Instead, the data suggest that $\delta^{13}\text{C}_{\text{cellulose}}$ and $\delta^{18}\text{O}_{\text{cellulose}}$ varied relatively independently from each other. Ferrio and Voltas (2005) previously noted such decoupling in pines from the Mediterranean region, which are adapted to temporary drought. There, $\delta^{13}\text{C}_{\text{cellulose}}$ recorded water availability, i.e. vapour pressure deficit, as a function of stomatal conductance. During seasonal intervals of dryness / drought, however, the $\delta^{18}\text{O}_{\text{cellulose}}$ no longer correlated well with precipitation $\delta^{18}\text{O}$, due to strong variability in leaf-water $\delta^{18}\text{O}$ arising from ^{18}O -enrichment during transpiration. In the Adam Creek sub-arctic wetland setting, where there is a low probability of water-deficit conditions, different types of stress may have been at play that also produced a decoupling of these isotopic parameters.

At Adam Creek, we have $\delta^{13}\text{C}_{\text{cellulose}}$ typical for modern boreal forests and observe a decrease in $\delta^{13}\text{C}_{\text{cellulose}}$ as the trees mature indicating an increase in stomatal conductance related to reduced water stress and/or decreasing temperatures. We also observe higher than expected $\delta^{18}\text{O}_{\text{cellulose}}$ for this latitude indicating higher rates of transpiration during drier conditions and/or warmer temperatures and hence higher $\delta^{18}\text{O}$ for precipitation feeding the trees. It is likely that because of the warmer temperatures indicated by the $\delta^{18}\text{O}$ data, carbon assimilation was not limited by temperature. Hence, the lowering of $\delta^{13}\text{C}_{\text{cellulose}}$ as the trees matured indicates an increase in water availability as roots grew deeper or the area gradually became inundated. Under these warm, humid conditions the $\delta^{18}\text{O}_{\text{cellulose}}$ would vary more strongly in response to the $\delta^{18}\text{O}$ of precipitation events.

4.3 Early-wood versus Late-Wood Cellulose Isotope Composition and Seasonality

Although early-wood cellulose contains some carbon and oxygen that is sourced from stored carbohydrates, Dickmann and Kozłowski (1970) and Kozłowski (1992) suggested that the use of stored carbohydrates on $\delta^{13}\text{C}_{\text{cellulose}}$ and $\delta^{18}\text{O}_{\text{cellulose}}$ was negligible in conifers. More recently, Weigl et al. (2008) showed for oak that $\delta^{13}\text{C}_{\text{cellulose}}$ and $\delta^{18}\text{O}_{\text{cellulose}}$ of both early and late-wood can be used as climate proxies. Other researchers (Brooks et al. 1998, McCarroll and Loader 2004, An et al. 2012, Fu et al. 2017) have also shown that early-wood $\delta^{13}\text{C}_{\text{cellulose}}$ and $\delta^{18}\text{O}_{\text{cellulose}}$ can provide some information about spring and early summer growth conditions. For example, the $\delta^{18}\text{O}_{\text{cellulose}}$ of early-wood from conifers from Yulong Snowy Mountains of southwestern China had significant positive correlation to May-July temperature and negative correlation to May-July cloud cover, relative humidity and precipitation (An et al. 2012, Fu et al. 2017). Brooks et al. (1998) observed for *Pinus banksiana* trees from central Canadian forest that high amounts of winter precipitation were correlated with higher $\delta^{13}\text{C}_{\text{cellulose}}$ of early-wood that year because high amounts of snow caused low soil temperatures which negatively influenced growth. In that study $\delta^{13}\text{C}_{\text{cellulose}}$ of late-wood was correlated with both winter and growing season precipitation. Disagreement on this point remains, however; Jäggi et al. (2002), for example, suggest for spruce that early-wood, compared to late-wood, is more strongly influenced by

biochemical isotopic fractionation during starch formation of the previous year than by climate conditions during cellulose formation.

If stored carbohydrates had a strong influence on early-wood $\delta^{13}\text{C}_{\text{cellulose}}$ and $\delta^{18}\text{O}_{\text{cellulose}}$ for the Adam Creek samples, we might expect to see a positive correlation between the isotopic compositions of late-wood of one year and the early-wood of the subsequent year (Kress et al. 2009). In this study, 4 out of 5 samples (all except AC-77-D1) showed significant correlations ($p < 0.01$ or $p < 0.05$) between $\delta^{13}\text{C}$ of early-wood and the previous year's late-wood (Table 4.6). Although this may be interpreted to mean that carbon in early-wood cellulose is partially sourced from the previous year, those samples also showed significant correlations between early-wood and late-wood of same year for $\delta^{13}\text{C}$ (Table 4.6). Hence, early-wood $\delta^{13}\text{C}_{\text{cellulose}}$ may therefore reflect growing season conditions.

Correlations between $\delta^{18}\text{O}$ of early-wood cellulose and the previous year's late-wood cellulose were only observed for samples AC-77-A2 and AC-77-E3 (Table 4.6). There is no consistent evidence of an oxygen carry-over effect between early-wood and the previous year's late-wood.

As such, it appears that analysis of both early- and late-wood $\delta^{13}\text{C}_{\text{cellulose}}$ and $\delta^{18}\text{O}_{\text{cellulose}}$ in the Adam Creek samples provides an opportunity to identify seasonal trends in temperature, humidity and precipitation. All five samples showed variation in the $\delta^{13}\text{C}_{\text{cellulose}}$ and $\delta^{18}\text{O}_{\text{cellulose}}$ between early and late-wood grown in the same year but a two-tailed t-test indicated that there was no significant difference in either $\delta^{18}\text{O}$ or $\delta^{13}\text{C}$ between early- and late-wood within each sample over the entire range of tree-rings sampled (Table 4.7).

Table 4.6 Pearson correlation (r) between EW (early-wood) and the previous year's LW (late-wood), and between EW and LW of same year for $\delta^{13}\text{C}_{\text{cellulose}}$ or $\delta^{18}\text{O}_{\text{cellulose}}$.

Samples	EW vs LW from the previous year		EW vs LW from the same year	
	$\delta^{18}\text{O}$	$\delta^{13}\text{C}$	$\delta^{18}\text{O}$	$\delta^{13}\text{C}$
AC-77-A2	0.53**	0.56**	0.52**	0.68**
AC-77-C3	0.41	0.61**	0.16	0.70**
AC-77-D1	0.18	0.39	0.75**	0.42
AC-77-E3	0.69*	0.68*	0.52	0.82**
AC-77-F1	0.61	0.91*	0.73	0.91*

* Correlation is significant at the 0.05 level (2-tailed)

**Correlation is significant at the 0.01 level (2-tailed)

Table 4.7 p-values for two-tailed t-test for $\delta^{13}\text{C}_{\text{cellulose}}$ or $\delta^{18}\text{O}_{\text{cellulose}}$ between early- and late-wood within each tree-ring for all samples.

Samples	p-values (p < 0.05)	
	$\delta^{13}\text{C}$	$\delta^{18}\text{O}$
AC-77-A2	0.19	0.38
AC-77-C3	0.22	0.37
AC-77-D1	0.7	0.29
AC-77-E3	0.39	0.58
AC-77-F1	0.7	0.65

We expect spring-early summer to be cooler than mid-late summer-autumn each year. A thirty-year record of temperature at Kapuskasing, Ontario, 100 km from Adam Creek (the closest weather station), shows that the average April-June temperatures (8 °C) are lower than July to October (12 °C) (Environment Canada 2014). Likewise, monthly precipitation amounts are highest for July, September and October. Lower temperatures should cause lower early-wood $\delta^{13}\text{C}_{\text{cellulose}}$ compared to late-wood, but greater water availability in mid-summer to autumn could cause late-wood $\delta^{13}\text{C}$ to be lower than early-wood. Cooler temperatures during early-wood formation should cause early-wood $\delta^{18}\text{O}$ to be lower than

late-wood, but increased precipitation later in the summer may also reduce ^{18}O -enrichment of plant water resulting from transpiration and thus also lower late-wood $\delta^{18}\text{O}_{\text{cellulose}}$.

Direct comparison of intra-ring $\delta^{13}\text{C}_{\text{cellulose}}$ or $\delta^{18}\text{O}_{\text{cellulose}}$ revealed a wide range of intra-ring amplitudes for $\Delta^{13}\text{C}_{\text{LW-EW}} = -1.1$ to $+1.4$ ‰ and $\Delta^{18}\text{O}_{\text{LW-EW}} = -2.6$ to $+3.1$ ‰ from early spring-early summer to mid-late summer-autumn each year (Figures 4.10 and 4.11). For the Adam Creek samples, therefore, both early-wood and late-wood $\delta^{13}\text{C}_{\text{cellulose}}$ and $\delta^{18}\text{O}_{\text{cellulose}}$ are variably higher or lower without a specific pattern being apparent.

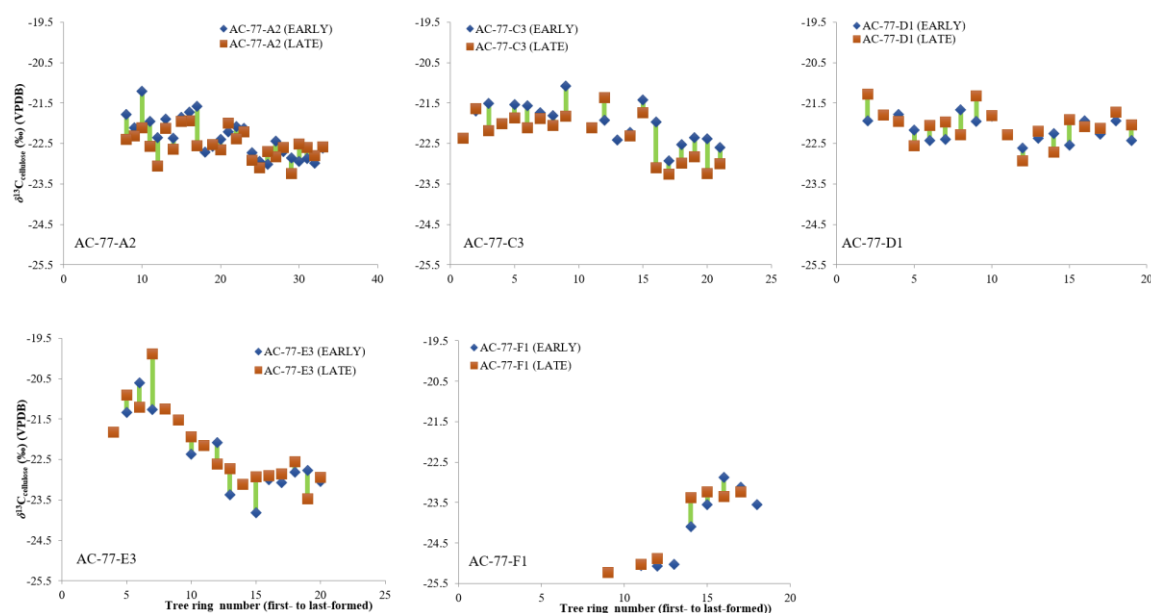


Figure 4.10 Comparison of same year, early-wood and late-wood $\delta^{13}\text{C}_{\text{cellulose}}$ for AC-77-A2, AC-77-C3, AC-77-D1, AC-77-E3 and AC-77-F1.

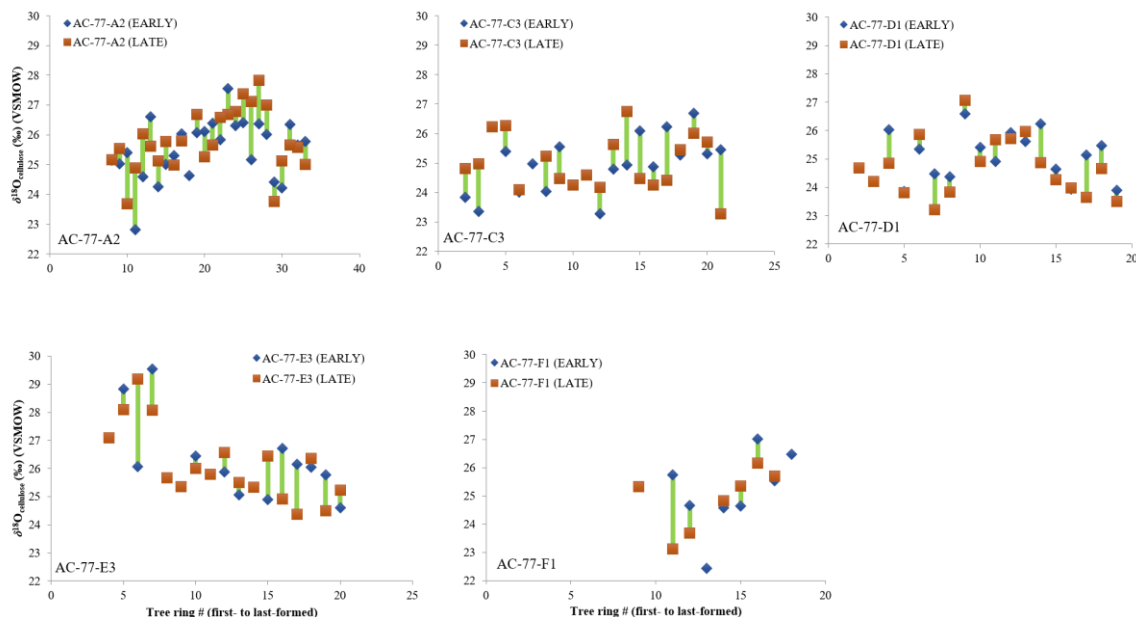


Figure 4.11 Comparison of same year, early-wood and late-wood $\delta^{18}\text{O}_{\text{cellulose}}$ for AC-77-A2, AC-77-C3, AC-77-D1, AC-77-E3 and AC-77-F1.

For some samples we gain some information about seasonal climate change. For example, the relatively small $\Delta^{13}\text{C}_{\text{LW-EW}}$ observed for AC-77-E3, especially in the latter half of that record (Figure 4.10), could indicate ever-increasing water availability associated with a rising water table during all parts of the growing season. A similar argument could be made for the first part of the record for AC-77-F1. Sample AC-77-C3 has higher $\delta^{13}\text{C}_{\text{cellulose}}$ for early-wood relative to late-wood for most years, which could indicate greater sensitivity to increased water availability later in the growing season than temperature changes.

For the trees in this study we do not observe consistent seasonal variations in $\delta^{13}\text{C}_{\text{cellulose}}$ or $\delta^{18}\text{O}_{\text{cellulose}}$ from year to year. This indicates growth was not limited by just one climate factor. In tree-ring # 6 for sample AC-77-E3, for example, early-wood $\delta^{13}\text{C}_{\text{cellulose}}$ was slightly higher than that of late-wood, but early-wood $\delta^{18}\text{O}_{\text{cellulose}}$ was much lower than that of latewood. In this year the tree might have utilized more water from snow melt during spring and early summer ($\delta^{13}\text{C}_{\text{cellulose}}$ slightly higher and $\delta^{18}\text{O}_{\text{cellulose}}$ much lower) and then experienced a temperature increase and associated evaporative leaf-water ^{18}O -enrichment

during mid-summer to autumn ($\delta^{13}\text{C}_{\text{cellulose}}$ slightly lower and $\delta^{18}\text{O}_{\text{cellulose}}$ much higher) (Figure 4.11). Overall, all samples in this study exhibited small to large year-to-year variations of $\delta^{13}\text{C}_{\text{cellulose}}$ and $\delta^{18}\text{O}_{\text{cellulose}}$ in both early-wood and late-wood, but these were not large enough to signal extreme seasonality. The trees were generally growing under favourable conditions during MIS 5a.

Other studies have reported a similar range of intra-ring variations in both $\delta^{13}\text{C}_{\text{cellulose}}$ and $\delta^{18}\text{O}_{\text{cellulose}}$, resulting from changes in microenvironments during tree growth (Barbour et al. 2002, Mayr et al. 2003, Leavitt 2002, Kress et al. 2009, Fu et al. 2017). Fu et al. (2017) found that early-wood $\delta^{13}\text{C}_{\text{cellulose}}$ was significantly higher than late-wood $\delta^{13}\text{C}_{\text{cellulose}}$ in conifers, while late-wood $\delta^{18}\text{O}_{\text{cellulose}}$ was higher than early-wood $\delta^{18}\text{O}_{\text{cellulose}}$. In that study, the early-wood $\delta^{13}\text{C}_{\text{cellulose}}$ mainly recorded a temperature signal whereas the late-wood carried a precipitation signal, but both early-wood and late-wood $\delta^{18}\text{O}_{\text{cellulose}}$ recorded a precipitation signal. An et al. (2012) observed higher early-wood $\delta^{18}\text{O}_{\text{cellulose}}$, which correlated with temperature and relative humidity than late-wood, which correlated with precipitation and relative humidity. Also, Mayr et al. (2003) found that the average $\delta^{13}\text{C}$ of early-wood (-24.9‰) and late-wood (-24.8‰) in subfossil Holocene oaks from fluvial deposits only differed slightly, as the result of water availability. Barbour et al.'s (2002) study of $\delta^{18}\text{O}_{\text{cellulose}}$ and $\delta^{13}\text{C}_{\text{cellulose}}$ of conifers from New Zealand showed that the greatest variation in $\delta^{13}\text{C}_{\text{cellulose}}$ was 4 to 6 ‰ over two seasons, where the driest site resulted greatest range in $\delta^{13}\text{C}$. Seasonal trends in $\delta^{18}\text{O}_{\text{cellulose}}$, however, were not as consistent and were likely driven by seasonal variation in the $\delta^{18}\text{O}$ of source water.

Compared to the results of Barbour et al. (2002), the seasonal trends of both $\Delta^{13}\text{C}_{\text{LW-EW}}$ (-1.1 to $+1.4\text{‰}$) and $\Delta^{18}\text{O}_{\text{LW-EW}}$ (-2.6 to $+3.1\text{‰}$) at Adam Creek were not as large. This comparison suggests that the change in climatic conditions between spring-early summer (early-wood) and mid-summer to autumn (late-wood) were not substantially different within the growing season during MIS 5a at Adam Creek.

4.4 Tree-ring Width and Seasonality

Tree-ring widths (TRW) vary in response to changes in growing conditions. Each annual tree-ring is composed of early- and late-wood. Trees that grow at low temperatures and/or under water stress exhibit decreased radial growth (Brooks et al. 1998). Girardin and Tarif (2005), for example, showed that the amount of radial growth in the trees of the boreal plains of Manitoba, Canada was positively correlated with precipitation amount and early summer temperatures, both of which affected early-wood growth. For the boreal forest in Churchill, Manitoba, Tardif et al. (2008) found that wider rings indicate years with warm early summers, whereas $\delta^{13}\text{C}_{\text{cellulose}}$ reflected overall growing season temperature. There, $\delta^{13}\text{C}_{\text{cellulose}}$ increased with long (warm) growing season, but there was no significant correlation between TRW and precipitation amount.

We measured TRW for early- and late-wood of all samples analyzed in this study (Table 3.2). For all samples, early-wood contributed more to the whole-wood TRW than late-wood. Figure 4.12 and Table 4.8 report TRW for sub-samples for which there are also isotopic data. As expected, TRW decreased in later tree-rings as the trees grew older, given that the radial growth of a tree decreases as the tree diameter increases (Figure 4.12). The TRWs of all samples were highly variable from year to year, indicating that growing conditions were also quite variable from year to year.

Table 4.8 Average tree-ring widths (TRW) for isotopically analyzed sub-samples.

Sample	Mean TRW (SD) Early-wood (μm)	Mean TRW (SD) Late-wood (μm)	Mean TRW (SD) Whole-wood (μm)	# of rings
AC-77-A2	339.2 (123.7)	89.9 (34.4)	420.3 (147.6)	26
AC-77-C3	204.5 (71.7)	76.4 (20.0)	282.3 (74.5)	17
AC-77-D1	199.1 (68.6)	52.4 (55.4)	254.1 (60.9)	18
AC-77-E3	191.3 (154.5)	92.4 (48.6)	277.2 (169.1)	17
AC-77-F1	277.4 (111.6)	175.1 (93.8)	457.3 (170.8)	8

SD = standard deviation

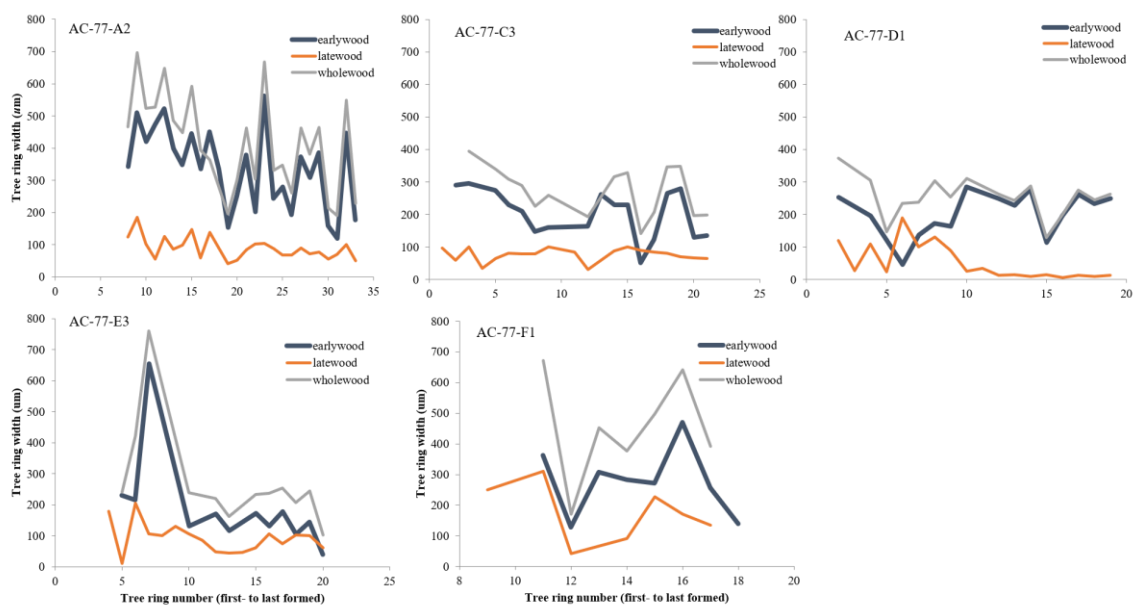


Figure 4.12 Tree-ring width (TRW) for whole tree-ring (whole-wood), early-wood and late-wood for AC-77-A2, AC-77-C3, AC-77-D1, AC-77-E3 and AC-77-F1.

Values of TRW for the whole tree-ring (early-wood + late-wood) were compared to $\delta^{13}\text{C}_{\text{cellulose}}$ and $\delta^{18}\text{O}_{\text{cellulose}}$ for whole tree-rings, early-wood and late-wood (Table 4.9) and the relationship between TRW and $\delta^{13}\text{C}_{\text{cellulose}}$ and $\delta^{18}\text{O}_{\text{cellulose}}$ for whole tree-rings is shown in Figures 4.13 and 4.14. The expectation was that TRW should increase under favourable growth conditions, as typified by sufficient water and/or warm temperatures. Growth during intervals of sufficient water should produce lower late-wood $\delta^{13}\text{C}_{\text{cellulose}}$, while late-wood $\delta^{18}\text{O}_{\text{cellulose}}$ should increase as with rising growing season temperatures and favourable growth temperatures. Previously, however, Anderson et al. (1998) showed that there was no significant correlation between Swiss spruce TRW and whole-ring cellulose isotopic data over the last 100 years, except during the warmest episode in the 1940s, where TRW decreased as both $\delta^{13}\text{C}_{\text{cellulose}}$ and $\delta^{18}\text{O}_{\text{cellulose}}$ increased during an extreme warm climatic event.

Table 4.9 Pearson correlation between TRW and $\delta^{13}\text{C}_{\text{cellulose}}$ or $\delta^{18}\text{O}_{\text{cellulose}}$.

Samples	$\delta^{13}\text{C}_{\text{cellulose}}$ (WW)	$\delta^{13}\text{C}_{\text{cellulose}}$ (LW)	$\delta^{13}\text{C}_{\text{cellulose}}$ (EW)	$\delta^{18}\text{O}_{\text{cellulose}}$ (WW)	$\delta^{18}\text{O}_{\text{cellulose}}$ (LW)	$\delta^{18}\text{O}_{\text{cellulose}}$ (EW)
AC-77-A2	0.43*	0.19	0.44*	-0.16	-0.15	-0.14
AC-77-C3	0.48	0.35	0.27	0.16	0.48	0
AC-77-D1	0.47	0.25	0.15	0.24	0.22	0.17
AC-77-E3	0.67*	0.79**	0.62*	0.77**	0.58*	0.72
AC-77-F1	0.23	0.08	0.26	0.45	0.15	0.69

WW = whole tree-ring; LW = late-wood; EW = early-wood

* Correlation is significant at the 0.05 level (2-tailed)

**Correlation is significant at the 0.01 level (2-tailed)

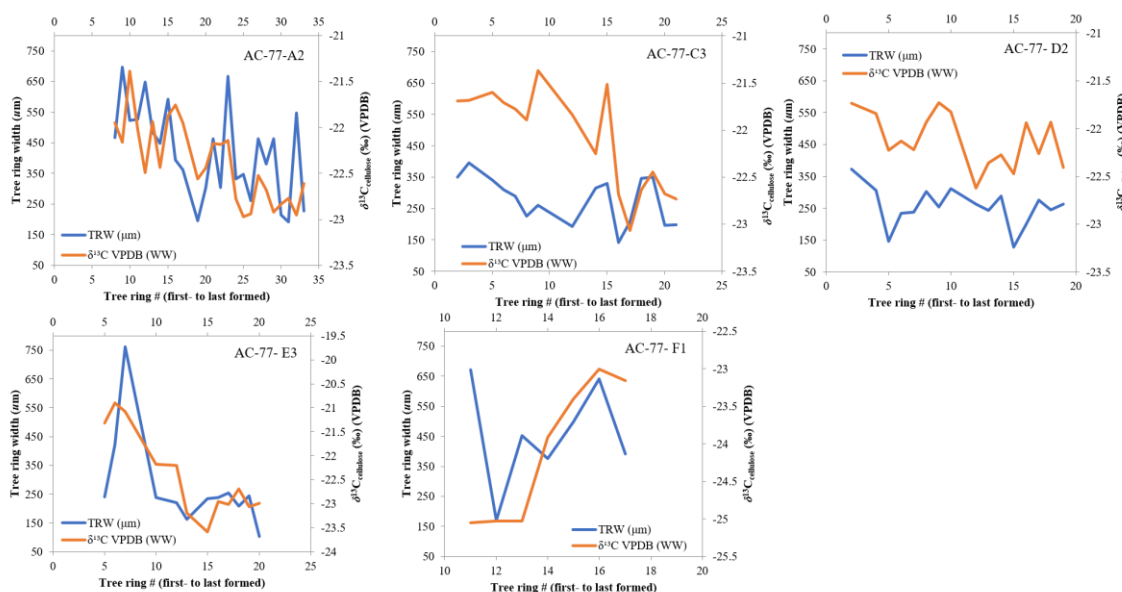


Figure 4.13 Comparison of whole (WW) tree-ring width (TRW) versus tree-ring # (age) with whole-ring $\delta^{13}\text{C}_{\text{cellulose}}$ versus tree-ring # for AC-77-A2, AC-77-C3, AC-77-D1, AC-77-E3 and AC-77-F1.

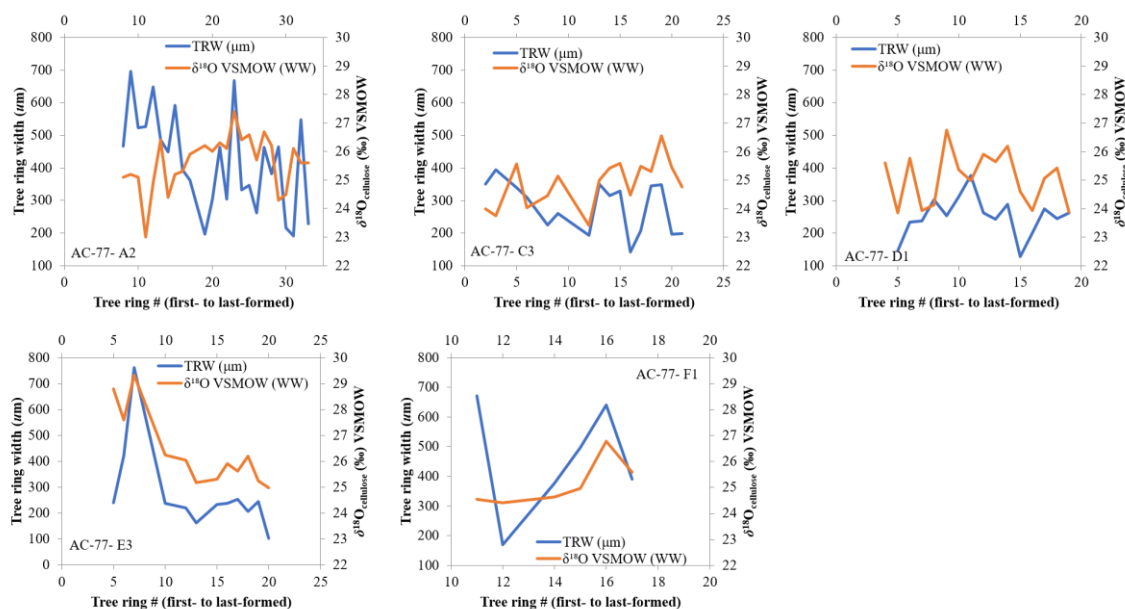


Figure 4.14 Comparison of whole (WW) tree-ring width (TRW) versus tree-ring # (age) with whole-ring $\delta^{18}\text{O}_{\text{cellulose}}$ versus tree-ring # for AC-77-A2, AC-77-C3, AC-77-D1, AC-77-E3 and AC-77-F1.

Except AC-77-E3, low positive or negative Pearson correlations (r) were obtained between TRW and both $\delta^{13}\text{C}_{\text{cellulose}}$ and $\delta^{18}\text{O}_{\text{cellulose}}$ for the Adam Creek samples (Table 4.9). This result is similar to what was reported by Anderson et al. (1998); Härdtle et al. (2013) also found no significant correlation between TRW and whole-ring $\delta^{13}\text{C}_{\text{cellulose}}$ of a modern oak tree (*Quercus petraea*) growing in Luxembourg. The lack of correlation may indicate that TRW is not influenced by factors such as carbon assimilation (carbon storage in the trunk or allocation of carbon to seeds) that can influence $\delta^{13}\text{C}_{\text{cellulose}}$ and mask any correlation when growing conditions are generally favourable.

Significant positive and high Pearson correlations between TRW and all wood components of $\delta^{13}\text{C}_{\text{cellulose}}$ were obtained for AC-77-E3 (Table 4.9) ($r = 0.67$, 0.79 and 0.62 for WW, LW and EW, respectively; $p < 0.01$ for LW and $p < 0.05$ for WW and EW; $n = 12$). A significant correlation between TRW and $\delta^{18}\text{O}_{\text{cellulose}}$ for AC-77-E3 ($r = 0.77$ and 0.58 for WW and LW, respectively; $p < 0.01$ for WW and $p < 0.05$ for LW; $n = 12$), consistent with the positive correlation between $\delta^{13}\text{C}_{\text{cellulose}}$ and $\delta^{18}\text{O}_{\text{cellulose}}$, was also obtained for this sample when all data were included (Table 4.9; see also Figure 4.9). In the case of

Anderson et al. (1998), extreme warmth beyond the tolerance of spruce likely limited growth. In contrast, the increased growth rate of AC-77-E3 associated with higher $\delta^{13}\text{C}_{\text{cellulose}}$ and $\delta^{18}\text{O}_{\text{cellulose}}$ likely reflected greater warmth and warm early summers (Tardif et al. 2008) while still remaining within the range of favourable growth conditions for spruce.

4.5 Climatic and Environment Conditions at Adam Creek during MIS 5a

Overall, the results for $\delta^{13}\text{C}_{\text{cellulose}}$ and $\delta^{18}\text{O}_{\text{cellulose}}$ obtained in this study suggest that the MIS 5a climate at Adam Creek was slightly warmer or similar to today. Allard et al. (2012) found that pollen taxa from the Missinaibi Formation in Hudson Bay Lowland were similar to modern pollen spectra, where *Picea* (spruce) was most abundant, which also suggests that climatic conditions during deposition of Missinaibi Formation was similar to present climate in the region (mean summer temperature of 15 °C; Climate Atlas of Canada (2019), with modern relative humidity of 63 % in month of July 2020 Environment Canada (2014)). Further to the south, Suh et al.'s (2020) study of $\delta^{13}\text{C}_{\text{alk}}$ and $\delta^2\text{H}_{\text{alk}}$ of plant waxes (*n*-alkanes) from Mississippi River Basin sediments also showed that MIS 5 was slightly warmer and characterized by lower global ice volumes than MIS 1.

Both $\delta^{18}\text{O}_{\text{cellulose}}$ and $\delta^{13}\text{C}_{\text{cellulose}}$ displayed inter- and intra- annual variations resulting from annual and seasonal fluctuations in growing season conditions, but there was no indication of climate stress that limited growth. Comparisons of $\delta^{13}\text{C}_{\text{cellulose}}$ and $\delta^{18}\text{O}_{\text{cellulose}}$ with modern boreal forest sites in North America suggest that trees from Adam Creek during MIS 5a experienced no intervals of significant water stress or lack of sunshine, but instead thrived in a similar to slightly warmer environment than today. The wetland environment in which the Adam Creek forest grew during MIS 5a would have been similar to today, and thus any water deficit stress was unlikely. Occasional forest flooding events could have occurred as the sample trees were found in peat layer above fluvial and below lacustrine sediments, but the isotope data do not indicate the trees suffered from sustained excess-water stress.

Chapter 5

5 Conclusions

In this study, tree-ring widths (TRW) and $\delta^{13}\text{C}_{\text{cellulose}}$ and $\delta^{18}\text{O}_{\text{cellulose}}$ of subfossil wood from Adam Creek, Ontario were measured to determine inter- and intra-annual paleoclimatic conditions during Marine Isotope Stage (MIS) 5, and interglacial substage 5a in particular. Early-wood representing spring to early summer and late-wood representing mid-summer to autumn were separated and their cellulose extracted and analyzed for $\delta^{13}\text{C}_{\text{cellulose}}$ and $\delta^{18}\text{O}_{\text{cellulose}}$, and the resulting environmental signals evaluated in terms of temperature and water availability.

There were no significant differences between early-wood and late-wood for either $\delta^{13}\text{C}_{\text{cellulose}}$ and $\delta^{18}\text{O}_{\text{cellulose}}$, which suggests that climatic conditions during spring-early summer and mid-summer-autumn climate were not significantly different. Variations in $\delta^{13}\text{C}_{\text{cellulose}}$ and $\delta^{18}\text{O}_{\text{cellulose}}$ from year to year were observed. A shift to lower $\delta^{13}\text{C}_{\text{cellulose}}$ as the trees matured most likely indicated increasing water availability, but not extensive flooding. The variations in $\delta^{18}\text{O}_{\text{cellulose}}$ indicate some year-to-year fluctuations in average weather conditions but are not diagnostic of extreme climatic events. The estimated value of $\delta^{18}\text{O}_{\text{precipitation}}$ at Adam Creek during MIS 5a is ~ 1 ‰ higher at present, which is diagnostic of slightly warmer and/or less humid conditions than at present.

Overall, there were no correlations between TRW and either $\delta^{13}\text{C}_{\text{cellulose}}$ or $\delta^{18}\text{O}_{\text{cellulose}}$ for most of the Adam Creek samples. This outcome suggests that the growth of these trees was not influenced by carbon storage, which can affect $\delta^{13}\text{C}_{\text{cellulose}}$ even under favourable growing conditions. The one exception was sample AC-77-E3, which showed significant positive correlations between TRW and both of $\delta^{13}\text{C}_{\text{cellulose}}$ and $\delta^{18}\text{O}_{\text{cellulose}}$. This pattern suggests that conditions during growth of this sample varied sufficiently to be recorded in the cellulose isotopic compositions.

5.1 Future Work

The trends we observed in the $\delta^{13}\text{C}_{\text{cellulose}}$ and $\delta^{18}\text{O}_{\text{cellulose}}$ signals of five different wood samples in this study enabled us to make general statement about MIS 5a growing-season conditions. Given an opportunity to sample, a comparison between the stable carbon- and oxygen-isotope compositions of modern and ancient spruce samples from Adam Creek would be most useful in interpreting the tree-ring records. The ability to position a weather station at the locality and collect water samples for isotopic analysis would further improve our ability to calibrate the isotopic records for the subfossil wood samples.

It would also be ideal to collect more wood samples from the Missinaibi Formation at Adam Creek, focusing on trunks that remain *in situ*. This would decrease some uncertainties concerning the provenance of the current sample materials. The ancient forest soils could also be examined for other proxies whose isotopic compositions could provide information about climatic conditions; such materials might include pedogenic carbonates, and terrestrial and lacustrine shells of molluscs. Analysis of $\delta^2\text{H}_{\text{cellulose}}$ for the subfossil wood samples could also provide more information about precipitation and soil water isotopic compositions, which would further aid in understanding evapo-transpiration and hence temperature and relative humidity during the MIS 5a growing season.

More broadly, subfossil wood samples should be gathered from various other interglacials and interstadials (e.g., MIS 7, 5, 3 and 1) in order to learn more about the variations in growing-season conditions and the larger implications for climatic patterns associated with Quaternary glacial-interglacial cycles.

References

- Allard, G., Roy, M., Ghaleb, B., Richard, P.J.H., Larouche, A.C., Veillette, J.J., and Parent, M. 2012. Constraining the age of the last interglacial-glacial transition in the Hudson Bay lowlands (Canada) using U-Th dating of buried wood. *Quaternary Geochronology*, **7**: 37–47. Elsevier B.V. doi:10.1016/j.quageo.2011.09.004.
- Alvarez, C., Bégin, C., Savard, M.M., Dinis, L., Marion, J., Smirnoff, A., and Bégin, Y. 2018. Relevance of using whole-ring stable isotopes of black spruce trees in the perspective of climate reconstruction. *Dendrochronologia*, **50**: 64–69. doi:10.1016/j.dendro.2018.05.004.
- An, W., Liu, X., Leavitt, S., Ren, J., Sun, W., Wang, W., Wang, Y., Xu, G., Chen, T., and Qin, D. 2012. Specific climatic signals recorded in earlywood and latewood $\delta^{18}\text{O}$ of tree rings in southwestern China. *Tellus B: Chemical and Physical Meteorology*, **64**: 18703. doi:10.3402/tellusb.v64i0.18703.
- Anderson, W.T., Bernasconi, S.M., and McKenzie, J.A. 1998. Oxygen and carbon isotopic record of climatic variability in tree ring cellulose (*Picea abies*): An example from central Switzerland (1913–1995). *Journal of Geophysical Research*, **103**: 31,625–31,636.
- Anderson, W.T., Bernasconi, S.M., McKenzie, J.A., Saurer, M., and Schweingruber, F. 2002. Model evaluation for reconstructing the oxygen isotopic composition in precipitation from tree ring cellulose over the last century. *Chemical Geology*, **182**: 121–137. doi:10.1016/S0009-2541(01)00285-6.
- Anderson, W.T., Sternberg, L.S.L., Pinzon, M.C., Gann-Troxler, T., Childers, D.L., and Duever, M. 2005. Carbon isotopic composition of cypress trees from South Florida and changing hydrologic conditions. *Dendrochronologia*, **23**: 1–10. doi:10.1016/j.dendro.2005.07.006.
- Barbour, M.M., Walcroft, A.S., and Farquhar, G.D. 2002. Seasonal variation in $\delta^{13}\text{C}$ and $\delta^{18}\text{O}$ of cellulose from growth rings of *Pinus radiata*. *Plant Cell and Environment*, **25**: 1483–1499. doi:10.1046/j.0016-8025.2002.00931.x.

- Bégin, C., Gingras, M., Savard, M.M., Marion, J., Nicault, A., and Bégin, Y. 2015. Assessing tree-ring carbon and oxygen stable isotopes for climate reconstruction in the Canadian northeastern boreal forest. *Palaeogeography, Palaeoclimatology, Palaeoecology*, **423**: 91–101. doi:10.1016/j.palaeo.2015.01.021.
- Bose, T., Sengupta, S., Chakraborty, S., and Borgaonkar, H. 2016. Reconstruction of soil water oxygen isotope values from tree-ring cellulose and its implications for paleoclimate. *Quaternary International*, **425**: 387–398. Elsevier Ltd. doi:10.1016/j.quaint.2016.07.052.
- Bowen, G.J., and Revenaugh, J. 2003. Interpolating the isotopic composition of modern meteoric precipitation. *Water Resources Research*, **39**: 1–13. doi:10.1029/2003WR002086.
- Brendel, O., Iannetta, P.P.M., and Stewart, D. 2000. A rapid and simple method to isolate pure Alpha-cellulose. *Phytochemical Analysis*, **11**: 7–10.
- Brooks, J.R., Flanagan, L.B., and Ehleringer, J.R. 1998. Responses of boreal conifers to climate fluctuations: indications from tree-ring widths and carbon isotope analyses. *Canadian Journal of Forest Research*, **28**: 524–533.
- Buhay, W.M., Timsic, S., Blair, D., Reynolds, J., Jarvis, S., Petrash, D., Rempel, M., and Bailey, D. 2008. Riparian influences on carbon isotopic composition of tree rings in the Slave River Delta, Northwest Territories, Canada. *Chemical Geology*, **252**: 9–20. doi:10.1016/j.chemgeo.2008.01.012.
- Cai, Q., Liu, Y., Duan, B., Li, Q., Sun, C., and Wang, L. 2018. Tree-ring $\delta^{18}\text{O}$, a tool to crack the paleo-hydroclimatic code in subtropical China. doi:10.1016/j.quaint.2017.10.038.
- Climate Atlas of Canada. 2019. Available from <https://climateatlas.ca/> [accessed 20 September 2012].
- Craig, H. 1961. Isotopic Variations in Meteoric Waters. *Science*, **133**: 1702–1703. Available from <http://www.jstor.org/stable/1708089>.
- Crann, C.A., Murseli, S., St-Jean, G., Zhao, X., Clark, I.D., and Kieser, W.E. 2017. First status report on radiocarbon sample preparation techniques at the A.E. Lalonde

- AMS Laboratory (Ottawa, Canada). Radiocarbon, **59**: 695–704.
doi:10.1017/RDC.2016.55.
- Dalton, A.S., Finkelstein, S.A., Barnett, P.J., and Forman, S.L. 2016. Constraining the Late Pleistocene history of the Laurentide Ice Sheet by dating the Missinaibi Formation, Hudson Bay Lowlands, Canada. *Quaternary Science Reviews*, **146**: 288–299. Elsevier Ltd. doi:10.1016/j.quascirev.2016.06.015.
- Dalton, A.S., Väiliranta, M., Barnett, P.J., and Finkelstein, S.A. 2017. Pollen and macrofossil-inferred palaeoclimate at the Ridge Site, Hudson Bay Lowlands, Canada: evidence for a dry climate and significant recession of the Laurentide Ice Sheet during Marine Isotope Stage 3. *Boreas*, **46**: 388–401. doi:10.1111/bor.12218.
- Dansgaard, W. 1964. Stable isotopes in precipitation. *Tellus*, **16**: 436–468.
doi:10.3402/tellusa.v16i4.8993.
- Daux, V., Edouard, J.L., Masson-delmotte, V., Stievenard, M., Hoffmann, G., Pierre, M., Mestre, O., Danis, P.A., and Guibal, F. 2011. Can climate variations be inferred from tree-ring parameters and stable isotopes from *Larix decidua*? Juvenile effects, budmoth outbreaks, and divergence issue. *Earth and Planetary Science Letters*, **309**: 221–233. Elsevier B.V. doi:10.1016/j.epsl.2011.07.003.
- Dickmann, D.I., and Kozlowski, T.T. 1970. Vegetative Reproductive. *Plant Physiology*, **45**: 284–288.
- Dodd, J.P., Patterson, W.P., Holmden, C., and Brasseur, J.M. 2008. Robotic micromilling of tree-rings: A new tool for obtaining subseasonal environmental isotope records. *Chemical Geology*, **252**: 21–30. doi:10.1016/j.chemgeo.2008.01.021.
- Duffy, J.E., Mccarroll, D., Barnes, A., Ramsey, C.B., Davies, D., Loader, N.J., Miles, D., and Young, G.H.F. 2017. Short-lived juvenile effects observed in stable carbon and oxygen isotopes of UK oak trees and historic building timbers. *Chemical Geology*, **472**: 1–7. doi:10.1016/j.chemgeo.2017.09.007.
- Dyke, A.S., and Prest, V.K. 1987. Late Wisconsinan and Holocene retreat of the Laurentide Ice Sheet. *Géographie physique et Quaternaire Late*, **41**: 237–263.
- Edwards, T.W., and Fritz, P. 1986a. Assessing meteoric water composition and relative

- humidity from ^{18}O and ^2H in wood cellulose: paleoclimatic implications for southern Ontario. *Applied Geochemistry*, **1**: 715–723.
- Edwards, T.W., and Fritz, P. 1986b. Assessing meteoric water composition and relative humidity from $\delta^{18}\text{O}$ and $\delta^2\text{H}$ in wood cellulose: paleoclimatic implications for southern Ontario, Canada. *Applied Geochemistry*, **1**: 715–723.
- Edwards, T.W.D., Birks, S.J., Luckman, B.H., and MacDonald, G.M. 2008. Climatic and hydrologic variability during the past millennium in the eastern Rocky Mountains and northern Great Plains of western Canada. *Quaternary Research*, **70**: 188–197. doi:10.1016/j.yqres.2008.04.013.
- Ehleringer, J.R., and Dawson, T.E. 1992. Water uptake by plants perspectives from stable isotope composition. *Plant Cell and Environment*, **15**: 1073–1082.
- Environment Canada, G. of C. 2014. No Title. Available from <https://www.agr.gc.ca/eng/agriculture-and-climate/agricultural-practices/climate-change-and-agriculture/climate-scenarios-for-agriculture/climate-change-scenarios/length-of-growing-season-in-ontario/?id=1363033977515>.
- Epstein, S., Thompson, P., and Yapp, C.J. 1977. Oxygen and hydrogen isotopic ratios in plant cellulose. *American Association for the Advancement of Science*, **198**: 1209–1215. Available from <http://www.jstor.org/stable/1745828>.
- Esau, K. 1960. *Anatomy of seed plants*. New York: Wiley.
- Evans, M.N., and Schrag, D.P. 2004. A stable isotope-based approach to tropical dendroclimatology. *68*: 3295–3305. doi:10.1016/j.gca.2004.01.006.
- Farley-Gill, L.D. 1980. Contemporary pollen spectra in the James Bay Lowland, Canada, and comparison with other forest-tundra assemblages. *Géographie physique et Quaternaire*, **34**: 321–334. doi:<https://doi.org/10.7202/1000415ar>.
- Farquhar, G., O’Leary, M., and Berry, J. 1982. On the relationship between carbon isotope discrimination and the intercellular carbon dioxide concentration in leaves. *Australian Journal of Plant Physiology*, **9**: 121. doi:10.1071/PP9820121.
- Ferrio, J.P., and Voltas, J. 2005. Carbon and oxygen isotope ratios in wood constituents

- of *Pinus halepensis* as indicators of precipitation, temperature and vapour pressure deficit. *Tellus Series B-Chemical and Physical Meteorology*, **57**: 164–173. doi:10.3402/tellusb.v57i2.16780.
- France, R. 1996. Carbon isotope ratios in logged and unlogged boreal forests: Examination of the potential for determining wildlife habitat use. *Environmental Management*, **20**: 249–255. doi:10.1007/BF01204009.
- Francey, R.J., and Farquhar, G.D. 1982. An explanation of $^{13}\text{C}/^{12}\text{C}$ variations in tree rings. *Nature*, **297**: 28–31. doi:10.1038/297028a0.
- Freyer, H.D. 1979. On the ^{13}C record in tree rings . Part I. ^{13}C Variations in northern hemispheric trees during the last 150 years. *Tellus*, **31**: 124–137.
- Fu, P.-L., Griebinger, J., Gebrekirstos, A., Fan, Z.-X., and Bräuning, A. 2017. Earlywood and latewood stable carbon and oxygen isotope variations in two pine species in southwestern China during the recent decades. *Frontiers in Plant Science*, **7**: 1–12. doi:10.3389/fpls.2016.02050.
- Gagen, M., McCarroll, D., and Edouard, J.-L. 2004. Latewood width, maximum density, and stable carbon isotope ratios of pine as climate indicators in a dry subalpine environment, French Alps. *Arctic, Antarctic, and Alpine Research*, **36**: 166–171. doi:10.1657/1523-0430(2004)036[0166:lwmdas]2.0.co;2.
- Gagen, M., McCarroll, D., Loader, N.J., Robertson, I., Jalkanen, R., and Anchukaitis, K.J. 2007. Exorcising the “segment length curse”: Summer temperature reconstruction since AD 1640 using non-detrended stable carbon isotope ratios from pine trees in northern Finland. *Holocene*, **17**: 435–446. doi:10.1177/0959683607077012.
- Gagen, M., McCarroll, D., Robertson, I., Loader, N.J., and Jalkanen, R. 2008. Do tree ring $\delta^{13}\text{C}$ series from *Pinus sylvestris* in northern Fennoscandia contain long-term non-climatic trends? **252**: 42–51. doi:10.1016/j.chemgeo.2008.01.013.
- Galewsky, J., Steen-Larsen, H.C., Field, R.D., Worden, J., Risi, C., and Schneider, M. 2016. Stable isotopes in atmospheric water vapor and applications to the hydrologic cycle. *Reviews of Geophysics*, **54**: 809–865. doi:10.1002/2015RG000512.

- Gartner, B.L., and Meinzer, F.C. 2005. 15 - Structure-function relationships in sapwood water transport and storage. *In* *Vascular Transport in Plants*. Academic Press. pp. 307–331.
- Gray, J., and Thompson, P. 1977. Climatic information from $^{18}\text{O}/^{16}\text{O}$ analysis of cellulose, lignin and whole wood from tree rings. *Nature*, **270**: 708–709.
- Griffith, J.D., Willcox, S., Powers, D.W., Nelson, R., and Baxter, B.K. 2008. Discovery of abundant cellulose microfibrils encased in 250 Ma permian halite: A macromolecular target in the search for life on other planets. doi:10.1089/ast.2007.0196.
- Griggs, C., Peteet, D., Kromer, B., Grote, T., Southon, J., Tree, C., and Ny, I. 2017. Rapid communication a tree-ring chronology and paleoclimate record for the Younger Dryas – Early Holocene transition from northeastern North America. **32**: 341–346. doi:10.1002/jqs.2940.
- Groffman, P.M., Kareiva, P., Carter, S., Grimm, N.B., Lawler, M.M., Matzek, V., and Tallis, H. 2014. Climate change impacts in the United States Ch. 18: Midwest. *In* *Climate change impacts in the United States: The third national climate assessment*. pp. 195–219. doi:10.7930/J0TD9V7H.
- Guerrieri, R., Jennings, K., Belmecheri, S., Asbjornsen, H., and Ollinger, S. 2017. Evaluating climate signal recorded in tree-ring $\delta^{13}\text{C}$ and $\delta^{18}\text{O}$ values from bulk wood and α -cellulose for six species across four sites in the northeastern US. *Rapid Communications in Mass Spectrometry*, **31**: 2081–2091. doi:10.1002/rcm.7995.
- Härdtle, W., Niemeyer, T., Assmann, T., Aulinger, A., Fichtner, A., Lang, A., Leuschner, C., Neuwirth, B., Pfister, L., Quante, M., Ries, C., Schuldt, A., and von Oheimb, G. 2013. Climatic responses of tree-ring width and $\delta^{13}\text{C}$ signatures of sessile oak (*Quercus petraea* Liebl.) on soils with contrasting water supply. *Plant Ecology*, **214**: 1147–1156. doi:10.1007/s11258-013-0239-1.
- Hays, J.D., Imbrie, J., and Shackleton, N.J.J.. 1976. Variations in the Earth's orbit: pacemaker of the ice ages. *Science*, **194**: 1121–1132. doi:10.1126/science.194.4270.1121.

- Hill, S.A., Waterhouse, J.S., Field, E.M., Switsur, V.R., and Ap rees, T. 1995. Rapid recycling of triose phosphates in oak stem tissue. *Plant, Cell & Environment*, **18**: 931–936. doi:10.1111/j.1365-3040.1995.tb00603.x.
- Holzkämper, S., Tillman, P.K., Kuhry, P., and Esper, J. 2012. Comparison of stable carbon and oxygen isotopes in *Picea glauca* tree rings and *Sphagnum fuscum* moss remains from subarctic Canada. *Quaternary Research*, **78**: 295–302. doi:10.1016/j.yqres.2012.05.014.
- Hook, B.A., Halfar, J., Bollmann, J., Gedalof, Z., Azizur Rahman, M., Reyes, J., and Schulze, D.J. 2015. Extraction of α -cellulose from mummified wood for stable isotopic analysis. *Chemical Geology*, **405**: 19–27. Elsevier B.V. doi:10.1016/j.chemgeo.2015.04.003.
- Hunter, R.D., Panyushkina, I.P., Leavitt, S.W., Wiedenhoeft, A.C., and Zawiskie, J. 2006. A multiproxy environmental investigation of Holocene wood from a submerged conifer forest in Lake Huron, USA. *Quaternary Research*, **66**: 67–77. doi:10.1016/j.yqres.2006.03.008.
- IBM. 2016. IBM SPSS - IBM Analytics.
- Johnson, K.R., and Ingram, B.L. 2004. Spatial and temporal variability in the stable isotope systematics of modern precipitation in China: Implications for paleoclimate reconstructions. *Earth and Planetary Science Letters*, **220**: 365–377. doi:10.1016/S0012-821X(04)00036-6.
- Joos, F., and Spahni, R. 2008. Rates of change in natural and anthropogenic radiative forcing over the past 20,000 years. *Proceedings of the National Academy of Sciences*, **105**: 1425–1430. doi:10.1073/pnas.0707386105.
- Kagawa, A., Sugimoto, A., and Maximov, T.C. 2006. Seasonal course of translocation, storage and remobilization of ^{13}C pulse-labeled photoassimilate in naturally growing *Larix gmelinii* saplings. *New Phytologist*, **171**: 793–804. doi:10.1111/j.1469-8137.2006.01780.x.
- Keeling, R.F., Piper, S.C., Bollenbacher, A.F., and Walker, S.J. 2010. Monthly atmospheric $^{13}\text{C}/^{12}\text{C}$ isotopic ratios for 11 SIO stations (1977-2008).

doi:10.3334/CDIAC/ATG.025.

- Keppler, F., Harper, D.B., Kalin, R.M., Meier-Augenstein, W., Farmer, N., Davis, S., Schmidt, H.L., Brown, D.M., and Hamilton, J.T.G. 2007. Stable hydrogen isotope ratios of lignin methoxyl groups as a paleoclimate proxy and constraint of the geographical origin of wood. *New Phytologist*, **176**: 600–609. doi:10.1111/j.1469-8137.2007.02213.x.
- Kerr-Lawson, L.J., Karrow, P.F., Edwards, T.W.D., and Mackie, G.L. 1992. A paleoenvironmental study of the molluscs from the Don Formation (Sangamonian?) Don Valley brickyard, Toronto, Ontario. *Canadian Journal of Earth Sciences*, **29**: 2406–2417. doi:10.1139/e92-188.
- Kozlowski, T.T. 1992. Carbohydrate Sources and Sinks in Woody Plants. *Botanical Review*, **58**: 107–222.
- Kress, A., Young, G.H.F., Saurer, M., Loader, N.J., Siegwolf, R.T.W., and McCarroll, D. 2009. Stable isotope coherence in the earlywood and latewood of tree-line conifers. *Chemical Geology*, **268**: 52–57. Elsevier B.V. doi:10.1016/j.chemgeo.2009.07.008.
- Leavitt, S.W. 2002. Prospects for reconstruction of seasonal environment from tree-ring $\delta^{13}\text{C}$: Baseline findings from the Great Lakes area, USA. *Chemical Geology*, **192**: 47–58. doi:10.1016/S0009-2541(02)00161-4.
- Leavitt, S.W., and Kalin, R. 1992. A new tree-ring width, $\delta^{13}\text{C}$ and ^{14}C investigation of the two creeks site. **34**: 792–797. Available from <http://strathprints.strath.ac.uk/16303/>.
- Li, Z., Nakatsuka, T., and Sano, M. 2015. Tree-ring cellulose $\delta^{18}\text{O}$ variability in pine and oak and its potential to reconstruct precipitation and relative humidity in central Japan. *Geochemical Journal*, **49**: 125–137. doi:10.2343/geochemj.2.0336.
- Lisiecki, L.E., and Raymo, M.E. 2005. A Pliocene-Pleistocene stack of 57 globally distributed benthic $\delta^{18}\text{O}$ records. *Paleoceanography*, **20**: 1–17. doi:10.1029/2004PA001071.
- Liu, Y., Cai, Q., Liu, W., Yang, Y., Sun, J., and Song, H. 2008. Monsoon precipitation variation recorded by tree-ring $\delta^{18}\text{O}$ in arid Northwest China since AD 1878. **252**:

- 56–61. doi:10.1016/j.chemgeo.2008.01.024.
- Loader, N.J., Robertson, I., and McCarroll, D. 2003. Comparison of stable carbon isotope ratios in the whole wood, cellulose and lignin of oak tree-rings. *Palaeogeography, Palaeoclimatology, Palaeoecology*, **196**: 395–407. doi:10.1016/S0031-0182(03)00466-8.
- Loader, N.J., Young, G.H., McCarroll, D., and Wilson, R.J. 2013a. Quantifying uncertainty in isotope dendroclimatology. *The Holocene*, **23**: 1221–1226. doi:10.1177/0959683613486945.
- Loader, N.J., Young, G.H.F., Grudd, H., and McCarroll, D. 2013b. Stable carbon isotopes from Torneträsk, northern Sweden provide a millennial length reconstruction of summer sunshine and its relationship to Arctic circulation. *Quaternary Science Reviews*, **62**: 97–113. Elsevier Ltd. doi:10.1016/j.quascirev.2012.11.014.
- Mayr, C., Frenzel, B., Friedrich, M., Spurk, M., Stichler, W., and Trimborn, P. 2003. Stable carbon- and hydrogen-isotope ratios of subfossil oaks in southern Germany: methodology and application to a composite record for the Holocene. *The Holocene*, **13**: 393–402. doi:10.1191/0959683603hl632rp.
- McCarroll, D., and Loader, N.J. 2004. Stable isotopes in tree rings. *Quaternary Science Reviews*, **23**: 771–801. doi:10.1016/j.quascirev.2003.06.017.
- McCarroll, D., and Pawellek, F. 2001. Stable carbon isotope ratios of *Pinus sylvestris* from northern Finland and the potential for extracting a climate signal from long Fennoscandian chronologies. *Holocene*, **11**: 517–526. doi:10.1191/095968301680223477.
- Miller, G.H., and Andrews, J.T. 2019. Hudson Bay was not deglaciated during MIS-3. *Quaternary Science Reviews*, **225**: 105944. Elsevier Ltd. doi:10.1016/j.quascirev.2019.105944.
- Mustoe, G.E. 2016. Density and loss on ignition as indicators of the fossilization of silicified wood. *IAWA Journal*, **27**: 98–111.
- Naulier, M., Savard, M.M., Bégin, C., Marion, J., Arseneault, D., and Bégin, Y. 2014.

- Carbon and oxygen isotopes of lakeshore black spruce trees in northeastern Canada as proxies for climatic reconstruction. *Chemical Geology*, **374–375**: 37–43. Elsevier B.V. doi:10.1016/j.chemgeo.2014.02.031.
- Naulier, M., Savard, M.M., Bégin, C., Marion, J., Nicault, A., and Bégin, Y. 2015. Temporal instability of isotopes-climate statistical relationships - A study of black spruce trees in northeastern Canada. *Dendrochronologia*, **34**: 33–42. Elsevier GmbH. doi:10.1016/j.dendro.2015.04.001.
- Nguyen, M., and Hicock, S. 2014. Glacial stratigraphy of the Ridge River area, northern Ontario: refining Wisconsinan glacial history and evidence for Laurentide Ice streaming. University of Western. Available from <http://ir.lib.uwo.ca/etd>.
- Poole, I., and Bergen, P.F.V. 2006. Physiognomic and chemical characters in wood as palaeoclimate proxies. *Plant Ecology*, **182**: 175–195. doi:10.1007/s11258-005-9025-z.
- Porter, T.J., Pisaric, M.F.J., Kokelj, S. V., and Edwards, T.W.D. 2009. Climatic signals in $\delta^{13}\text{C}$ and $\delta^{18}\text{O}$ of tree-rings from white spruce in the Mackenzie Delta region, northern Canada. *Arctic, Antarctic, and Alpine Research*, **41**: 497–505. doi:10.1657/1938-4246-41.4.497.
- Ramsey, C.B. 2009. Bayesian analysis of radiocarbon dates. *Radiocarbon*, **51**: 337–360. doi:10.2458/azu_acku_pk6812_yaa85_2009.
- Reimer, P.J., Bard, E., Bayliss, A., Beck, W.J., Blackwell, P.G., Ramsey, C.B., Buck, C.E., Cheng, H., Edwards, R.L., Friedrich, M., Grootes, P.M., Guilderson, T.P., Haflidason, H., Hajdas, I., Hatté, C., Heaton, T.J., Hoffmann, D.L., Hogg, A.G., Hughen, K.A., Kaiser, K.F., Kromer, B., Manning, S.W., Niu, M., Reimer, R.W., Richards, D.A., Scott, E.M., Southon, J.R., Staff, R.A., Turney, C.S.M., and Plicht, J. van der. 2013. Intcal13 and marine13 radiocarbon age calibration curves 0–50,000 years cal BP. *Radiocarbon*, **55**: 1869–1887. doi:10.1017/S0033822200048864.
- Riechelmann, D.F.C., Maus, M., Dindorf, W., Konter, O., Schöne, B.R., and Esper, J. 2016. Comparison of $\delta^{13}\text{C}$ and $\delta^{18}\text{O}$ from cellulose, whole wood, and resin-free whole wood from an old high elevation *Pinus uncinata* in the Spanish central

- Pyrenees. *Isotopes in environmental and health studies*, **6016**: 1–12.
doi:10.1080/10256016.2016.1161622.
- Riley, J. 2003. *Flora of the Hudson Bay Lowlands and its postglacial origins*. NRC Press.
- Roden, J.S., Bowling, D.R., McDowell, N.G., Bond, B.J., and Ehleringer, J.R. 2005. Carbon and oxygen isotope ratios of tree ring cellulose along a precipitation transect in Oregon, United States. *Journal of Geophysical Research: Biogeosciences*, **110**: n/a-n/a. doi:10.1029/2005jg000033.
- Roden, J.S., and Ehleringer, J.R. 1999. Hydrogen and oxygen isotope ratios of tree-ring cellulose for riparian trees grown long term under hydroponically environments. *Oecologia*, **121**: 467–477.
- Roden, J.S., Lin, G., and Ehleringer, J.R. 2000. A mechanistic model for interpretation of hydrogen and oxygen isotope ratios in tree-ring cellulose. *Geochimica et Cosmochimica Acta*, **64**: 21–35. doi:10.1016/S0016-7037(99)00195-7.
- Saurer, M., Siegenthaler, U., and Schweingruber, F. 1995. The climate-carbon isotope relationship in tree rings and the significance of site conditions. *Tellus, Series B*, **47 B**: 320–330. doi:10.3402/tellusb.v47i3.16051.
- Schubert, B.A., and Hope Jahren, A. 2015. Global increase in plant carbon isotope fractionation following the last glacial maximum caused by increase in atmospheric $p\text{CO}_2$. *Geology*, **43**: 435–438. doi:10.1130/G36467.1.
- Schweingruber, F.H. 2007. *Wood structure and environment*. Edited By T.E. Timell and R. Wimmer. Springer Berlin Heidelberg.
- Scripps. 2019. The keeling curve. Available from <https://scripps.ucsd.edu/programs/keelingcurve/>.
- Seftigen, K., Linderholm, H.W., Loader, N.J., Liu, Y., and Young, G.H.F. 2011. The influence of climate on $^{13}\text{C}/^{12}\text{C}$ and $^{18}\text{O}/^{16}\text{O}$ ratios in tree ring cellulose of *Pinus sylvestris* L. growing in the central Scandinavian Mountains. *Chemical Geology*, **286**: 84–93. Elsevier B.V. doi:10.1016/j.chemgeo.2011.04.006.
- Sensula, B., and Pazdur, A. 2013. Influence of climate change on carbon and oxygen

- isotope fractionation factors between glucose and alpha-cellulose of pine wood. *Geochronometria*, **40**: 145–152. doi:10.2478/s13386-013-0104-y.
- Siegenthaler, U., Stocker, T.F., Monnin, E., Lüthi, D., Schwander, J., Stauffer, B., Raynaud, D., Barnola, J.M., Fischer, H., Masson-Delmotte, V., and Jouzel, J. 2005. Stable carbon cycle – climate relationship during the Late Pleistocene. *Science*, **301**: 1313–1317. doi:10.1126/science.1120130.
- Skinner, R.G. 1973. Quaternary stratigraphy of the Moose River basin, Ontario. Geological Survey of Canada, 77 pages. doi:10.1017/CBO9781107415324.004.
- Stauffer, B., Flückiger, J., Monnin, E., Schwander, J., Barnola, J.M., and Chappellaz, J. 2002. Atmospheric CO₂, CH₄ and N₂O records over the past 60,000 years based on the comparison of different polar ice cores. *Annals of Glaciology*, **35**: 202–208. doi:10.3189/172756402781816861.
- Stokes, C.R., Tarasov, L., Blomdin, R., Cronin, T.M., Fisher, T.G., Gyllencreutz, R., Hättestrand, C., Heyman, J., Hindmarsh, R.C.A., Hughes, A.L.C., Jakobsson, M., Kirchner, N., Livingstone, S.J., Margold, M., Murton, J.B., Noormets, R., Peltier, W.R., Peteet, D.M., Piper, D.J.W., Preusser, F., Renssen, H., Roberts, D.H., Roche, D.M., Saint-Ange, F., Stroeven, A.P., and Teller, J.T. 2015. On the reconstruction of palaeo-ice sheets: Recent advances and future challenges. *Quaternary Science Reviews*, **125**: 15–49. doi:10.1016/j.quascirev.2015.07.016.
- Stokes, M.A., and Smiley, T.L. 1968. An introduction to tree-ring dating. University of Chicago Press., Chicago.
- Suess, H.E. 1955. Radiocarbon Concentration in Modern Wood. *American Association for the Advancement of Science*, **122**: 415–417. doi:10.1210/jcem-10-10-1361.
- Suh, Y.J., Diefendorf, A.F., Freimuth, E.J., and Hyun, S. 2020. Last interglacial (MIS 5e) and Holocene paleohydrology and paleovegetation of midcontinental North America from Gulf of Mexico sediments. *Quaternary Science Reviews*, **227**: 106066. Elsevier Ltd. doi:10.1016/j.quascirev.2019.106066.
- Tardif, J.C., Conciatori, F., and Leavitt, S.W. 2008. Tree rings, $\delta^{13}\text{C}$ and climate in *Picea glauca* growing near Churchill, subarctic Manitoba, Canada. *Chemical Geology*,

252: 88–101. doi:10.1016/j.chemgeo.2008.01.015.

Tieszen, L.L. 1991. Natural variations in the carbon isotope values of plants: implications for archaeology, ecology and palaeoecology. *Journal of Archaeological Science*, **18**: 227–248.

Treydte, K.S., Schleser, G.H., Helle, G., Frank, D.C., Winiger, M., Haug, G.H., and Esper, J. 2006. The twentieth century was the wettest period in northern Pakistan over the past millennium. **440**: 1179–1182. doi:10.1038/nature04743.

United States Geological Survey; USGS. 2020. Available from <https://isotopes.usgs.gov/lab/referencematerials.html> [accessed 13 April 2020].

Vaganov, E.A., Schulze, E.D., Skomarkova, M. V., Knohl, A., Brand, W.A., and Roscher, C. 2009. Intra-annual variability of anatomical structure and $\delta^{13}\text{C}$ values within tree rings of spruce and pine in alpine, temperate and boreal Europe. *Oecologia*, **161**: 729–745. doi:10.1007/s00442-009-1421-y.

Voelker, S.L., Stambaugh, M.C., Guyette, R.P., Feng, X., Grimley, D.A., Leavitt, S.W., Panyushkina, I., Grimm, E.C., Marsicek, J.P., Shuman, B., and Brandon Curry, B. 2015. Deglacial hydroclimate of midcontinental North America. *Quaternary Research (United States)*, **83**: 336–344. University of Washington. doi:10.1016/j.yqres.2015.01.001.

Voelker, S.L., Wang, S.Y.S., Dawson, T.E., Roden, J.S., Still, C.J., Longstaffe, F.J., and Ayalon, A. 2019. Tree-ring isotopes adjacent to Lake Superior reveal cold winter anomalies for the Great Lakes region of North America. *Scientific Reports*, **9**: 1–10. Springer US. doi:10.1038/s41598-019-40907-w.

Waterhouse, J.S., Switsur, V.R., Barker, A.C., Carter, A.H.C., and Robertson, I. 2002. Oxygen and hydrogen isotope ratios in tree rings: How well do models predict observed values? *Earth and Planetary Science Letters*, **201**: 421–430. doi:10.1016/S0012-821X(02)00724-0.

Weigl, M., Grabner, M., Helle, G., Schleser, G.H., and Wimmer, R. 2008. Characteristics of radial growth and stable isotopes in a single oak tree to be used in climate studies. *Science of the Total Environment*, **393**: 154–161.

doi:10.1016/j.scitotenv.2007.12.016.

Wright, W.E. 2008. Statistical evidence for exchange of oxygen isotopes in holocellulose during long-term storage. *Chemical Geology*, **252**: 102–108.

doi:10.1016/j.chemgeo.2008.01.016.

Xu, C., Ge, J., Nakatsuka, T., Yi, L., Zheng, H., and Sano, M. 2016. Potential utility of tree ring $\delta^{18}\text{O}$ series for reconstructing precipitation records from the lower reaches of the Yangtze River, southeast China. *Journal of Geophysical Research: Atmospheres*, **121**: 3954–3968. doi:10.1002/2015JD023610.Received.

² Sample ID	Ring segment i.d. ¹	Ring #	Late/ Early	TRW ¹ (μm)	TRW whole ring (μm)	δ ¹⁸ O VSMOW (‰)	Δ _{LW-EW} (‰)	annual weighted average δ ¹⁸ O VSMOW	3-yr average δ ¹⁸ O VSMOW whole-ring (‰)	5-yr average δ ¹⁸ O VSMOW whole-ring (‰)	δ ¹³ C VPDB (‰)	Δ _{LW-EW} (‰)	annual weighted average δ ¹³ C VPDB (‰)	3-yr average δ ¹³ C VPDB whole-ring (‰)	5-yr average δ ¹³ C VPDB whole-ring (‰)
AC77A2.23	86	43	LATE	76	735										
AC77A2.24	85	43	EARLY	659											
AC77A2.25	84	42	LATE	71	439										
AC77A2.26	83	42	EARLY	368											
AC77A2.27	82	41	LATE	92	361										
AC77A2.28	81	41	EARLY	269											
AC77A2.29	80	40	LATE	52	403										
AC77A2.30	79	40	EARLY	351											
AC77A2.31	78	39	LATE	64	699										
AC77A2.32	77	39	EARLY	635											
AC77A2.33	76	38	LATE	117	327										
AC77A2.34	75	38	EARLY	210											
AC77A2.35	74	37	LATE	139	363										
AC77A2.36	73	37	EARLY	224											
AC77A2.37	72	36	LATE	117	386										
AC77A2.38	71	36	EARLY	269											
AC77A2.39	70	35	LATE	51	490										
AC77A2.40	69	35	EARLY	439											
AC77A2.41	68	34	LATE	109	263										
AC77A2.42	67	34	EARLY	154											
AC77A2.43	66	33	LATE	50	228	+25.0					-22.6				
AC77A2.44	65	33	EARLY	178		+25.8	-0.8	+25.6	+25.8	+25.2	-22.6	0.0	-22.6	-22.8	-22.8
AC77A2.45	64	32	LATE	100	548	+25.6					-22.8				
AC77A2.46	63	32	EARLY	448		+25.7	-0.1	+25.6	+25.4	+25.3	-23.0	0.2	-23.0	-22.9	-22.8
AC77A2.47	62	31	LATE	71	191	+25.7					-22.6				
AC77A2.48	61	31	EARLY	120		+26.4	-0.7	+26.1	+24.9	+25.5	-22.9	0.3	-22.8	-22.8	-22.7
AC77A2.49	60	30	LATE	55	215	+25.1					-22.5				
AC77A2.50	59	30	EARLY	160		+24.2	0.9	+24.5	+25.0	+25.5	-22.9	0.4	-22.8	-22.8	-22.8
AC77A2.51	58	29	LATE	78	464	+23.8					-23.2				
AC77A2.52	57	29	EARLY	386		+24.4	-0.7	+24.3	+25.7	+25.9	-22.9	-0.4	-22.9	-22.7	-22.8

² Sample ID	Ring segment i.d. ¹	Ring #	Late/ Early	TRW ¹ (μm)	TRW whole ring (μm)	δ ¹⁸ O VSMOW (‰)	Δ _{LW-EW} (‰)	annual weighted average δ ¹⁸ O VSMOW	3-yr average δ ¹⁸ O VSMOW whole-ring (‰)	5-yr average δ ¹⁸ O VSMOW whole-ring (‰)	δ ¹³ C VPDB (‰)	Δ _{LW-EW} (‰)	annual weighted average δ ¹³ C VPDB (‰)	3-yr average δ ¹³ C VPDB whole-ring (‰)	5-yr average δ ¹³ C VPDB whole-ring (‰)
AC77A2.53	56	28	LATE	72	381	+27.0	1.0	+26.2	+26.2	+26.3	-22.6	0.1	-22.7	-22.7	-22.8
AC77A2.54	55	28	EARLY	309		+26.0					-22.7				
AC77A2.55	54	27	LATE	90	463	+27.8	1.5	+26.7	+26.3	+26.6	-22.8	-0.4	-22.5	-22.8	-22.7
AC77A2.56	53	27	EARLY	373		+26.4					-22.4				
AC77A2.57	52	26	LATE	68	261	+27.1	2.0	+25.7	+26.2	+26.4	-22.7	0.3	-22.9	-22.9	-22.6
AC77A2.58	51	26	EARLY	193		+25.2					-23.0				
AC77A2.59	50	25	LATE	68	347	+27.4	1.0	+26.6	+26.8	+26.6	-23.1	-0.2	-23.0	-22.6	-22.5
AC77A2.60	49	25	EARLY	279		+26.4					-22.9				
AC77A2.61	48	24	LATE	88	332	+26.8	0.5	+26.4	+26.6	+26.4	-22.9	-0.2	-22.8	-22.4	-22.3
AC77A2.62	47	24	EARLY	244		+26.3					-22.7				
AC77A2.63	46	23	LATE	105	667	+26.7	-0.9	+27.4	+26.6	+26.4	-22.2	-0.1	-22.1	-22.2	-22.3
AC77A2.64	45	23	EARLY	562		+27.6					-22.1				
AC77A2.65	44	22	LATE	102	304	+26.6	0.7	+26.1	+26.1	+26.1	-22.4	-0.3	-22.2	-22.3	-22.3
AC77A2.66	43	22	EARLY	202		+25.8					-22.1				
AC77A2.67	42	21	LATE	85	463	+25.7	-0.7	+26.3	+26.1	+25.9	-22.0	0.2	-22.2	-22.4	-22.2
AC77A2.68	41	21	EARLY	378		+26.4					-22.2				
AC77A2.69	40	20	LATE	52	303	+25.3	-0.9	+26.0	+26.0	+25.7	-22.7	-0.3	-22.4	-22.3	-22.1
AC77A2.70	39	20	EARLY	251		+26.1					-22.4				
AC77A2.71	38	19	LATE	42	196	+26.7	0.6	+26.2	+25.8	+25.4	-22.5	0.0	-22.6	-22.1	-22.1
AC77A2.72	37	19	EARLY	154		+26.1					-22.6				
AC77A2.73	36	18	LATE	153	489										
AC77A2.74	35	18	EARLY	336		+24.6					-22.7				
AC77A2.75	34	17	LATE	138	363	+25.8	-0.2	+25.9	+25.5	+25.5	-22.6	1.0	-21.9	-21.9	-22.0
AC77A2.76	33	17	EARLY	225		+26.0					-21.6				
AC77A2.77	32	16	LATE	59	394	+25.0	-0.3	+25.3	+25.0	+25.2	-21.9	0.2	-21.8	-22.0	-22.1
AC77A2.78	31	16	EARLY	335		+25.3					-21.7				
AC77A2.79	30	15	LATE	147	592	+25.8	0.8	+25.2	+25.4	+24.8	-22.0	0.1	-21.9	-22.1	-22.2
AC77A2.80	29	15	EARLY	445		+25.0					-21.9				
AC77A2.81	28	14	LATE	99	448	+25.1	0.9	+24.4	+25.2	+24.8	-22.6	0.3	-22.4	-22.3	-22.1
AC77A2.82	27	14	EARLY	349		+24.2					-22.4				

² Sample ID	Ring segment i.d. ¹	Ring #	Late/ Early	TRW ¹ (μm)	TRW whole ring (μm)	δ ¹⁸ O VSMOW (‰)	Δ _{LW-EW} (‰)	annual weighted average δ ¹⁸ O VSMOW	3-yr average δ ¹⁸ O VSMOW whole-ring (‰)	5-yr average δ ¹⁸ O VSMOW whole-ring (‰)	δ ¹³ C VPDB (‰)	Δ _{LW-EW} (‰)	annual weighted average δ ¹³ C VPDB (‰)	3-yr average δ ¹³ C VPDB whole-ring (‰)	5-yr average δ ¹³ C VPDB whole-ring (‰)
AC77C3.19	44	22	LATE	99	173										
AC77C3.20	43	22	EARLY	74											
AC77C3.21	42	21	LATE	64	199	+23.3	-2.2	+24.8	+25.6	+25.5	-23.0	-0.4	-22.7	-22.6	-22.7
AC77C3.22	41	21	EARLY	135		+25.5					-22.6				
AC77C3.23	40	20	LATE	67	197	+25.7	0.4	+25.4	+25.8	+25.5	-23.2	-0.9	-22.7	-22.6	-22.7
AC77C3.24	39	20	EARLY	130		+25.3					-22.4				
AC77C3.25	38	19	LATE	70	349	+26.0	-0.7	+26.6	+25.8	+25.5	-22.8	-0.5	-22.4	-22.7	-22.5
AC77C3.26	37	19	EARLY	279		+26.7					-22.4				
AC77C3.27	36	18	LATE	80	346	+25.5	0.2	+25.3	+25.1	+25.3	-23.0	-0.4	-22.6	-22.8	-22.4
AC77C3.28	35	18	EARLY	266		+25.3					-22.5				
AC77C3.29	34	17	LATE	85	208	+24.4	-1.8	+25.5	+25.2	+25.2	-23.3	-0.3	-23.1	-22.4	-22.3
AC77C3.30	33	17	EARLY	123		+26.2					-22.9				
AC77C3.31	32	16	LATE	90	142	+24.3	-0.6	+24.5	+25.2	+24.8	-23.1	-1.1	-22.7	-22.2	-21.9
AC77C3.32	31	16	EARLY	52		+24.9					-22.0				
AC77C3.33	30	15	LATE	100	329	+24.5	-1.6	+25.6	+25.3	+24.9	-21.7	-0.3	-21.5	-21.9	-21.8
AC77C3.34	29	15	EARLY	229		+26.1					-21.4				
AC77C3.35	28	14	LATE	87	316	+26.7	1.8	+25.4	+24.6	+24.7	-22.3	-0.1	-22.3	-21.8	-21.8
AC77C3.36	27	14	EARLY	229		+24.9					-22.2				
AC77C3.37	26	13	LATE	88	350	+25.6	0.8	+25.0	+24.5	+24.6	-22.4				
AC77C3.38	25	13	EARLY	262		+24.8					-21.4				
AC77C3.39	24	12	LATE	30	193	+24.2	0.9	+23.4	+24.3	+24.4	-21.9	0.6	-21.8	-21.7	-21.7
AC77C3.40	23	12	EARLY	163		+23.3					-21.9				
AC77C3.41	22	11	LATE	85	100	+24.6					-22.1				
AC77C3.42	21	11	EARLY	15											
AC77C3.43	20	10	LATE	86	171	+24.3									
AC77C3.44	19	10	EARLY	85											
AC77C3.45	18	9	LATE	100	260	+24.5	-1.1	+25.1	+24.9	+24.8	-21.8	-0.8	-21.4	-21.7	-21.7
AC77C3.46	17	9	EARLY	160		+25.6					-21.1				
AC77C3.47	16	8	LATE	78	226	+25.2	1.2	+24.5	+24.5	+24.6	-22.1	-0.2	-21.9	-21.8	-21.7
AC77C3.48	15	8	EARLY	148		+24.0					-21.8				

² Sample ID	Ring segment i.d. ¹	Ring #	Late/ Early	TRW ¹ (μm)	TRW whole ring (μm)	δ ¹⁸ O VSMOW (‰)	Δ _{LW-EW} (‰)	annual weighted average δ ¹⁸ O VSMOW	3-yr average δ ¹⁸ O VSMOW whole-ring (‰)	5-yr average δ ¹⁸ O VSMOW whole-ring (‰)	δ ¹³ C VPDB (‰)	Δ _{LW-EW} (‰)	annual weighted average δ ¹³ C VPDB (‰)	3-yr average δ ¹³ C VPDB whole-ring (‰)	5-yr average δ ¹³ C VPDB whole-ring (‰)
AC77C3.49	14	7	LATE	79	289	+24.9	-0.1	+25.0	+24.9	+24.5	-21.9	-0.2	-21.8	-21.7	-21.7
AC77C3.50	13	7	EARLY	210		+25.0					-21.7				
AC77C3.51	12	6	LATE	80	310	+24.1	0.1	+24.0	+24.5		-22.1	-0.5	-21.7	-21.7	
AC77C3.52	11	6	EARLY	230		+24.0					-21.6				
AC77C3.53	10	5	LATE	65	340	+26.3	0.9	+25.6	+24.4		-21.9	-0.3	-21.6	-21.7	
AC77C3.54	9	5	EARLY	275		+25.4					-21.5				
AC77C3.55	8	4	LATE	34	74	+26.2					-22.0				
AC77C3.56	7	4	EARLY	40											
AC77C3.57	6	3	LATE	100	395	+25.0	1.6	+23.8			-22.2	-0.7	-21.7		
AC77C3.58	5	3	EARLY	295		+23.3					-21.5				
AC77C3.59	4	2	LATE	60	350	+24.8	1.0	+24.0			-21.6	0.1	-21.7		
AC77C3.60	3	2	EARLY	290		+23.8					-21.7				
AC77C3.61	2	1	LATE	97		+21.4					-22.4				
Adam Creek -77-D-1															
AC77D1.1	44	22	LATE	8	187										
AC77D1.2	43	22	EARLY	179											
AC77D1.3	42	21	LATE	15	221										
AC77D1.4	41	21	EARLY	206											
AC77D1.5	40	20	LATE	11	155										
AC77D1.6	39	20	EARLY	144											
AC77D1.7	38	19	LATE	12	262	+23.5	-0.4	+23.9	+24.8	+24.6	-22.0	0.4	-22.4	-22.2	-22.2
AC77D1.8	37	19	EARLY	250		+23.9					-22.4				
AC77D1.9	36	18	LATE	10	244	+24.7	-0.8	+25.4	+24.8	+25.0	-21.7	0.2	-21.9	-22.0	-22.2
AC77D1.10	35	18	EARLY	234		+25.5					-21.9				
AC77D1.11	34	17	LATE	13	275	+23.6	-1.5	+25.1	+24.5	+25.1	-22.1	0.1	-22.3	-22.2	-22.3
AC77D1.12	33	17	EARLY	262		+25.1					-22.3				
AC77D1.13	32	16	LATE	5	200	+24.0	0.0	+23.9	+24.9	+25.3	-22.1	-0.1	-21.9	-22.2	-22.3
AC77D1.14	31	16	EARLY	195		+23.9					-21.9				
AC77D1.15	30	15	LATE	15	128	+24.3	-0.4	+24.6	+25.5	+25.5	-21.9	0.6	-22.5	-22.4	-22.3
AC77D1.16	29	15	EARLY	113		+24.6					-22.5				

² Sample ID	Ring segment i.d. ¹	Ring #	Late/ Early	TRW ¹ (μm)	TRW whole ring (μm)	δ ¹⁸ O VSMOW (‰)	Δ _{LW-EW} (‰)	annual weighted average δ ¹⁸ O VSMOW	3-yr average δ ¹⁸ O VSMOW whole-ring (‰)	5-yr average δ ¹⁸ O VSMOW whole-ring (‰)	δ ¹³ C VPDB (‰)	Δ _{LW-EW} (‰)	annual weighted average δ ¹³ C VPDB (‰)	3-yr average δ ¹³ C VPDB whole-ring (‰)	5-yr average δ ¹³ C VPDB whole-ring (‰)
AC77E3.34	45	23	EARLY	100											
AC77E3.35	44	22	LATE	70	150										
AC77E3.36	43	22	EARLY	80											
AC77E3.37	42	21	LATE	37	92										
AC77E3.38	41	21	EARLY	55											
AC77E3.39	40	20	LATE	62	103	+25.2	0.6	+25.0	+25.5	+25.6	-22.9	0.1	-23.0	-22.9	-22.9
AC77E3.40	39	20	EARLY	41		+24.6					-23.0				
AC77E3.41	38	19	LATE	100	244	+24.5	-1.3	+25.3	+25.7	+25.7	-23.5	-0.7	-23.1	-22.9	-23.1
AC77E3.42	37	19	EARLY	144		+25.8					-22.8				
AC77E3.43	36	18	LATE	102	208	+26.4	0.3	+26.2	+25.9	+25.6	-22.6	0.3	-22.7	-22.9	-23.1
AC77E3.44	35	18	EARLY	106		+26.0					-22.8				
AC77E3.45	34	17	LATE	75	254	+24.4	-1.8	+25.6	+25.6	+25.6	-22.9	0.2	-23.0	-23.2	-23.0
AC77E3.46	33	17	EARLY	179		+26.1					-23.1				
AC77E3.47	32	16	LATE	106	238	+24.9	-1.8	+25.9	+25.5	+25.7	-22.9	0.1	-23.0	-23.2	-22.8
AC77E3.48	31	16	EARLY	132		+26.7					-23.0				
AC77E3.49	30	15	LATE	62	234	+26.4	1.5	+25.3	+25.5	+26.4	-22.9	0.9	-23.6	-23.0	-22.4
AC77E3.50	29	15	EARLY	172		+24.9					-23.8				
AC77E3.51	28	14	LATE	46	171	+25.3					-23.1				
AC77E3.52	27	14	EARLY	125											
AC77E3.53	26	13	LATE	45	162	+25.5	0.4	+25.2	+25.8	+26.9	-22.7	0.7	-23.2	-22.5	-21.9
AC77E3.54	25	13	EARLY	117		+25.1					-23.4				
AC77E3.55	24	12	LATE	49	220	+26.6	0.7	+26.0	+27.2	+27.6	-22.6	-0.5	-22.2	-21.8	-21.5
AC77E3.56	23	12	EARLY	171		+25.9					-22.1				
AC77E3.57	22	11	LATE	85	174	+25.8					-22.2				
AC77E3.58	21	11	EARLY	89											
AC77E3.59	20	10	LATE	107	239	+26.0	-0.4	+26.2	+27.7		-21.9	0.4	-22.2	-21.4	
AC77E3.60	19	10	EARLY	132		+26.4					-22.4				
AC77E3.61	18	9	LATE	130	217	+25.4					-21.5				
AC77E3.62	17	9	EARLY	87											
AC77E3.63	16	8	LATE	100	190	+25.7					-21.3				

² Sample ID	Ring segment i.d. ¹	Ring #	Late/ Early	TRW ¹ (μm)	TRW whole ring (μm)	δ ¹⁸ O VSMOW (‰)	Δ _{LW-EW} (‰)	annual weighted average δ ¹⁸ O VSMOW	3-yr average δ ¹⁸ O VSMOW whole-ring (‰)	5-yr average δ ¹⁸ O VSMOW whole-ring (‰)	δ ¹³ C VPDB (‰)	Δ _{LW-EW} (‰)	annual weighted average δ ¹³ C VPDB (‰)	3-yr average δ ¹³ C VPDB whole-ring (‰)	5-yr average δ ¹³ C VPDB whole-ring (‰)
AC77F1.22	39	20	EARLY	120											
AC77F1.23	38	19	LATE	69	179										
AC77F1.24	37	19	EARLY	110											
AC77F1.25	36	18	LATE	174	314										
AC77F1.26	35	18	EARLY	140		+26.5					-23.5				
AC77F1.27	34	17	LATE	135	391	+25.7	0.1	+25.6	+25.8	+25.3	-23.2	-0.1	-23.2	-23.2	-23.4
AC77F1.28	33	17	EARLY	256		+25.5					-23.1				
AC77F1.29	32	16	LATE	170	641	+26.2	-0.9	+26.8	+25.5	+25.1	-23.4	-0.5	-23.0	-23.4	-24.1
AC77F1.30	31	16	EARLY	471		+27.0					-22.9				
AC77F1.31	30	15	LATE	227	498	+25.3	0.7	+25.0	+24.7		-23.2	0.3	-23.4	-24.1	
AC77F1.32	29	15	EARLY	271		+24.6					-23.5				
AC77F1.33	28	14	LATE	92	376	+24.8	0.3	+24.6	+24.5		-23.4	0.7	-23.9	-24.7	
AC77F1.34	27	14	EARLY	284		+24.6					-24.1				
AC77F1.35	26	13	LATE	146	453						-25.0				
AC77F1.36	25	13	EARLY	307		+22.4					-24.9				
AC77F1.37	24	12	LATE	42	170	+23.7	-1.0	+24.4			-25.1	0.2	-25.0		
AC77F1.38	23	12	EARLY	128		+24.7					-25.0				
AC77F1.39	22	11	LATE	310	672	+23.1	-2.6	+24.5			-25.0	0.0	-25.0		
AC77F1.40	21	11	EARLY	362		+25.7					-25.1				
AC77F1.41	20	10	LATE	168	575										
AC77F1.42	19	10	EARLY	407											
AC77F1.43	18	9	LATE	250	733	+25.3					-25.2				
AC77F1.44	17	9	EARLY	483											
AC77F1.45	16	8	LATE	249											

¹ TRW = tree ring width² Sample name code: e.g., AC-77-A2.1; AC-77-A = subfossil wood bundle; 2 = wood fragment number from AC-77-A2; .1 = ring number from center of wood fragment.

Curriculum Vitae

Name:	Jumin Lee
Post-secondary Education and Degrees:	<p>Department of Earth Sciences The University of Western Ontario London, Ontario, Canada 2016 – 2020 M.Sc.</p> <p>Specialization in Environmental Science (Honors) University of Windsor Windsor, Ontario, Canada 2013 – 2016 B.Sc.</p> <p>Major in Biology The University of Western Ontario London, Ontario, Canada 2008 – 2013 B.Sc.</p>
Honours and Awards:	<p>Western Graduate Research Scholarship (WGRS) \$1000 (CDN)/term Sept. 2017 – Apr.2018</p> <p>Western Graduate Research Scholarship (WGRS) \$1000 (CDN)/term Sept. 2016 – Apr.2017</p> <p>Dean's Honor List Sept. 2013 – April 2016</p>
Related Work Experience	<p>Teaching Assistant (Supervisor: Dr. Sheri Molnar) Geology 1022B: Earth Rocks The University of Western Ontario Jan. 2018 - April 2018</p> <p>Teaching Assistant (Supervisor: Dr. Alysha McNeil) Geology 1081A: Resources, Environment & Sustainability in a Material Society The University of Western Ontario Sept. 2017 - Dec. 2018</p> <p>Teaching Assistant (Supervisor: Dr. Elizabeth Webb) Geology 2240G: Catastrophic Events in Earth History The University of Western Ontario</p>

Jan. 2017 - April 2017

Teaching Assistant (Supervisor: Dr. Cam Tsujita)
Geology 1081A: Resources, Environment & Sustainability in a
Material Society
The University of Western Ontario
Sept. 2016 - Dec. 2016

Publications:

Weisener, C.G., **Lee, J.**, Chaganti, S.R., Reid, T., Falk, N. and Drouillard, K.
“Investigating sources and sinks of N₂O expression from freshwater microbial
communities in urban watershed sediments.” Chemosphere, 188. 2017.